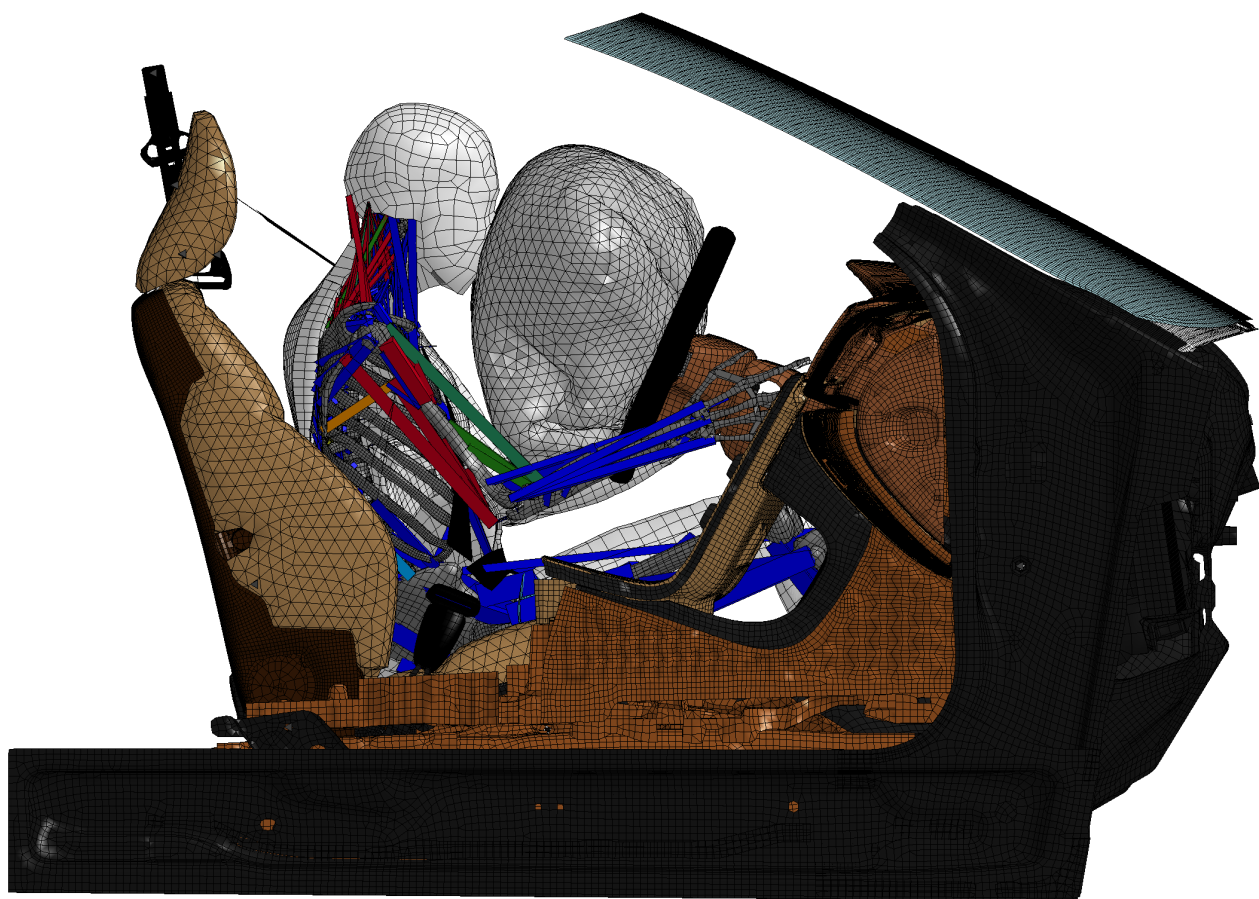




CHALMERS
UNIVERSITY OF TECHNOLOGY



Industrialisation of a Finite Element Active Human Body Model for Vehicle Crash Simulations

Master's thesis in Solid and Structural Mechanics

ERIK ELIASSON
JACOB WASS

Department of Applied Mechanics
CHALMERS UNIVERSITY OF TECHNOLOGY
Göteborg, Sweden 2015

MASTER'S THESIS 2015:52

Industrialisation of a Finite Element Active Human Body Model for Vehicle Crash Simulations

ERIK ELIASSON
JACOB WASS



Department of Applied Mechanics
Division of Vehicle Safety
CHALMERS UNIVERSITY OF TECHNOLOGY
Göteborg, Sweden 2015

Industrialisation of a Finite Element Active Human Body Model for Vehicle Crash Simulations
ERIK ELIASSON
JACOB WASS

© ERIK ELIASSON , JACOB WASS, 2015

Master's thesis 2015:52
ISSN 1652-8557
Department of Applied Mechanics
Division of Vehicle Safety
Chalmers University of Technology
SE-412 96 Göteborg
Sweden
Telephone: +46 (0)31-772 1000

Cover:

The SAFER AHBM in a 70 km/h crash event just as the air bag is deployed. The model is partly blanked to show muscles and muscle activation.

Chalmers Reproservice
Göteborg, Sweden 2015

Industrialisation of a Finite Element Active Human Body Model for Vehicle Crash Simulations

Master's thesis in Solid and Structural Mechanics

ERIK ELIASSON

JACOB WASS

Department of Applied Mechanics

Division of Vehicle Safety

Chalmers University of Technology

ABSTRACT

The Total HUMAN Model for Safety (THUMS), developed by Toyota, is a numerical finite element model of the human body to enable studies of vehicle accidents by computer aided simulations. Recently a new muscle package, referred to as the SAFER Active Human Body Model (AHBM) which provides the THUMS with active muscle response, was developed in a PhD project at Chalmers University of Technology. This enable studies of pre-crash events, such as emergency braking. The objective of this thesis is to industrialise the SAFER AHBM used by the automotive industry to make it a reliable tool in development. Industrialisation of the model, in this context, includes making the model easier to use, solving numerical instability issues when entering the crash phase, reducing computational time, and calibration and validation of the industry version of the SAFER AHBM.

A method for positioning the SAFER AHBM was developed to aid the user when evaluating new driving scenarios. The positioning is conducted via a constraint based simulation where the model is placed in the desired position by prescribing nodal displacements. The model was also calibrated and validated with respect to experimental data from volunteers in a pre-crash scenario. Calibration was done using a radial basis function meta-model which was sampled by two Design of Experiment (DOE) iterations consisting of 48 and 24 simulations, respectively. The parameter test matrix was constructed using a space-filling design algorithm with the controller gains as parameters. The goal functions for the calibration and validation were head rotation, head vs. sternum relative X -displacement, belt force, steering wheel force and frequency content of all responses.

Positioning of the model is done with high precision by prescribing displacements (rotations) for key nodes in the model, e.g. ankles, wrists, head, neck, spine and hips. After the simulation is completed the user has the possibility to extract element stresses which can be used as input to a new simulation starting from the positioned state. This enables both seat squashing and positioning to be done in one simulation. Calibration of the model resulted in seventeen new controller gains for the PID-control system which improved the model response compared to experimental data. The model response now fits within one standard deviation for all the goal functions (except head rotation for which it over rotates slightly) and exhibits a stable response towards small perturbations. It was found that the muscle control system is very sensitive and easily experiences closed loop instability, especially for variations in the derivative gain. The model was also shown to complete a full pre-crash crash simulation without termination due to numerical instabilities.

Keywords: finite element, human body model, active muscles, feedback control, model calibration, model validation, positioning of HBM, posture modifications of HBM

PREFACE

This thesis presents the work done in a master project on industrialisation of the SAFER Active Human Body model (AHBM) under the Applied Mechanics department at Chalmers University of Technology. Examiner for the project was Jonas Östh, researcher at SAFER (Chalmers Vehicle and Traffic Safety Centre) and supervisor was Bengt Pipkorn, technical specialist at Autoliv Development AB. The thesis work was conducted in the facilities at SAFER, located at Lindholmen, and many of the simulations were carried out on the CASPER computer cluster at SAFER.

ACKNOWLEDGEMENTS

We would like to thank SAFER and Autoliv Development AB for hosting, helping and supporting us through this master thesis. A special thanks is directed to Jonas Östh and Bengt Pipkorn for their supportive and dedicated supervision of the work. It has been a fun and challenging project with a comprehensive learning outcome within many engineering disciplines. We would also like to thank Jona Olafsdottir, Manuel Mendoza-Vazquez and Karin Brohlin at SAFER, Krystoffer Mroz and Dan Brase at Autoliv, and Merete Östmann at Volvo for their support and inputs throughout the project.

NOMENCLATURE

AHBM	Active Human Body Model
Autoliv	Autoliv Development AB
DOE	Design Of Experiments
DOF	Degree Of Freedom
FE	Finite Element
GHBMC	Global Human Body Model Consortium
HBM	numerical Human Body Model
HUMOS	HUman Model for Safety
LHS	Latin Hypercube Sampling
MB	Multi-Body
MPI	Message Parsing Interface
NRMS	Normalised Root-Mean-Square
ODE	Ordinary Differential Equation
ORM	Objective Rating Method
PMHS	Post-Mortem Human Subject
R&D	Research and Development
RMS	Root-Mean-Square
THUMS	Total HUman Model for Safety

CONTENTS

Abstract	i
Preface	iii
Acknowledgements	iii
Nomenclature	v
Contents	vii
1 Introduction	1
1.1 Objectives	3
1.2 Deliverables	3
1.3 Limitations	3
1.4 Tools	3
2 Theory	4
2.1 Explicit and implicit solvers	4
2.2 Calibration	5
2.2.1 Sequential Methods	5
2.2.2 Single Iteration Methods	6
2.2.3 Metamodelling Techniques	6
2.2.4 Calibration Of Goal Functions	7
2.3 Musculoskeletal Model	8
2.3.1 Hill-Type Muscle Model	8
2.3.2 Neuromuscular Feedback Control System	9
3 Positioning	11
3.1 Method	13
3.2 Results	17
4 Calibration and Validation	19
4.1 Method	21
4.1.1 Calibration	21
4.1.2 Validation	24
4.2 Results	25
5 Discussion	31
6 Conclusions	36
7 Future Work	37
References	38
Appendices	40
A Positioning Manual	41
A.1 Example Positioning File	45
B MATLAB code	48
C Calibration Results	57
D SAFER AHBM Industrial Version Bug Fixes	59

1 Introduction

In 2010 the governments of the world declared 2011-2020 as the Decade of Action for Road Safety and invited the World Health Organization (WHO) to prepare a report to assess the state of global road safety at the onset of the Decade [10]. The report found that during 2010 there were over 1,240,000 traffic related fatalities around the world and another 20 to 50 million who sustain non-fatal injuries. These accidents are not only devastating to the individuals involved, but also come with a huge cost for society. A report done by the Transport Research Laboratory (2000) [13] makes a crude estimate of US\$ 518 billion for the annual cost of road crashes worldwide. Most of these accidents are related to excessive speed, drunk-driving and absence of adequate safety systems, such as seat belts and helmets [10]. This needs to be countered by both legislation and technical improvements, motivating the need to understand crash events and related injuries, so that traffic systems can be more efficient and save lives.

During the past decades considerable effort has been put into understanding occupant responses and injuries in vehicle impact scenarios. A result of such research is the development of anthropomorphic test devices (ATD), commonly known as crash test dummies, like Hybrid III, SID, BioRID etc. which are used for physical testing of crash safety measures for vehicles. These ATDs are complemented with numerical models which are used extensively in industry and research, see Figure 1.1a. However, since physical test dummies are made for repeated testing, they have a different physiology compared with real humans, some examples of this are the joints, ribcage and neck system. With increasing computational power available, an effort towards bridging this difference has been the development of numerical Models of the Human Body (HBM), see Figure 1.1b. Two modelling approaches are commonly utilised: a Multi-Body systems (MB) method, which connects a system of flexible and rigid bodies to approximate the kinematics of a full human body, and the Finite Element (FE) method, which divides the body into a large number of small elements for which both kinematic and constitutive equations are solved. The MB approach is useful because the simulation is fast and it gives the possibility to run large parametric studies when evaluating a new design, while having a reliable kinematic response. However, what the MB approach lacks is a realistic geometrical representation of the human body and injury predictive possibilities of bones, joints and soft tissues. On the other hand the FE method facilitates the study of injury risk at tissue level and is better suited for contact simulations but comes with a much higher computational cost, making large parameter studies more complex and time consuming. Today, the FE modelling approach has become the favoured method for researchers and companies such as Autoliv, Volvo Cars, Daimler, Volkswagen, etc. and is more or less industry standard for occupant modelling.

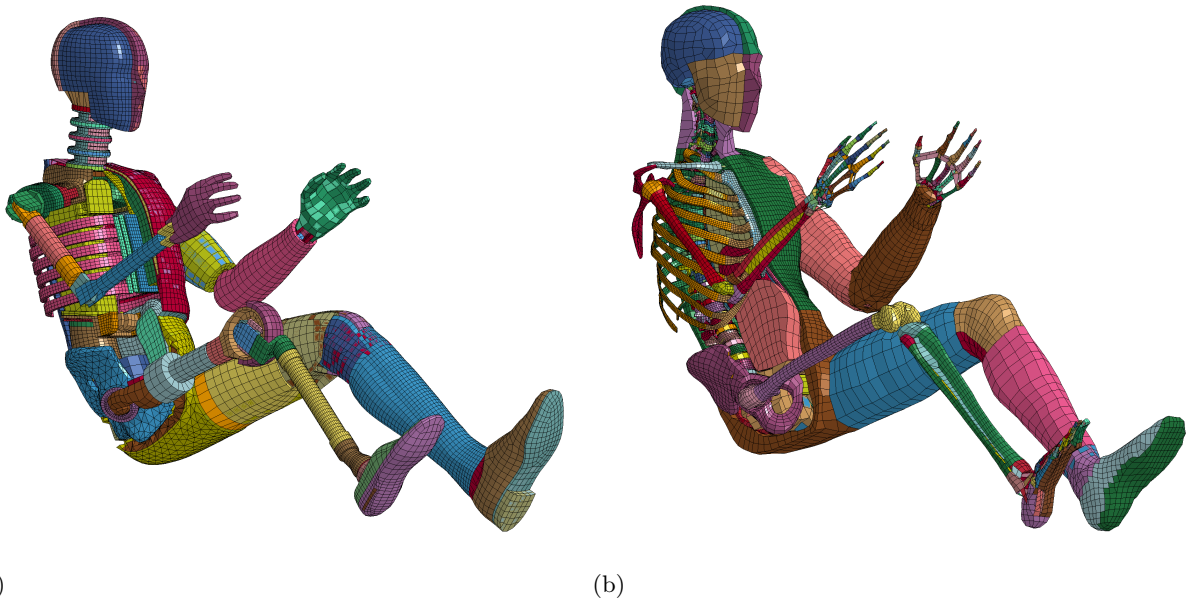


Figure 1.1: Comparison of a Dummy model (LSTC, Livermore, CA, USA) and the THUMS model [12], partly blanked.

A number of whole body FE HBMs exist which are solved using commercial explicit FE solvers, e.g. the HUMOS [27], the THUMS [12] and the GHBMC [9] models. This thesis makes use of the THUMS version 1.52 (Toyota 2000-2001, [25]) which includes over 150,000 finite elements to represent a 50th percentile American male occupant, see Figure 1.1b. This is not the latest version of THUMS (THUMS version 4 Toyota 2011) but it is the model used by Autoliv today. One reason for this is the number of finite elements used in THUMS version 4 (1.8 million) which, at the present, makes it more of a research tool than an industry tool due to the long simulation times. Another reason is the development work put into the model by Autoliv to enhance the performance of e.g. the rib cage. However, even such complex models as THUMS version 4 are simplifications of the mechanical properties of the biological tissues that comprise an actual human response and many aspects yet remain to be investigated.

Recently, active muscular control was implemented for the THUMS model by Östh (2014) [35], referred to as SAFER AHBM see Figure 1.2. The goal for Östh was to study the muscular response of car occupants subjected to pre-crash interventions, and to model them in a numerical human model with active muscles. The muscle model utilised was a Hill-type model [33] which represent the muscles by 1D beam elements stretching between two nodes. The control of the muscles are achieved by a proportional, integral and derivative (PID) feedback control, where the current position of the model is compared to a reference position in order to calculate the error in position. This error will generate a signal to the activation dynamics of the muscles which makes the muscles contract/relax accordingly, see Section 2.3 for further theory on muscle mechanics and control theory. Using THUMS with an active muscle control facilitates the study of pre-crash scenarios, where muscle activation highly influence the position of the driver due to longer events and lower loads compared to crash scenarios [38].

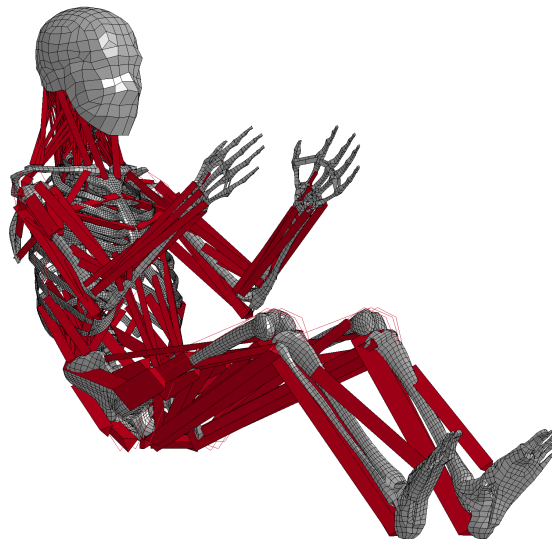


Figure 1.2: *The SAFER AHBM model with red lines indicating active muscles.*

Autoliv has used the passive THUMS model for many years in their development work of new safety systems for crash scenarios [25]. This model has worked well enough for fast, high load scenarios, which are present in crashes, since the kinematic response of the driver mainly is a result of the geometry, mass and stiffness of the models. In high speed events, the addition of active muscles will have low impact on the simulation outcome, due to the high forces and fast scenarios. However, when trying to simulate a real accident, the pre-crash scenario needs to be included for Autoliv to continue improving the performance of their safety systems. This is because the belt pre-tension systems, occupant position, and airbag timings govern much of the outcome in the subsequent crash, and thereby the risk of injury or fatality. Hence, the need to include a realistic pre-crash phase, with active muscle control prior to crash analysis, has increased in recent time. Before Autoliv can fully make use of the active muscle model they need to ensure that a validated response compared to experimental data is achieved. The model also needs to be numerically stable throughout a full crash simulation and run with a feasible simulation time and scaling in distributed simulations with Message Parsing Interface (MPI) technology. For the model to be effective in industry work it should also be as easy as possible to include in simulation setups used for evaluating Autoliv's safety systems.

1.1 Objectives

The objective of this study is to industrialise a model developed in a doctoral thesis project at Chalmers University of Technology (2014) [35] to be used in the development work at Autoliv, Volvo and SAFER. Industrialisation, in this context, refers to ensuring a calibrated and validated model response, making the model easy to use, solving numerical instability issues when entering the crash phase and improving computational time so that a combined pre-crash crash simulation can be completed over night. The goal is to deliver a model that satisfies this industrialisation definition and is shown to be ready for use in a combined pre-crash crash simulation for evaluation of different belt and airbag systems.

1.2 Deliverables

- A method for positioning the SAFER AHBM in a car interior
- A setup for combined pre-crash and crash simulations
- Calibrated SAFER AHBM with respect to experimental data for pre-crash analysis
- Validated SAFER AHBM with respect to experimental data
- A computationally stable SAFER AHBM through a full pre-crash crash scenario

1.3 Limitations

The work is restricted to sagittal plane motion since this is the current state of the active muscle model, *e.g.* no lateral collisions or lateral pre-crash events will be considered. Furthermore, the work is limited to the industry version of the THUMS model used by Autoliv (version 1.52) and updates and modifications will, as far as possible, be limited to the active muscle model and not to the original THUMS model. Since this thesis' objective is to industrialise the already developed active muscle model, it will be restricted to modifying the parameters of the muscle control system and muscle material properties, when calibration is conducted, meaning that no new muscles will be added to the model and no material changes within the original THUMS will be evaluated to ensure a validated response.

1.4 Tools

All pre- and post-processing in this thesis was done using LS-PREPOST[®] (LSTC Inc., Livermore, CA, USA) and MATLAB[®] (The Mathworks Inc., Natick, MA, USA). Simulations was done using LS-DYNA[®] r8.0 revision 98312 (LSTC Inc., Livermore, CA, USA) while the calibration was set up using LS-OPT[®] v4.2 (LSTC Inc., Livermore, CA, USA). The cluster used for the computations run with Intel[®] Xeon[®] CPU X5550 2.67GHz (Intel Inc., Santa Clara, CA, USA) and each simulation was done using MPI with 8CPU, unless otherwise stated.

2 Theory

2.1 Explicit and implicit solvers

Differential equations, such as the equations of motion, can be solved by analytical or numerical methods. The exact solution can be obtained analytically for simpler problems, however in real problems this is rarely an option. Instead the equation is discretized in time and solved for numerically (e.g. FEM) at each time step by using either an explicit or an implicit solution strategy. To highlight the difference between these solvers a simple example, which is commonly used when discussing explicit and implicit methods, is presented. Consider the following ordinary differential equation (ODE) with initial values:

Find $x = x(t)$ such that

$$\begin{cases} \dot{x} = f(x, t) \\ x(t_0) = x_0 \end{cases} \quad (2.1)$$

If time, t , is discretized as $t \in [t_0, t_0 + \Delta t, t_0 + 2\Delta t, \dots, t_0 + n\Delta t]$, the differential equation above can be rewritten in a discrete time equivalent form as

$$\dot{x}_n = f(x_n, t_n) \quad (2.2)$$

The derivative at a given step n can be approximated as

$$\dot{x}_n = \frac{x_{n+1} - x_n}{\Delta t} \quad (2.3)$$

which makes it possible to rewrite Equation 2.2 on the following form

$$\frac{x_{n+1} - x_n}{\Delta t} = f(x_n, t_n) \quad (2.4)$$

$$x_{n+1} = x_n + \Delta t f(x_n, t_n) \quad (2.5)$$

Since the current step is known the proceeding step in the calculation can be solved for *explicitly*. This method is called *Forward Euler's method*, or simply Euler's method, and presents the simplest explicit integration scheme [29]. Now considering the same ODE but changing the approximation of the derivative at a given step n as

$$\dot{x}_n = \frac{x_n - x_{n-1}}{\Delta t} \quad (2.6)$$

it is possible to rewrite Equation 2.2 on the following form

$$\frac{x_n - x_{n-1}}{\Delta t} = f(x_n, t_n) \quad (2.7)$$

$$x_n = x_{n-1} + \Delta t f(x_n, t_n) \quad (2.8)$$

By reindexing n this can be rewritten as

$$x_{n+1} = x_n + \Delta t f(x_{n+1}, t_{n+1}) \quad (2.9)$$

Since only the current step is known, and x_{n+1} appears on both sides of Equation 2.9, the proceeding step in the calculation depends *implicitly* on this equation. This method is called *Backward Euler's method* and is the simplest implicit integration scheme. The solution to Equation 2.9 normally needs to be found iteratively by e.g. the Newton-Raphson method [29].

The two examples presented highlights the major differences between an explicit and an implicit solver. Namely that for an explicit solver you always get the next step directly by solving a simple equation while for an implicit solution you need to solve (possibly) multiple iterations involving inversion of large matrices before convergence is met. This means that for each step in the simulation the implicit solver takes more time to compute the result. However, the implicit solver is unconditionally stable while the explicit solver is not. This means that the implicit solver has the possibility to take significantly larger time steps compared to the explicit

solver, resulting in a shorter total time even though each individual step takes longer time to compute. Explicit solvers handles nonlinearities with relative ease since the time step is already very small but for implicit solvers this becomes a problem. If the implicit solver is to capture highly nonlinear responses the time step needs to be reduced in order to find a converged solution. This means that the advantages of having a long time step in order to save computational time is no longer possible to maintain. In general the trade-off between advantages and disadvantages for the two solution methods result in implicit solvers being used for static or slower dynamical simulations while explicit solvers are used for high speed, short duration and highly nonlinear simulations. For example, in this thesis a commercial software called LS-Dyna (LSTC, Livermore, CA, USA) is used to solve the motion equations numerically. The software uses an explicit solver which is based on a version of the central difference theorem to determine accelerations and velocities in dynamic simulations [20].

As already mentioned the explicit solver has a limit on the time step in order to obtain a stable solution. This is called the *Courant-Friedrichs-Lewy condition* (CFL) [5] which states that for each (x,t) the mathematical domain of dependence is contained in the numerical domain of dependence [30]. This means that if the amplitude of a wave, moving through a discrete spatial grid, is to be computed at discrete time steps of equal duration the time step need to be longer than the time it take for the wave to move between adjacent grid points. For an explicit FE problem this condition puts a hard limit on the time step as the time it takes for a sound wave to travel across an element. In the case of a 3D continuum this can be calculated as

$$c = \frac{E(1 - \nu)}{(1 + \nu)(1 - 2\nu)\rho} \quad (2.10)$$

$$\Delta t = \frac{l}{c} \quad (2.11)$$

where c is the wave speed and l is the length of the element [20]. From Equation 2.10 and Equation 2.11 it is clear that fine meshes, stiff materials and low densities will increase the total simulation time.

2.2 Calibration

In model calibration the problem is to find a set of model parameters p that minimise the difference between test data \mathbf{y} and the model response $\mathbf{f}(t, \mathbf{p})$. This can be done by various methods dependent on the characteristics of the model and the available computational resources. In general, the problem can be formulated as a minimisation of a goal function $Q(p)$, as in Equation 2.12:

$$p^* = \underset{p}{\operatorname{argmin}} [Q(p)] \quad (2.12)$$

Typically this minimisation is solved by a sequential optimisation algorithm or a single iteration method, both will be explained in brief below. It can consist of one goal or several sub-goals, common constructions are as the sum of squared residuals (SSR), a root-mean-square value (RMS) [29], or by the Objective Rating Method (ORM) [11]. Below is an example of a goal function expressed as a SSR (Equation 2.13) where n is the number of data points.

$$Q(p) = \sum_{i=1}^n r_i^2 = \sum_{i=1}^n (y_i - f_i(t, \mathbf{p}))^2 \quad (2.13)$$

See Section 2.2.4 for more explanations of goal functions.

2.2.1 Sequential Methods

The Gauss-Newton method is a sequential algorithm that evaluates a Taylor expansion of the goal function to find extreme values (minima/maxima). $Q(p)$ is differentiated with respect to p and solved at zero, the partial derivative is denoted $\mathbf{J}_k = \partial Q / \partial \mathbf{p}$ [29]. The algorithm usually needs an iterative solution strategy in non-linear problems and faces the risk of finding local minima instead of global minima. Many strategies such as the Levenberg-Marquart, Steepest descent, and Conjugate gradient search methods have been developed to improve the performance of the original Gauss-Newton method [8]. Below, in Equation 2.14, the foundation of

non-linear least squares is given as an example of problems that can be solved with the Gauss-newton method (the initial guess is marked with an index k) [8].

$$\begin{aligned}
0 = \frac{dQ(\mathbf{p})}{d\mathbf{p}} &= \sum_{i=1}^n r_i \frac{\partial r_i(\mathbf{p})}{\partial \mathbf{p}} \approx \sum_{i=1}^n \frac{\partial r_i(\mathbf{p}^k)}{\partial \mathbf{p}} \left(y_i - f_i(t, p^k) - \sum_{i=1}^n \frac{\partial r_i(\mathbf{p}^k)}{\partial \mathbf{p}} (\mathbf{p} - \mathbf{p}^k) \right) \quad (2.14) \\
&\implies (\mathbf{J}^T \mathbf{J})_k \Delta \mathbf{p}_k = \mathbf{J}_k^T \Delta \mathbf{y}_i \\
&\implies \mathbf{p}_{k+1} = \mathbf{p}_k + (\mathbf{J}^T \mathbf{J})_k^{-1} \mathbf{J}_k^T \Delta \mathbf{y}_i
\end{aligned}$$

The equation has to be solved iteratively until a certain criteria is met, for example when the function value changes less than a certain percent per iteration. The major disadvantage of the Gauss-Newton method is its inaccurate performance if the initial guess is far from the optimum, or if the chosen parameters have little influence on the goal function. That is because the method is built around the idea to find a zero derivative of the goal function in its parameters, thereby all local minima satisfies the equations [8]. The derivative will be close to zero, also if a parameter have no influence on the goal function, whereas no useful information can be calculated. This concept is refereed to as the sensitivity of a parameter. It can be measured with sensitivity measures such as the ANOVA (ANalysis Of VAriance) [29] or GSA (Global Sensitivity Analysis). Both are statistical methods using the concept of variance to analyse the variation of outputs as a consequence of varying the inputs of a model [21].

2.2.2 Single Iteration Methods

The other alternative in calibration is the single iteration-, or design of experiments (DOE) method. Its main idea is to set up a number of experiments with parameters varied such that the desired model variations can be observed. To do so, one has to construct a test matrix of varied parameters that maximises the probability of capturing the model behaviour. This can be done with different methods dependent on the initial knowledge of the model and computational resources. One method is the full factorial design that produces a matrix with each possible combination of parameter variations, see Figure 2.1a. This method requires that the parameters are discrete or divided into discrete subsets and will easily result in a large number of experiments. The number of experiments (n) can be calculated as $n = x^y$, where x is the number of variations per parameter and y is the number of parameters [8]. Another method is to simply distribute the parameters randomly. This makes it possible to choose the number of experiments, but has the downside that two parameters can end up close to each-other and therefore not provide useful information about the model variation, see Figure 2.1b. A better method is the Latin Hypercube Sampling (LHS) method, which distribute parameters on non-overlapping equally probable intervals and then selects points in each interval on the basis of a given probability distribution [8]. In multivariate problems, the selection can be done randomly, or by more sophisticated methods such as the maxi-mini method, which is an optimisation that maximises the minimal distance between the selected points, see Figure 2.1c. In either of the selection methods one parameter per interval is chosen. The maxi-mini method can also be used directly as a method to design a parameter space. Then the parameters are first distributed randomly and then moved according to the maxi-mini goal with some sequential optimisation algorithm [21]. LS-OPT uses an algorithm called simulated annealing which is a derivative-free method of finding a global minima/maxima [21], see Figure 2.1d.

2.2.3 Metamodelling Techniques

It can sometimes be useful to build a less complex surrogate model of the input-output relationship obtained by varying model parameters \mathbf{p} in a complex model. The surrogate model, also called a metamodel, can be constructed by different methods to capture trends and perform statistics on a set of results. A powerful tool is regression analysis, which is fitting a linear model to the input-output relationship and calculating statistics, such as the sum of squared residuals or R^2 -values, which quantify trends in the model response and makes it possible to understand how to make improvements in the model [21]. Linear regression is useful if the response of the model is linear in its parameters. In case $Q(\mathbf{p})$ is non-linear, other techniques are used. One is to fit polynomials to the response data, which has the drawback that the analyst has to choose the polynomial order[21]. Therefore it is common to use other types of basis functions to construct metamodels. One popular methods are neural networks with Radial Basis Functions (RBF) summed together [23]. The most general

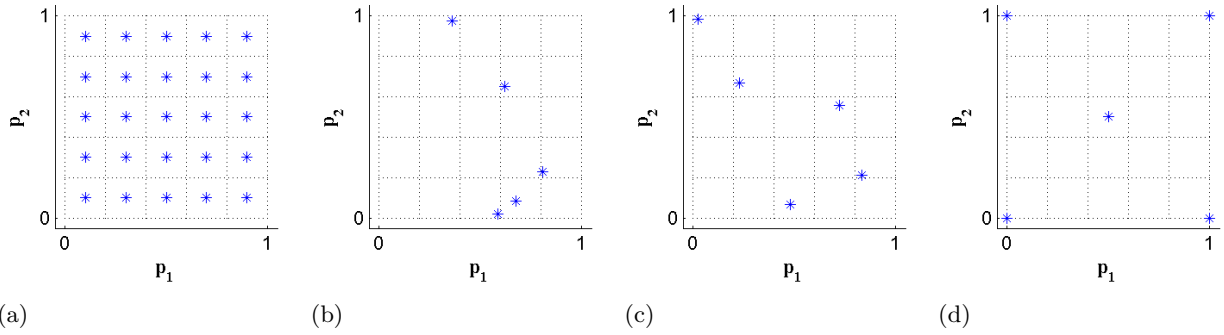


Figure 2.1: *Parameter space sampling methods: (a) Full Factorial, (b) Random, (c) Latin-Hypercube, (d) Maxi-mini with simulated annealing*

form of a RBF can be stated as

$$h(\mathbf{p}) = \phi\left(\frac{(\mathbf{p} - \mathbf{p}_i)^T(\mathbf{p} - \mathbf{p}_i)}{r^2}\right) \quad (2.15)$$

where \mathbf{p} is the function variables, p_i is the tested parameters (or centres), r^2 is the euclidean distance squared and ϕ is the basis function. Some common basis functions ϕ are: Gaussian- ($\phi(z) = e^{-z}$), multiquadratic-, inverse multiquadratic- and the Cauchy function [23]. Finally the metamodel is constructed with the RBF:s added together as a weighted sum, which is called a radial basis network.

$$f(\mathbf{p}) = \sum_{i=1}^n w_i h_i(\mathbf{p}) \quad (2.16)$$

To find the appropriate weights, a sequential optimisation can be used to minimise a cost function that describes the difference between the metamodel $f(\mathbf{p})$ and the test data $y(\mathbf{p})$. Typically this cost function is minimised by a Gauss-Newton algorithm [23]. Many additions and variations are available to improve and adjust the performance of the RBF-networks, for example an additional linear term which is used in LS-Opt [21].

2.2.4 Calibration Of Goal Functions

When assessing if a good fit between the reference and response curve has been obtained, several different measurements can be taken into account, e.g shape, amplitude, frequency etc. Depending on the calibration objective the importance of different measurements can then be weighed to create the best fit for the current problem. For example, a standard RMS comparison can lead to a fairly good RMS value for two curves with similar amplitude and low frequency behaviour even though the response curve includes a lot more high frequencies than the reference. This would result in a response which has a mean value that follows the reference well but with an added variation on top of the mean value. For some systems this might not be a problem and the result is taken as a good fit, for other systems the high frequency behaviour might be completely unphysical and make the parameter setting useless. An alternative method to RMS for mathematical comparison of different curves, where both shape and amplitude is considered, is the Objective Rating Method (ORM) function [11]. This function is defined as

$$ORM = 1 - \sqrt{\frac{\int \left(\max(|r(t)|, |c(t)|) \times \left(1 - \frac{\max(0, r(t) \times c(t))}{\max(\delta, r(t)^2, c(t)^2)} \right)^2 \right) dt}{\int \max(|r(t)|, |c(t)|) dt}} \quad (2.17)$$

where r and c are abbreviations for reference and comparison respectively and δ is a small value used to avoid division by zero. If the goal is to find the best fit for multiple objectives simultaneously the separate measurements can also be grouped as

$$ORM_{group} = 1 - \sqrt{\frac{\sum (W \times (1 - ORM)^2)}{\sum W}} \quad (2.18)$$

where W is a weight factor which sets the contribution of each ORM value to the grouped value. The results range from 0% to 100%, where 100% represent a perfect match.

When trying to calibrate unstable systems with non-linear responses it can also be of extra interest to target the high frequency content of the response curve. An option is then to transform the response curves from time domain to frequency domain via Fourier transform [29] defined as

$$F(\omega) = \mathcal{F}(f(t)) = \int_{-\infty}^{\infty} f(t)e^{-i\omega t} dt \quad (2.19)$$

This makes it possible to assess the frequency content in both the reference and response curve respectively. To assess the fit between the frequency contents an ORM function can be used to compare the curves. Combining this measurement with an RMS-value of the difference between the reference and response curve, via Equation 2.18, makes it possible to individually weight the importance of each output so that an adequate trade-of between all the responses can be obtained.

2.3 Musculoskeletal Model

The active muscle model package developed by Östh (2014) [35] consists of beam muscle elements modelled with the LS-Dyna material model, *MAT_MUSCLE material (type 156) [19], and a feedback control system which utilises PID controllers to activate the muscles. A brief description of the muscle material model and neuromuscular control system are described in the following sections.

2.3.1 Hill-Type Muscle Model

When performing a movement or maintaining a posture the central nervous system (CNS) activates the muscle fibres to generate a force along the muscle which are connected to skeletal parts in the body. The force makes the skeletal structure execute the task at hand by bending a joint or counteract an applied force, for instance. The Hill-type muscle model used in the SAFER AHBM represents a force generating muscle connected between two points [33]. The Hill muscle model is a purely phenomenological model and of relatively low complexity, compared to more advanced cross-bridge (biochemical) models. It has been shown to be suitable for transient events as it provides accurate force response in a wide range of conditions [3]. The mechanical properties of the muscles are described by three elements, see Figure 2.2; The Parallel Elastic (PE) element representing stiffness of the passive muscle tissue; The Series Elastic (SE) element representing the tendon stiffness by which the muscle is connected to the bone structure; and the Contractile Element (CE) representing the active force which the muscle generate when activated by a nervous stimulation. The contractile force of an individual muscle element is defined as

$$F = N_a(t)f_l(t)f_v(t)F_{max} \quad (2.20)$$

where F_{max} is the maximum contractile force that the muscle can generate, f_l and f_v are scale factors that are functions of the current muscle length and shortening velocity and N_a is the muscle activation level, $N_a \in [0, 1]$. The response of this muscle element is highly non-linear since the PE element has a non-linear stiffness characteristic as well as a rate dependent term to model its viscoelastic properties. At the same time the CE element is a function of $N_a(t)$, $f_l(t)$ and $f_v(t)$ where both the force-length and force-velocity relations are non-linear, see Figure 2.3.

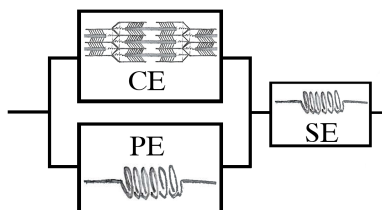


Figure 2.2: *Hill-type model representation, reprinted from [35] with permission.*

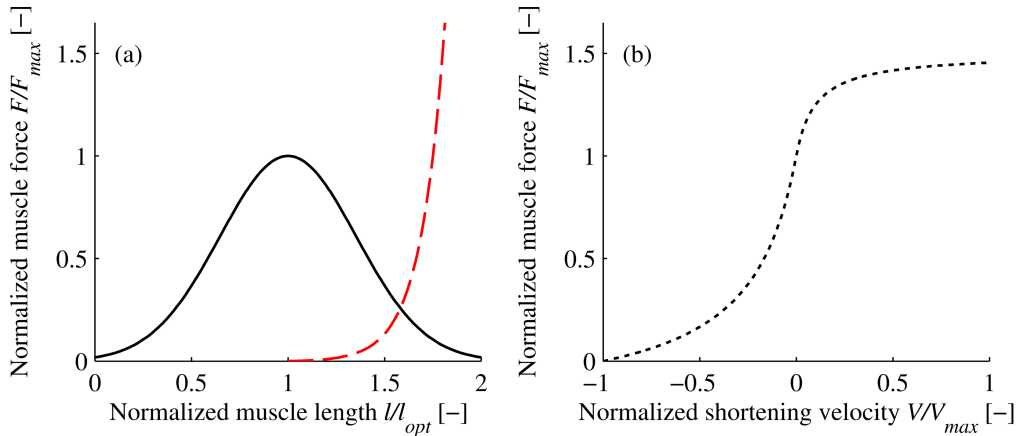


Figure 2.3: *Normalised force-length and force-velocity curves, reprinted from [35] with permission.*

2.3.2 Neuromuscular Feedback Control System

A feedback system refers to two (or more) dynamical systems connected in such a way that each system influences the other and that their dynamics are coupled [34]. A closed-loop feedback control system uses continuous measurements of the output signal of the system $y(t)$, to compute a control signal $u(t)$, by comparing the output signal to a reference signal $r(t)$. The error between the current state of the system and the desired state is hence computed as

$$e(t) = r(t) - y(t) \quad (2.21)$$

and works as an input to the regulator which computes the control signal.

A general feedback control system consists of a regulator and a system that is controlled, usually this is a dynamical system. Disturbance to the system dynamics and delays of the measured output signal can be added to further mimic the reality. If the disturbance to the system makes the output signal deviate from the desired reference signal, the task for the regulator is to compensate the system with a controlling signal such that the desired output is achieved. For a stable dynamical system with small delays and not too large disturbances this is normally not a difficult task. However, if the dynamical system in itself is unstable or the signal delay is significant, even the smallest of disturbances can be enough to make a stable control impossible. The regulator is commonly modelled as a proportional-integral-derivative (PID) controller [34]. The control signal, is then formed entirely from the error, $e(t)$, by the sum of three terms as

$$u(t) = K_p e(t) + K_i \int_0^t e(\tau) d\tau + K_d \frac{de(t)}{dt} \quad (2.22)$$

The control implemented in the SAFER AHBM is based on a closed-loop feedback control with a PID-regulator, see Figure 2.4. Identifying the different components in a classical feedback control system, the controller is the CNS, the musculoskeletal models are a part of the dynamical system (HBM) and the neural delay is the time it takes for the CNS to perceive the posture and position of individual limbs. For this specific feedback system, the output signals $y(t)$ are measured as joint angles and the input signal $r(t)$ is reference joint angles. Due to the time needed for a nerve signal to go back and forth to the CNS, T_{de} , the output signal is delayed, $y_d(t)$, before the error is computed as

$$e(t) = r(t) - y(t - T_{de}) \quad (2.23)$$

The SAFER AHBM has seven PID-controllers, one for the lumbar back, one for the cervical spine, one for the head, two for the shoulders and two for the elbows. The angles are measured both between internal points within the SAFER AHBM model and against a vertical axis. The purpose of the choice of controllers is to achieve posture control and a biofidelic response of the SAFER AHBM in pre-crash events. A figure explaining the individual controller locations and measured angles can be seen in Figure 2.5

The activation signal computed by the PID-regulator, $u(t)$, goes through a model for the muscles activation dynamics, to compute $N_a(t)$, before being sent to the muscle material model. The muscle activation dynamics

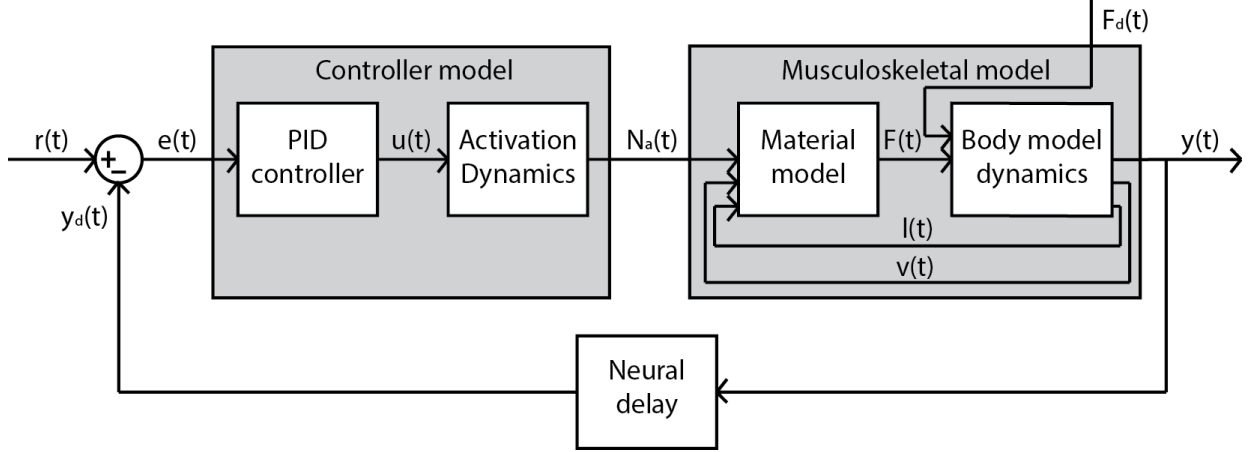


Figure 2.4: Closed-loop feedback control system of the musculoskeletal model.

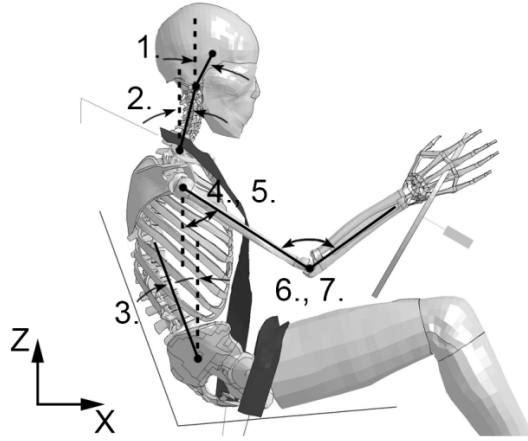


Figure 2.5: PID-controller angle definitions. The head (1), cervical spine (2), lumbar (3), and shoulder (4, 5) angle controllers all use the angle of the body part with respect to the vertical axis, while the elbow (6, 7) controllers utilise the relative angle between the corresponding humerus and ulna. Soft tissues of the trunk, neck, and upper extremities are not shown. Reprinted with permission from [35].

are represented by two low-pass filters in series, one for the intermediate neural excitation level $N_e(t)$ and one for the activation level $N_a(t)$ representing the muscles contraction dynamics [32].

$$T_{ne} \frac{dN_e}{dt} = u(t) - N_e(t) \quad (2.24)$$

$$T_{na} \frac{dN_a}{dt} = N_e(t) - N_a(t) \quad (2.25)$$

The contraction dynamics have different time constants if the muscle is tensing or relaxing so T_{na} is split into two, T_{naa} for activation and T_{nad} for deactivation. Depending on the muscles current length l and shortening velocity v the material model computes a force, $F(t)$, for the resulting activation level which combined with a potential disturbing force, $F_d(t)$, gives a moment to the joint. In this model the derivative part of Equation 2.22 is also filtered by a low-pass filter of first-order with a time constant, T_f , which smoothens and delays the activation signal as

$$T_f \frac{d^2 e_f(t)}{dt^2} = \frac{de(t)}{dt} - \frac{de_f(t)}{dt} \quad (2.26)$$

where $e_f(t)$ is the filtered signal [32].

3 Positioning

A method for positioning numerical HBMs (in this thesis the industry version of THUMS) has been developed to facilitate positioning and posture adjustment for a specific test of interest. The test environment can be a belted occupant in the seat of a car, a test setup on an impact sled, or any environment that represents the boundary conditions of interest in an analysis of the human body. Since the original posture of the HBMs are not always suitable for all types of tests, an easy to use and fast method is needed to be able to obtain useful results for various testing environments. This section describes the developed method, which is named the Prescribed Displacement method, exemplifies how to use it for in seat- and in space- positioning, and compares it with an existing method developed by David Poulard and a group of researchers at the University of Virginia (2014) [26].

Review of Existing Methods

A few different methods to personalise an HBM position and posture are used today. The first is to simply change the coordinates of the associated parts. Practically this can be done by defining rotation centres in natural joints, e.g. rotating an entire leg around a defined axis through the rotation centre of the hip. A new model can be saved when the desired posture is obtained. However, since the joints lack a well defined rotational axis in biofidelic FE models such as THUMS, the drawback is a high risk of mesh distortion when the rotation is applied. This method is instead better suited for ATD models since they have well defined rotational joints and is commonly used today. Tools utilising the joint rotation and translation method for positioning are available in software, such as Ls-PrePost [7] and Oasys PRIMER [22]. Attempts to use the joint rotation transformation methods together with computer graphic algorithms, such as OpenGL, to morph the mesh, have been evaluated by Jani et al. (2012) [14]. Their method permits control over joint angles, such as the knees, but also face a risk of distorting the FE-mesh in critical areas around the modified joints. Therefore, post positioning mesh smoothing is sometimes necessary to obtain adequate mesh quality. A similar approach was suggested by Desai et al. (2012) [6], utilising rigid body joint rotations together with a local dual Kriging algorithm to smoothen the FE-mesh at critical areas. Both the method by Jani et al. and Desai et al. have the advantage that they can be set up and solved in a pre-processor, without solving FE-equations, but at the same time, the disadvantage that there is a risk of model distortion and unphysical geometries. Both methods require knowledge of correct anatomy and handling of mesh smoothing algorithms, such as the local dual Kriging method, which can be complex for the user.

Another method is to set up a simulation with boundary conditions and loads which force the HBM into the desired position. HBMs consist of many deformable finite elements in various parts with different material properties, each connected together with constraints or penalising contact definitions. This means that no other posture can be obtained without introducing stresses and initialising contact forces in the model. Conducting a simulation based positioning with applied forces will move the positioned state away from the initial point of equilibrium and hence initialise internal stresses. This means that the model will try to spring back to an equilibrium state as soon as the positioning constraints are released, assuming that the material model used is partly an elastic material. The advantage of this method, when it comes to FE HBMs, is that the risk of distorting the FE-mesh is lower. The disadvantage is that it takes longer time to set-up and simulate, compared to applying a rotation at a specified joint.

One version of the simulation method has been developed by Poulard et al. (2015) [26] in a study to compare and validate pre-impact postures of THUMS against Post-Mortem Human Subjects (PMHS). Their method, which is sometimes called a Marionette method, utilise cables and dampers which pulls the body parts of THUMS to a specified goal position, see the following section for further details. LS-PrePost includes an application, called "THUMS positioning", for positioning the THUMS model through a simulation based method which is similar to Poulard et al.'s [18]. Finally, another simulation based method, which can be used to obtain a seated version of HBM models, is to apply translations and rotations to the HBM to get it close to the desired position above the seat and then start a simulation with a gravitational load pulling the HBM down into the seat. This method is referred to as seat drop-down, and has the advantage that it is easy to set up, but it lacks in precision and repeatability. In Table 3.1, a subjective comparison between the different methods is given to clarify their differences.

The European Commission is currently funding a project on the subject of HBM positioning and scaling, called the PIPER project (Position and Personalise Advanced Human Body Models for Injury Prediction). It has the objective to develop new tools to position and personalise advanced HBMs to be used in R&D by 2017.

The methods researched upon is built around ideas to be able to adopt HBMs to personal geometrical variations and postures of human subjects through pre-processor simulations. This includes adaptive re-meshing to avoid mesh distortion during the positioning phase as well as the possibility to scale the model in order to obtain various body types, e.g. short, tall, fat, skinny, young or old. The project was launched in 2013 and has a budget of 4M €[24].

Table 3.1: Subjective comparison of methods to adjust the position and posture of HBMs

Method	Setup time	Computational time	Postural changes	FE-mesh compatible	Precision
Whole body Translation and Rotations	<i>fast</i>	<i>fast</i>	<i>no</i>	<i>yes</i>	<i>good</i>
Joint angle modifications	<i>fast</i>	<i>fast</i>	<i>yes</i>	<i>no</i>	<i>good</i>
Joint angle mod. & FE-mesh smooth	<i>slow</i>	<i>fast</i>	<i>yes</i>	<i>yes</i>	<i>good</i>
Marionette method	<i>slow</i>	<i>slow</i>	<i>yes</i>	<i>yes</i>	<i>moderate</i>
Seat drop-down	<i>medium</i>	<i>slow</i>	<i>yes</i>	<i>yes</i>	<i>poor</i>

Positioning With The Marionette Method

This section describes the Marionette method developed by Poulard et al. (2015) [26] which is later used as comparative data for the evaluation of the method developed in this thesis. In their study, Poulard et al. used six PMHS' to test their method of positioning the THUMS using pulling cables attached to the pelvis, L3, T11, T6, T1 and head. The qualitative measures used to evaluate the results focused on geometrical differences in the spinal posture of the THUMS and the PMHS by measuring the models lean angle, error in position and error in angle, see Figure 3.1 and Table 3.2. In the study conducted by Poulard et al. the geometries of the PMHS' spines were also scaled lengthwise with the angles between the vertebral bodies (T1, T6, T11, L3) and pelvis kept constant. This was done to match the size of the THUMS' spine, since all the individual PMHS' had different anatomical sizes. The scaled PMHS positions are called the normalised postures and was used as goal positions when setting up the pulling cables. Using the Marionette method they achieved a near perfect fit of lean angle $0.1 \pm 0.1^\circ$ but still reported some errors in position and angle for all body segments combined, 7.67 ± 1.49 mm and $4.7 \pm 0.8^\circ$ respectively [26].

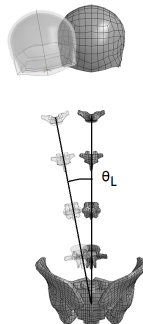


Figure 3.1: Lateral lean angle, θ_L , between a vertical axis and the midpoint of the posterior inferior iliac spine and the centre of the T1 vertebral body.

Industrial Demands On The Process

The requirements from Autoliv on the positioning method was that it should be easy to use, that it should minimise the work required by the user, that it should be general in the sense that it is not specific to a certain car, seat or THUMS model, and finally that the simulation time should not exceed an over-night simulation. The term *positioning* mainly refers to acquiring the correct posture of the HBM prior to a certain test. However, industry usually also include concepts such as *seat squashing* and *belt fitting* in this term. Seat squashing is a simulation where the HBM is positioned in the seat so that the equilibrium deformations and element stresses are acquired. This is done in order to start each simulation as close to equilibrium as possible, avoiding an initial settling phase. Belt fitting is a procedure where the belt is fitted on top of the positioned model as close

Table 3.2: Qualitative measures of the difference in posture between PMHS and the THUMS.

Measure	Unit	Explanation
θ_L	$^{\circ} deg$	Lateral lean angle between a vertical axis and the midpoint of the posterior inferior iliac spine and the centre of the T1 vertebral body.
Error Position	mm	The euclidean distance between the the centre of a reference part (head,T1,T6,T11,L3,Pelvis) in the THUMS to the PMHS.
Error Angles	$^{\circ} deg$	The difference in angle of reference parts in the THUMS to the PMHS, measured in the global coordinate system.

to the surface as possible while avoiding initial contact penetrations. Ideally all these steps would be done in one simulation, without input from the user between different steps, so that a complete positioning could be conducted in one go.

3.1 Method

The developed method is simulation based and utilises prescribed nodal displacements that force the HBM into the wanted position, hereby called the Prescribed Displacement method. This chapter explains the method, in which two simulation setups are suggested dependent on if the user wants to position the HBM in a seat or in space. The steps of positioning are explained in the two subsections below. For a complete users guide on how to implement the method; see Appendix A.

Simulation Setup

The Prescribed Displacement method works by prescribing the motion on a set of nodal Degrees Of Freedom (DOF) inside the HBM. In LS-DYNA this functionality is called: *Prescribed Motion Node*. The positioning includes a prescribed motion phase, conducted with a continuous ramp to minimise the risk of numerical instabilities, which sometimes can be caused by sudden discontinuities, and a settling phase where the new position is fixed, see Figure 3.2.

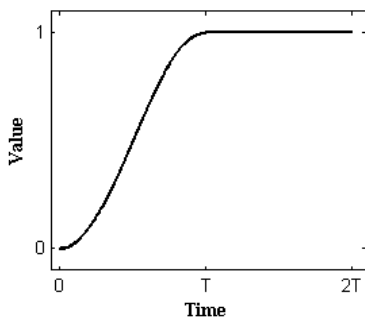


Figure 3.2: Continuous ramp curve defining the prescribed motion in the positioning method (T is the movement phase while $2T$ is the full positioning, including a settling phase).

Setting up a positioning simulation can be split into two steps, when positioning an HBM into a seat both steps are needed but for positioning in space it is sufficient to consider only step two. The first step involves translation and rotation of the HBM into a position where the model is as close to the seat as possible, without introducing initial contact penetrations at any points between the HBM and the seat. The second step is to define the prescribed displacements needed to reach the desired position and to decide which DOFs that should be constrained and which that should be left free. Some constraints can be released at the end of the positioning phase in order to reach a state of equilibrium with minimised internal stresses. This is important since the prescribed motions used to position the HBM can impose unphysical stresses in the model that will make it spring back to a more relaxed state. An example of which body parts and DOFs that have been successfully used with the developed method to position the SAFER AHBM can be seen in Table 3.3. Contact

definitions that might interfere with the positioning, such as the belt and possibly also the steering wheel, should be deactivated during the positioning simulation.

Table 3.3: Simulation times and list of body parts with their corresponding DOFs used in the positioning method. None specified DOFs were kept free during the simulation while DOFs listed under "Release DOF" were prescribed until *Release time* was met. The entire positioning was done during the *Position time* while the rest of the simulation was included for stabilisation.

Prescribed Body part	In seat		Prescribed Body Part	In space	
	DOF	Release DOF		DOF	Release DOF
Hands	x,y,z	-	Hands	x,y,z	-
Feet	x,y,z	x,z	Feet	x,y,z	-
Femoral heads	x,y,z	x,z	Pelvis	x,y	-
Head	x,y	-	Head	x,y	-
Shoulders	y,z	y,z	T1	x,y	-
T1	x,y	x	T6	x,y	-
T8	x,y	x	T11	x,y	-
L2	x,y	x	L3	x,y	-
Position time, T	150 ms			150 ms	
Release time	300 ms			-	
Total time	500 ms			300 ms	
	*Gravity is considered			*Gravity is not considered	

Extracting A New Positioned Model From Simulation Results

When the simulation is finished the obtained nodal coordinates and stresses are saved and updated into a new model. This is done with a script implemented in MATLAB, hereafter referred to as the Post Positioning Script. The Post Positioning Script reads an ASCII formatted result file called *dynain*, which is obtained from the Ls-PrePost software. It copies the nodal coordinates from the saved state in the *dynain* file into the chosen model keyword files, without re-structuring the original file. Also, the initial stresses are included by creating a new keyword file that contains the initial stresses for all elements it finds in the keyword files that the user wants to update. The model with updated nodal coordinates, together with the created initial stress keyword file, makes the new model. When the keyword file containing the element stresses is included in subsequent simulations, the stress state needs to be added in an initialisation phase of the simulation via a special type of algorithm called dynamic relaxation. Dynamic relaxation is an algorithm, similar to FE (see Section 2.1), that uses modal damping and artificial lumped masses to find a state of equilibrium with as few iterations as possible [1]. This is done to ensure that the contact forces build up in equilibrium with the element stresses and to initialise stresses and deformations in such a way that the simulation is able to start from a state of pre-load [18]. For this model, the pre-load is the force built up between the HBM and the seat as well as all internal element forces, e.g. the initial stresses in muscles and the vertebrae that holds the HBMs posture and the internal stresses of the seat cushion.

It is possible to start a simulation directly from a saved state in the *dynain* file without updating the coordinate values of the original file, by including the *dynain* file as an input to the simulation. However, since e.g. belt fitting needs to be done after the positioning is conducted it is important to be able to save a model with updated nodal coordinates so that one can work with the correct geometry. Also, the muscle control system in the SAFER AHBM needs updated reference angles applicable to the new postural position. See Appendix B for the MATLAB code of the Post Positioning Script and for the MATLAB code that updates the reference angles of the muscle control system.

Positioning The SAFER AHBM To Match Voluntary Test Data Of A Pre-Crash Scenario

The SAFER AHBM is positioned in a seat to match the average person that participated as voluntary drivers in a study of an autonomous braking scenario. The study was conducted by Östh et al. (2013) [37], to obtain test data on occupant response and their seated positions. Film-markers were placed on their head, shoulders, sternum, elbows and wrists. These can be seen in Figure 3.3 as boxes representing one standard deviation from the average seated position. The developed Prescribed Displacement method was used to match the

average values of the positions seen in the voluntary study, with the main goal of matching the displacement in longitudinal driving direction (X -direction). The FE model of a vehicle interior equivalent to the one used in the volunteer tests was supplied by Autoliv, to be used in the simulation setups for the present thesis.

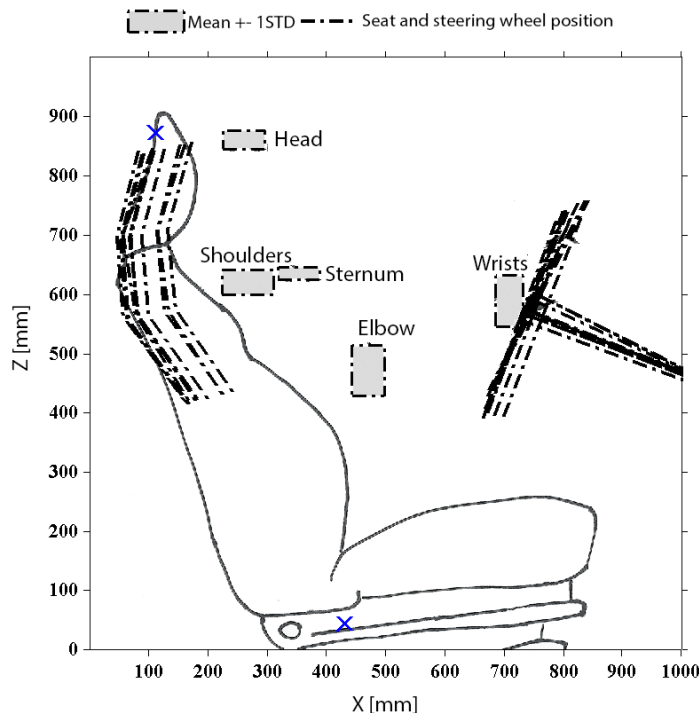


Figure 3.3: Seated position of drivers in a pre-crash scenario [37], boxes mark average ± 1 std of seated positions for head, shoulders, sternum, elbows and wrists.

Positioning Comparison to Previous Method

A positioning, replicating that which was reported by Poulard et al. (2015) [26], was desired in order to evaluate the developed Prescribed Displacement method. However, the article by Poulard et al. does not specify the full three dimensional error in position, nor if the global coordinate system used for measuring error angles is the THUMS'- or the PMHS'-global coordinate system. This means that it is not possible to achieve an exact positioning compared to any of the PMHS' using the reported data. In order to still do a rough evaluation, comparing the two methods and showing the potential of the Prescribed Displacement method, one of the PMHS' was selected (PMHS 1569) as a goal position. Using the figures presented by Poulard et al. the error in lateral direction (Y -dir) and the head error angle (X -dir) was approximated by manual measurements, see Table 3.4 for both Poulard et al.'s reported values and the measured values. The simulation setup utilised these measurements to replicate the normalised PMHS 1569 posture by positioning the SAFER AHBM with the developed Prescribed Displacement method. The measured vertebrae displacements was prescribed in the Y -direction while keeping the X -direction constrained and the Z -direction free. Displacement of hands and feet were constrained in all translational DOFs to keep the model in space. Rotation was only prescribed around the X -axis for head and pelvis while being free for all other segments and directions. The global coordinate system used is a Cartesian coordinate system located so that the X -axis points towards the driving direction, the Y -axis points laterally towards the right side of the HBM and the Z -axis is positive in the direction of gravity. The full simulation setup is presented in Table 3.5.

Table 3.4: Difference in posture between PMHS 1569 and the initial position of the THUMS, as reported by Poulard et al. and as measured from their reported figures.

*Error position is the Euclidian distance including all three dimensions without specifying them respectively. Error angles are defined in either THUMS' or the PMHS' global coordinate system but is not clearly stated.

**Figures only show Y-Z plane so error position was measured in y-direction while error angle was measured as rotation around the THUMS' x-axis. Since vertebrae angles were difficult to measure from the figures only error angle for head and pelvis was included, leaving the remaining rotational DOFs free.

PMHS 1569 vs. THUMS Initial						
Segment	Poulards data*			Measured**		
	Error pos. [mm]	Error ang. X [°] Y [°]		Z [°]	Error pos. y-dir [mm]	Error ang. x-dir X [°]
Head	18.4	0.2	-37.1	-9.9	28.3	12.5
T1	0.0	0.7	-8.4	-11.0	0.0	-
T6	15.5	-2.7	-0.3	2.3	0.0	-
T11	22.5	4.7	-8.4	-3.9	14.1	-
L3	38.4	12.1	-12.2	22.1	24.7	-
Pelvis	73.9	4.0	-5.7	1.3	56.5	0.0
Average	28.1	4.1	12.0	8.4	20.6	-

Table 3.5: List of body segments with their corresponding DOFs used in the evaluation of the developed Prescribed Displacement method. The positioning is conducted by moving each segment the prescribed displacement in 150 ms and then keeping it fixed for another 150 ms. A "-" indicates DOFs which were kept free for the positioning. Gravity was not included.

Comparison setup						
Prescribed Body part	DOF	Prescribed Displacements				
		X [mm]	Y [mm]	Z [mm]	X [°]	
Head	x,y,rx	0.0	28.3	-	12.5	
T1	x,y	0.0	0.0	-	-	
T6	x,y	0.0	0.0	-	-	
T11	x,y	0.0	14.1	-	-	
L3	x,y	0.0	24.7	-	-	
Pelvis	x,y,rx	0.0	56.5	-	0.0	
Hands	x,y,z	0.0	0.0	0.0	-	
Feet	x,y,z	0.0	0.0	0.0	-	
Position time, T	150 ms					
Total time	300 ms					

Mesh Quality Assessment

To ensure that the developed method for positioning does not create large distortions of the FE mesh a study of mesh quality for the model, before and after positioning, was also conducted. Poor quality of the finite element mesh leads to bad accuracy and efficiency for the model and should hence be avoided [15]. The qualitative measures used to evaluate the mesh were aspect ratio, interior angles and element Jacobian, as recommended by Burkhart et al. (2013) [4]. These measurements checks whether the elements have a symmetric shape and possess a positive volume which is crucial to achieve accurate displacement and stress results. The recommended limits are as follows [4]; 1) Less than 5% of the elements should have an aspect ratio above 3, 2) Less than 5% of the triangular/quadrilateral faced elements should have an internal angle deviation that exceeds 60°/70° respectively (minimum angle 30°/20° and maximum angle 150°/160°) and 3) Less than 5% of the elements should have a Jacobian below 0.7, preferably with the smallest Jacobian greater than 0.2.

3.2 Results

Using the developed Prescribed Displacement method the SAFER AHBM was positioned according to the average posture found in an experimental study on driver kinematics in braking events [37]. Using target nodes on the SAFER AHBM on representative locations, all markers could be placed within one standard deviation of the experimental mean value in X -direction. However, since the THUMS has a shorter sitting height (875 mm) than the volunteers (946,5 mm) in the study, the position in Z -direction is slightly lower, see Figure 3.4. From the simulation, both deformations and stresses were extracted from the SAFER AHBM and the seat to be used as starting values for subsequent simulations. With the data resources described in Section 1.4 a full positioning with a short settling phase (total simulation time 500 ms) took approximately 9 hours if only the seat and the SAFER AHBM was included and approximately 21 hours if the positioning was conducted with the full car interior model.

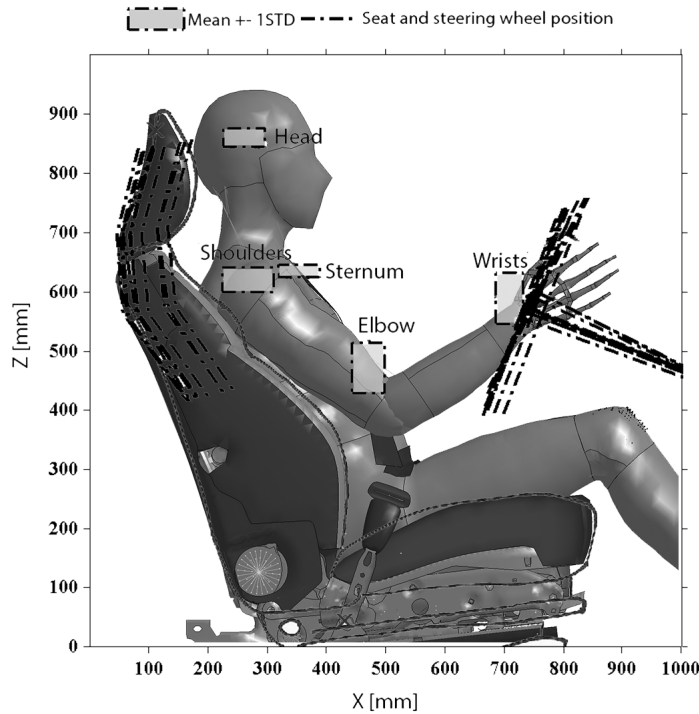


Figure 3.4: *The SAFER AHBM positioned according to the average posture found in an experimental study on driver kinematics [37].*

Results from the positioning done with the Prescribed Displacement method using a measured PMHS position from Poulard et al.'s data [26] can be seen in Table 3.6 and Figure 3.5. The table shows the difference in posture between initial and positioned SAFER AHBM compared to the posture of some selected body segments on PMHS 1569. The measurements used to evaluate the result are *Error in position [mm]*, *Error in angle [°]* and *Lean angle [°]* as explained in the method section. As can be seen from the table the average error in position is 0.3 mm while the head angle error is 0.05°. The lean angle for this position is 6.8°, compared with a lean angle of 6.7° corresponding to PMHS 1569, resulting in an error in lean angle of 0.1°. With the data resources described in Section 1.4 a positioning in space with a short settling phase (total simulation time 300 ms) took approximately 3 hours and 15 min.

Table 3.6: Comparison of the SAFER AHBM and the measured position of PMHS 1569 [26], before and after positioning of the SAFER AHBM with the Prescribed Displacement method. A "-" indicates DOFs which were kept free for the positioning.

PMHS 1569 vs. SAFER AHBM				
Segment	Initial		Positioned	
	Error pos. y-dir [mm]	Error ang. x-dir X [°]	Error pos. y-dir [mm]	Error ang. x-dir X [°]
Head	28.3	12.5	0.0	0.05
T1	0.0	-	1E-6	-
T6	0.0	-	4E-6	-
T11	14.1	-	0.0	-
L3	24.7	-	0.0	-
Pelvis	56.5	0.0	1.9	0.0
<i>Average</i>	<i>20.6</i>	-	<i>0.3</i>	-

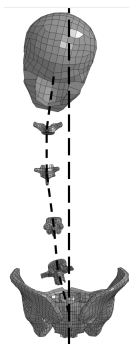


Figure 3.5: The SAFER AHBM positioned according to the measured position of PMHS 1569 from Poulard et al.'s article[26].

Mesh Quality Assessment

After positioning the SAFER AHBM according to the volunteer study and the PMHS 1569 posture, a comparison of mesh quality with the original model was conducted. The results show that both positionings had very little effect on the overall mesh quality with the biggest deterioration being 31 shell elements (out of 86154) falling below the Jacobian limit of 0.7 after a positioning in the seat was conducted, see Table 3.7. The results also show a poor mesh quality for the original THUMS model where almost all indicators fail the limits suggested by Burkhart et al. (2013) [4].

Table 3.7: Mesh quality assessment for the original THUMS model and the positioned SAFER AHBM.

		Original	Seat Pos.	PMHS 1569 Pos.
		[Nr. of failed]	[Nr. of failed]	[Nr. of failed]
Aspect Ratio				
- Max value of 3,	Shell:	5712 ($\approx 7\%$)	5726 ($\approx 7\%$)	5725 ($\approx 7\%$)
	Solid:	20839 ($\approx 32\%$)	20792 ($\approx 31\%$)	20837 ($\approx 32\%$)
Internal Angles				
- Tria faces, $30^\circ \leq \theta \leq 150^\circ$,	Shell:	954 ($\approx 21\%$)	953 ($\approx 21\%$)	956 ($\approx 21\%$)
	Solid:	862 ($\approx 28\%$)	867 ($\approx 28\%$)	863 ($\approx 28\%$)
- Quad faces, $20^\circ \leq \theta \leq 160^\circ$,	Shell:	16 ($\approx 0\%$)	18 ($\approx 0\%$)	16 ($\approx 0\%$)
	Solid:	722 ($\approx 1\%$)	722 ($\approx 1\%$)	721 ($\approx 1\%$)
Jacobian				
- Min value of 0.7,	Shell:	2325 ($\approx 3\%$)	2356 ($\approx 3\%$)	2332 ($\approx 3\%$)
	Solid:	17742 ($\approx 27\%$)	17746 ($\approx 27\%$)	17745 ($\approx 27\%$)

4 Calibration and Validation

This section describes the method used to do calibration and validation of the SAFER AHBM. Four different setups were created in LS-PrePost, to represent a pre-crash with two different belt systems, a frontal crash, and finally a combined pre-crash and crash scenario. The model was calibrated for a pre-crash scenario triggered by autonomous braking with a passive belt system, and validated against a scenario of autonomous braking with an active belt system. Below are descriptions of how the different setups were constructed, followed by a description of the method used in the calibration and thereafter the validation. Focus is put into finding a stable set of parameters for the muscle control system, that minimise the difference between the average volunteer in the test data and the response of the SAFER AHBM.

Pre-crash

The pre-crash scenario only involves driver contacts with the seat, belt and floor respectively (plus a firm grip on the steering wheel). Therefore, the interior model was reduced significantly. The reduction of the model has a large influence on the simulation time, which is important when conducting a calibration study. The setup used includes the SAFER AHBM, seat, belt, floor and a simplified model of a steering wheel, see Figure 4.1. The belt model includes a retractor with a constant force of 3 N, to remove belt slack, and a displacement-force controlled film-spool element that determines the initial belt pay-out. The film-spool element gives a gradually increasing belt force up to 32 mm of belt payout (50 N belt force) after which an increased stiffness locks the belt from being payed out any further. This is done to model the effect of a locked belt-system. From the experiments, a deceleration pulse was extracted representing an autonomous braking event from 70 km/h to 20 km/h in 2.5 s. The calibration simulations were limited to the initial 1.5 s of the autonomous braking event to reduce simulation time, resulting in a speed reduction of 37 km/h, see Figure 4.2.

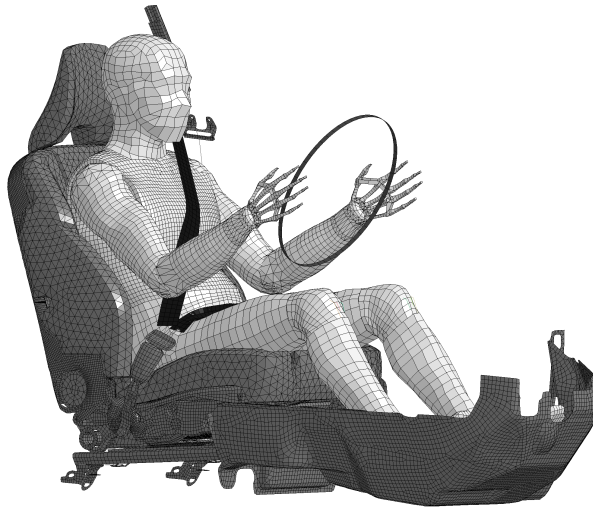


Figure 4.1: *HBM model positioned in seat with floor and simplified steering wheel included for a calibration run of pre-crash simulations.*

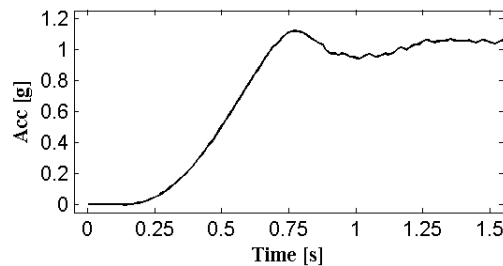


Figure 4.2: *Average autobrake pulse from experimental study by Östh et. al. (2013) [37].*

Crash

Compared to the pre-crash scenario, a crash scenario includes contacts between the driver and the rest of the interior. Hence, for this simulation, the full interior needs to be included, see Figure 4.3. The crash pulse used in the simulation was supplied by Autoliv and is taken from a real world accident of a full frontal impact, see Figure 4.4. The crash pulse is equivalent to a speed change of 72 km/h in 150 ms, resulting in a stopping distance of 1.5 m. The belt geometry is the same as the one used in the pre-crash setup but with some modifications to the retractor, pretensioner and load limiter. The pretensioner is activated 10 ms after the onset of the crash pulse, causing 50 mm of shoulder belt and 45 mm of lap belt to be payed in during the following 8 ms, forcing the driver back and down into the seat. In reality this pull-in is accomplished by a pyrotechnic system that rapidly pulls the seat belt. Once the belt has been pulled in it is locked during the upcoming crash. The load limiter is defined with an upper limit of 4 kN where it fails and allows plastic deformation. This decreases the high load on the ribcage and pelvis, that otherwise could be crushed by the belt system. The airbag is deployed 30 ms after the crash onset in order to catch the head and torso of the driver during deceleration.

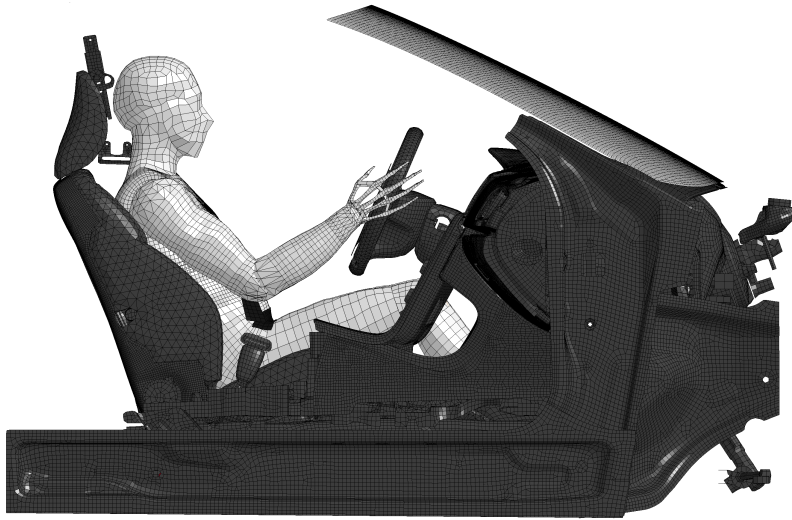


Figure 4.3: *SAFER AHBM model positioned in full interior model for a crash simulations.*

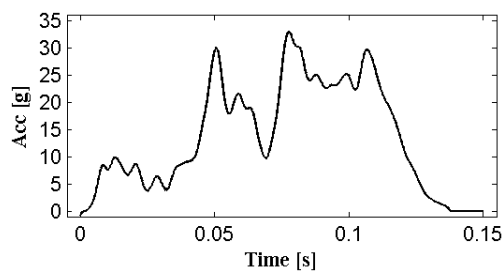


Figure 4.4: *Real world crash pulse from a full frontal impact in 72 km/h.*

Full crash scenario

The full crash scenario includes both a pre-crash (braking) and a crash. This simulation is meant to replicate a real world accident were the driver brakes from approximately 110 km/h to 72 km/h in 1.5 s and then does a full frontal impact where the vehicle makes a complete stop in 150 ms. The setup is the same as the one used for the crash scenario, see Figure 4.3, but with modified timings to allow for the pre-crash scenario. The acceleration curve used for the full crash scenario is a combination of the pre-crash curve and the crash curve, see Figure 4.5.

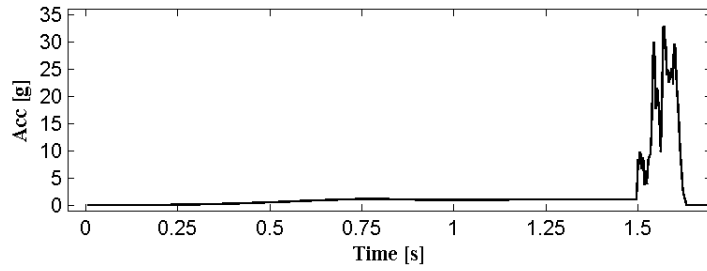


Figure 4.5: *Pulse for a full crash scenario of a vehicle braking from 110 km/h to 72 km/h in 1.5 s and then does a full frontal impact.*

4.1 Method

First, the un-calibrated model was tested in the combined pre-crash/crash to ensure that the simulations could finish with normal termination without causing numerical instabilities or errors. This was done, since the model changes possibly could affect its response. Thereafter, a DOE study was conducted to understand the influence of different parameters on the model response. A second DOE study with contracted variable ranges was run around the best point found in the first DOE study. These two studies are referred to as batch 1 and batch 2, from now on. This strategy was formed, to first widely scope the parameter space and then tune in the area of best solutions. The parameters used are the proportional, integral and derivative constants of the PID-controllers in the muscle control system and the scenario is the pre-crash event with a standard restraint. Finally, once the calibration was done, an attempt to further improve the model response was made by increasing the co-contraction and passive damping of the muscles. These changes were primarily done to counteract the high frequency content of the model response and to improve its stability for varying boundary conditions. After the calibration was done, the SAFER AHBM was tested in a slightly different scenario with an active seat belt pulling, to validate the model.

4.1.1 Calibration

The calibration data was obtained from an experimental study on driver kinematics in autonomous braking events, conducted by Östh et al. (2013) [37]. The data extracted from the study includes eleven male volunteers driving a passenger car on ordinary roads, being subjected to autonomous braking events with standard restraints. The test vehicle used in the experiments was a Volvo V60 T4, model year 2012, in which the seats had leather upholstery. The volunteers were allowed to partially adjust the driver seat and steering wheel to find a comfortable position. In each test film markers were attached to the volunteers to capture the kinematics for head, sternum and shoulder via film analysis. Further, interaction forces for the foot rest, brake pedal, steering wheel, shoulder and lap belt were recorded as well as seat indentations and belt pay-out. The calibration data can be seen in Figure 4.6.

Calibration Goal Functions

The DOE was done using LSTC's software LS-OPT (see Section 1.4), with a single iteration method utilising RBF as the meta-modelling technique, explained in Section 2.2.3 and Section 2.2.4. The objectives when assessing the best parameter combinations were to match the experimental curves of the displacement of the head and sternum together with the axial force in the steering wheel column and seat belt. The curves are presented in Figure 4.6. The match of the curves was quantified utilising normalised RMS-values (NRMS) of the difference between the model response and the experimental curves, with the normalising factor being the RMS value of one standard deviation in the calibration data, see Figure 4.6. This choice of normalising factor has the effect that 0 is a perfect match, 1 is comparable to 1 standard deviation, and higher than 1 is worse than 1 standard deviation.

$$RMS_{norm} = \frac{\sqrt{\frac{1}{T} \int (\bar{y}_{ref} - f(t, \mathbf{p}))^2}}{\sqrt{\frac{1}{T} \int (\sigma_{ref})^2}} \quad (4.1)$$

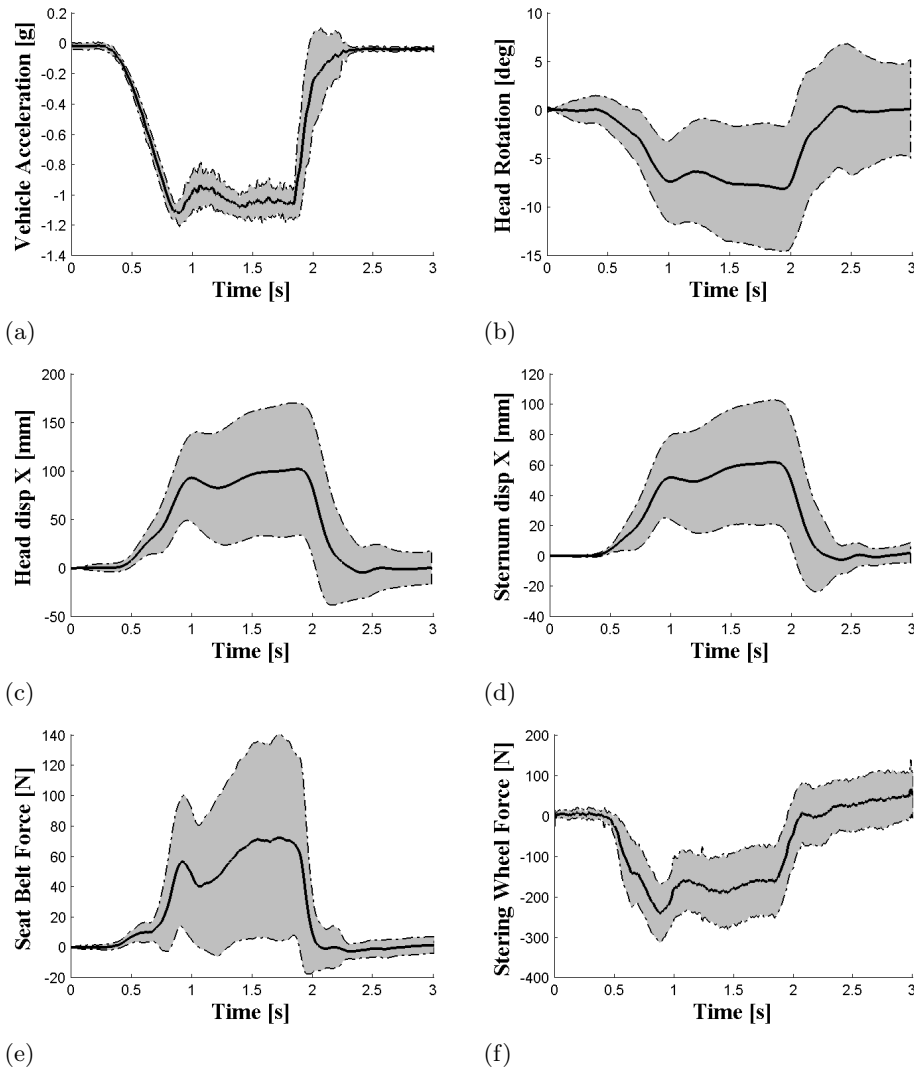


Figure 4.6: Reference curves for calibration. The solid line within the filled area is the mean value \pm one standard deviation. (a) Brake Pulse: Vehicle acceleration [g], (b) Head rotation about the y -axis [deg], (c) Head displacement in the X -direction [mm], (d) Sternum displacement in the X -direction [mm], (e) Change in seat belt force [N], (f) Change in axial steering column force [N]

The model has a tendency to become unstable in the control loop. Therefore, an objective to match the frequency content of the output signals to the frequency content of the reference curves was also added. This was done by evaluating a Fast Fourier Transform (FFT) of the responses and calculating the amplitudes in the range of 1 Hz to 7 Hz, where most of the unwanted behaviour of the instabilities could be characterised. The difference between the frequency content in the model and the experimental curves was also quantified with NRMS values. A combined goal function was formulated as an equally weighted euclidean norm, summarising the NRMS values. It was used to find the best trade-off between each of the measured responses, for further explanation, see Section 2.2.4.

Parameter Sampling

In the first calibration DOE batch, six parameters in the muscular control system was varied in 48 simulations. A maximum of 48 simulations was used because of restrictions on time. To sample the design space a space-filling design with the mini-maxi algorithm solved by simulated annealing was used, see Section 2.2 for further details. The muscle control system in the SAFER AHBM has seven PID-controllers with 3 parameters each, totalling 21 parameters. Therefore, to restrict the 21 parameters to only six, some of the controller gains were linked

together. First, symmetrical control was assumed between the arms, meaning that the parameters of the PID-controllers for the left and right arm were mirrored for the shoulders and elbows, respectively. Secondly, it was noted that the influence on all the goal functions were low for the muscles in the Lumbar back, compared to other muscles in the SAFER AHBM. Therefore the PID-controller parameters in the Lumbar back was not taken into account, and left at their original values. To further limit the number of parameters it was noted, by examination of the response curves in the study by Östh et al. (2013) [38], that the volunteer’s response followed the general shape of the acceleration pulse. This indicates that the volunteers stays at the new equilibrium, reached by the braking event, rather than forcing the body back through the deceleration field before the deceleration has stopped. This, together with the fact that Lennartsson (2002) [17] states that significantly large integral contribution of a PID-controller can lower the stability margins of the system, was used as motivation for constraining all integral gains to be a set scale factor of 50% to the proportional gain. The elbows and cervical spine controllers were seen to have the most significant influence on the response, and was hence left with both proportional and derivative gain as calibration parameters, while head and shoulder controllers were seen to have medium influence on the response, and was hence left with only proportional gain as calibration parameter, see Table 4.1 for the full calibration setup. These phenomena were found by analysing the global sensitivity measure of variance in a calibration study of the SAFER AHBM conducted by Östh et. al. (2011) [38]. The results of the analysis can be seen in Figure C.1 in Appendix C.

Table 4.1: Setup of batch 1 and batch 2 for calibration of PID-controller gains in SAFER AHBM to match volunteer data on driver kinematics in autonomous braking events. Each parameter in the controller model is specified with its initial value and range used in the calibration, C indicates a constant value. The Units are Kp [Nm/rad] Kd [Nms/rad] Ki [Nm/(s rad)], as the torque that the controllers wants to apply to its joint.

Calibration setup	Batch 1			Batch 2		
Calibration Method	Single Iteration			Single Iteration		
Sampling Method	Mini-maxi			Mini-maxi		
Metamodel Method	RBF network			RBF network		
Nr. of parameters	6			4		
Nr. of simulations	48			24		
Nr. of CPU	8 CPU x 3 Nodes			8 CPU x 3 Nodes		
Total Simulation Time	2 weeks			1 week		
Parameters	variable	Init	Range	variable*	Init.	Range
Head Kp	KH	0.86	[0.40 2.50]	KpH	1.100	[0.800 1.50]
Head Ki	0.50*KH	0.43	[0.20 1.25]	C	0.350	-
Head Kd	0.68*KH	0.58	[0.26 1.67]	KdH	0.025	[0.015 0.15]
Cervical spine Kp	KpC	1.30	[0.50 3.00]	KpC	1.350	[1.200 1.70]
Cervical spine Ki	0.5*KpC	0.65	[0.50 3.00]	C	0.670	-
Cervical spine Kd	KdC	0.46	[0.20 1.00]	KdC	0.050	[0.050 0.25]
Shoulders Kp	KS	1.05	[0.00 2.00]	C	0.280	-
Shoulders Ki	0.50*KS	0.53	[0.00 1.00]	C	0.140	-
Shoulders Kd	0.41*KS	0.44	[0.00 0.82]	C	0.110	-
Elbows Kp	KpE	2.00	[1.00 2.50]	C	1.010	-
Elbows Ki	0.50*KpE	1.00	[0.50 1.25]	C	0.510	-
Elbows Kd	KdE	0.06	[0.00 0.50]	C	0.250	-
Lumbar Back Kp	C	1.12	-	C	1.120	-
Lumbar Back Ki	C	0.56	-	C	0.560	-
Lumbar Back Kd	C	0.16	-	C	0.160	-

The second calibration batch was set up considering knowledge gained by the responses seen in the first batch. This was done by selecting the response curves (see Figure 4.6) that insufficiently matched the reference data, as priority for further improvement. An insufficient match was considered if the response curve was outside the corridor of one standard deviation from the average volunteer (NRMS ≥ 1.00). Thereafter, the GSA-measure was used to rank the calibration parameters after the influence they had on the insufficient responses, see Section 2.2.4. This information was used to select four parameters to be further tuned in the second calibration batch, see Table 4.1.

For the final simulations, the best parameter setting found was used to test the effect of increased co-

contraction and passive damping as a way to improve the model stability and to counteract the high frequency content of the response. This was done by altering the head and cervical spine muscles' co-contraction, from 3% to 10%, and passive damping, from 4 [kNs m⁻²] to 200 [kNs m⁻²].

4.1.2 Validation

The validation data was obtained from an experimental study on driver kinematics in autonomous braking events with an active seat belt system, conducted at Autoliv 2013. The data extracted from the study includes three male volunteers driving a passenger car on ordinary roads, being subjected to autonomous braking events. The test vehicle used in the experiments was the same as the vehicle used in the volunteer tests done by Östh et al. (2013) [37], with the addition of an active seat belt. The active seat belt works by generating a force in the seat belt which pulls the driver back into the seat at 600 ms after the autonomous braking event is initiated. In each test, film markers was attached to the volunteers to capture the kinematics of the head and shoulder via film analysis. Further, interaction forces at the foot rest, brake pedal, steering wheel, shoulder and lap belt was recorded as well as seat indentations and belt pay-out. The validation data extracted can be seen in Figure 4.7, together with the curves used for calibration.

For the simulations, the same setup was used as in the calibrations, with the addition of an active seat belt and change of acceleration curve to the one extracted from the validation data Figure 4.7. A *pretensioner element* with a time-force functionality following the mean belt force in Figure 4.7, was included in LS-Dyna to model the active pulling of the seat belt. If, at any time, the seat belt force gets greater than the current force delivered by the pretensioner, a *retractor element* locks. The belt characteristics are then governed by a displacement-force relationship, representing the stiffness of a locked belt system [18]. The simulation outputs, used as reference to determine the model behaviour was: head X-displacement, shoulder X-displacement and seat-belt force as well as frequency content in the outputs. NRMS values were used to quantify the fit of the model response to the validation data. The normalisation factors used were calculated from the standard deviation seen in the validation data.

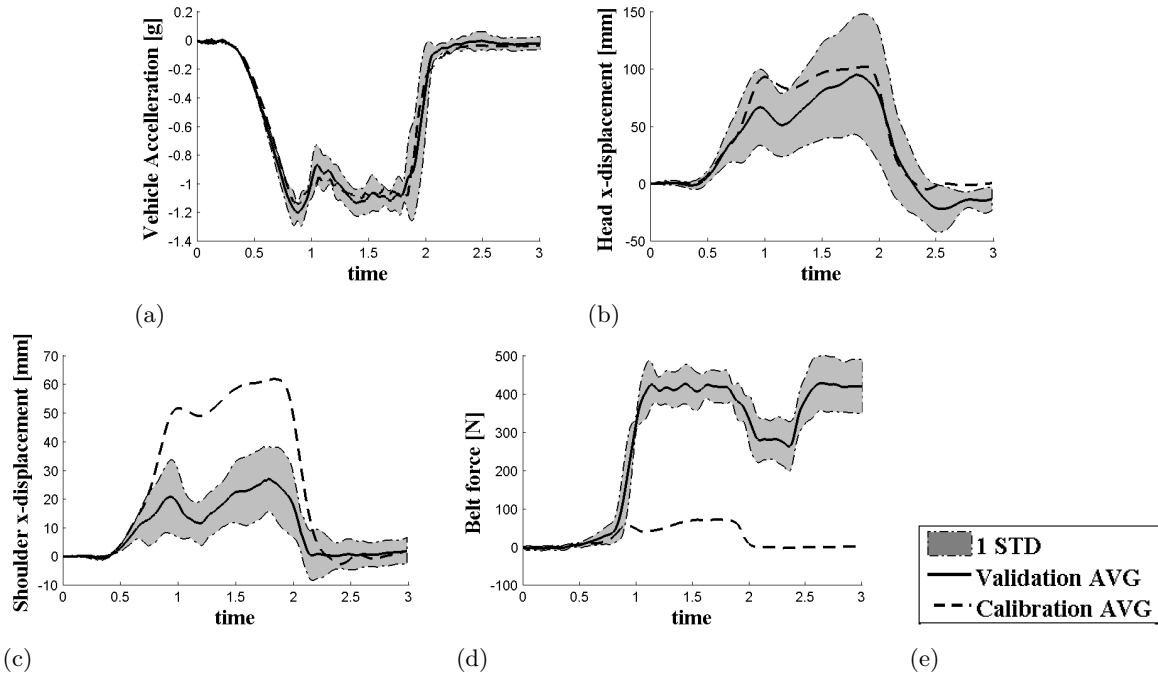


Figure 4.7: Reference curves for validation and calibration. The solid line within the filled area is the mean value \pm one standard deviation from the validation data set, and the dashed line is the mean value from the calibration data set. (a) Brake Pulse: Vehicle acceleration [g], (b) Head displacement in the X-direction [mm], (c) Shoulder displacement in the X-direction [mm], (e) Change in diagonal seat belt force [N]

4.2 Results

The pre-crash, crash, and combined pre-crash crash scenarios were set up and run until normal termination. Solutions to numerical issues have been found and incorporated into the SAFER AHBM. These issues were hourglassing of finite elements, unnecessarily bad scaling properties of some muscle contact definitions, or error terminations due to muscle nodes running through slip rings. For further details, see appendix D. A series plot of the combined pre-crash crash scenario can be seen in Figure 4.8. Thereafter, calibration Batch 1 and Batch 2 were run, resulting in a stable kinematic response within one standard deviation from the average volunteer in all responses, except the response of the head rotation and head X -displacement. The parameter settings resulting in the best response was tested in the validation setup to confirm the calibrated results. Results for both the calibration batches and the validations are given below.

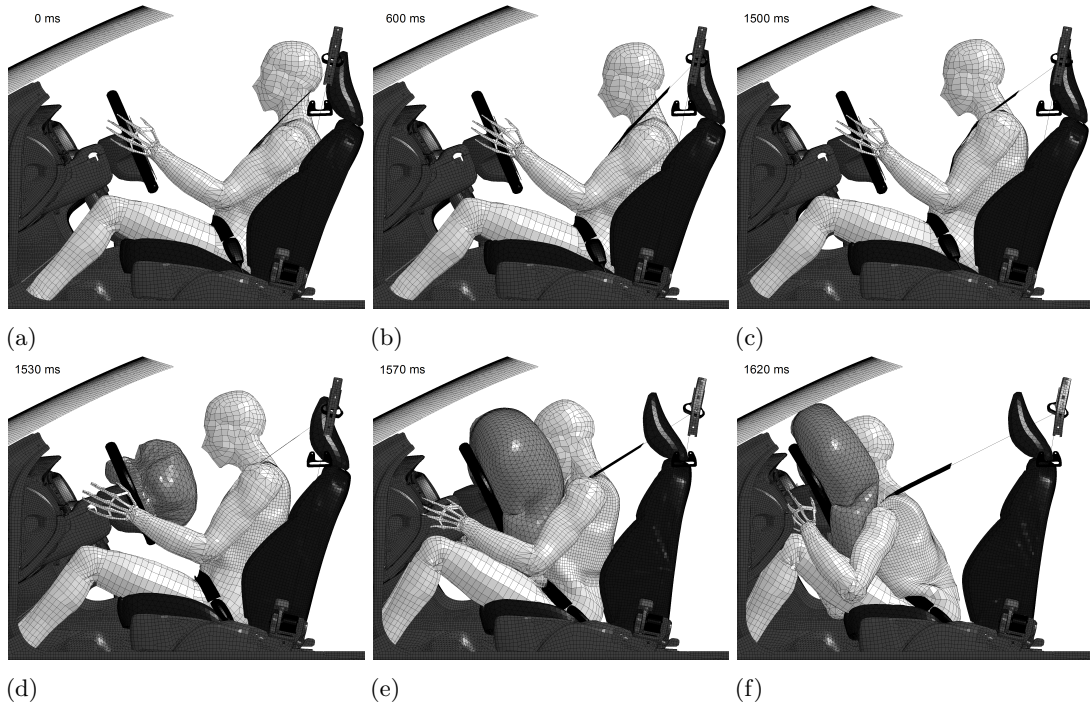


Figure 4.8: *Series plot of the combined pre-crash crash simulation. ((a) 0 ms, (b) 600 ms, (c) 1500 ms, (d) 1530 ms, (e) 1570 ms, (d) 1620 ms)*

Calibration results

When using the computer resources specified in Section 1.4, one calibration simulation acquired 36 hours to complete on eight CPUs, 55 hours on four CPUs or 146 hours on one CPU. Hence, the most efficient setup was determined to be a single iteration method with one simulation per CPU, executing eight jobs in parallel per node. Three computer nodes with eight CPUs each was available for two weeks for Batch 1, totalling 48 calibration simulations, and for one week for Batch 2, totalling 24 calibration simulations, which resulted in a total of 72 calibration simulations.

The first calibration batch were run until normal termination, quantifying the difference between the average volunteer and the SAFER AHBM model for each parameter set. NRMS values, for both the combined and individual goal functions, are presented together with their corresponding parameters in Table 4.2. The combined goal function express how well the tested parameter set performed in terms of trying to fit all the response outputs. The best combined result was achieved by simulation 1.17 scoring a 3.27, which can be compared to the worst score which was 11.42. The average combined value in Batch 1 was 6.06 and one standard deviation was 1.39. Most combinations of parameters were able to match the sternum X -displacement, steering wheel force and seat belt force curves within one standard deviation. However, for the responses measured on the head, few of the tested combinations were able to match within one standard deviation. The response curves for simulation 1.17 can be seen in Figure 4.10.

Table 4.2: Results of calibration Batch 1; showing the tested parameter sets sorted after NRMS values for the seven best and three worst scoring combined values. The following abbreviations are used for the comparative NRMS values: *HR* - Head Rotation, *HX* - Head X-displacement, *StX* - Sternum X-displacement, *SBF* - Seat Belt Force, *SWF* - Steering Wheel Force, *Fr* - frequency amplitude

Batch 1	Parameters							Normalised RMS								
SimID	KH	KpC	KdC	KS	KpE	KdE	Comb	HR	HRFr	HX	HXFr	StX	StFr	SBF	SWF	
1.17	0.71	1.35	0.23	0.28	1.01	0.49	3.27	1.92	2.15	0.19	0.85	0.44	0.22	0.66	0.39	
1.35	0.44	2.91	0.54	0.03	2.45	0.49	3.70	1.65	2.53	0.58	0.65	1.03	0.69	0.78	0.63	
1.20	0.60	2.96	0.26	1.82	1.58	0.44	4.25	1.77	3.27	0.26	0.54	0.65	0.61	0.77	0.82	
1.8	0.40	2.89	0.31	1.05	1.11	0.03	4.27	2.35	2.44	0.68	1.62	0.63	1.15	0.67	0.88	
1.14	0.87	2.92	0.95	0.43	1.01	0.01	4.43	1.65	3.03	0.61	1.43	0.71	1.75	0.65	0.73	
1.30	2.44	0.53	0.34	0.23	1.01	0.48	4.84	0.90	4.05	0.36	0.30	0.64	0.76	0.67	0.90	
1.36	1.17	0.52	0.92	1.22	1.01	0.01	4.90	2.47	3.29	1.07	1.29	0.63	1.27	0.64	0.91	
...																
...																
1.42	2.46	2.94	0.70	0.02	1.76	0.33	7.89	3.08	6.72	0.96	1.16	1.00	1.01	0.75	0.82	
1.34	2.50	1.53	0.98	0.59	1.65	0.50	10.27	3.48	8.43	0.66	1.09	0.84	1.70	0.68	1.42	
1.43	2.31	1.05	0.91	1.95	2.49	0.43	11.42	3.05	9.88	0.58	0.36	0.96	1.52	0.70	1.49	
Normalising factors:								0.07	3e-3	44.8	2.42	26.88	1.50	0.04	0.07	

In Batch 1, the parameters governing the muscle control regulator in the elbow (*KdE* and *KpE*) were found as the most influential parameters for the combined response, with a 37.1% score in the GSA for *KdE* and a 20.8% for *KpE*. Also the score for the parameter *KH* in the head regulator was found as the second most influential parameter with a score of 21.3%. When analysing the individual influence for the head rotation (*blue*, *green* coloured) in Figure 4.9 the results indicate that the head parameter *KH* and cervical spine parameters (*KpC* and *KdC*) were most influential. The response for head rotation and displacement had the worst matches with experimental data compared to the other responses, as can be seen in Table 4.2, with the majority of the NRMS values above 1.00, indicating that the deviation from the average volunteer was higher than one standard deviation. Therefore, Batch 2 was focused on finding improved controller gains for the head and cervical spine parameters.

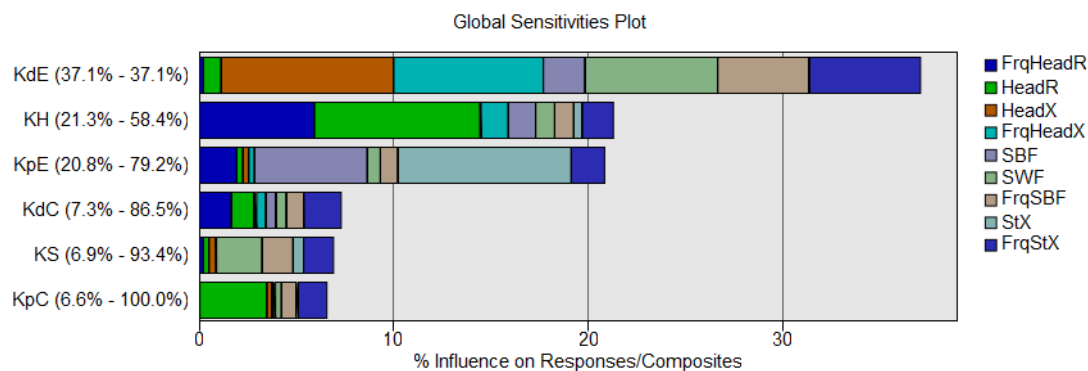


Figure 4.9: Global Sensitivity analysis for all parameters in the first calibration batch.

In Batch 2, none of the tested parameter sets were able to match the head rotation curve within one standard deviation. The best combination of parameters tested in Batch 2 was found in simulation 2.3, with $KpH = 1.50$, $KdH = 0.15$, $KpC = 1.62$ and $KdC = 0.25$. The value of the combined goal function for this set of parameters was 4.95, which was worse than the combined value of the 1.17-simulation at 3.27 in the first batch. However the 2.3-simulation showed an improvement in the match of the head rotation, from an NRMS value of 1.92 in the first batch to 1.25 in the second, see Table 4.3. The reason that the 2.3-simulation had a worse combined score compared to the best simulation (1.17) in the first batch comes from the higher frequency content in head rotation, with an NRMS value of 4.40 instead of 2.15. The response curves for the 2.3-simulation, together with others, can be seen in Figure 4.10.

Table 4.3: Results of calibration Batch 2; showing the tested parameter sets sorted after NRMS values for the seven best and three worst scoring combined values. The following abbreviations are used for the comparative NRMS values: *HR* - Head Rotation, *HX* - Head *X*-displacement, *StX* - Sternum *X*-displacement, *SBF* - Seat Belt Force, *SWF* - Steering Wheel Force, *Fr* - frequency amplitude

Batch 2	Parameters					RMS normalised							
SimID	KpH	KdH	KpC	KdC	Comb	HR	HRFr	HX	HXFr	StX	StFr	SBF	SWF
2.3	1.50	0.15	1.62	0.25	4.95	1.25	4.40	0.31	1.24	0.32	0.49	0.62	0.48
2.11	0.81	0.14	1.65	0.25	4.98	2.12	4.13	0.42	1.13	0.31	0.47	0.62	0.48
2.6	1.14	0.15	1.47	0.19	5.06	1.74	4.39	0.40	1.18	0.31	0.46	0.61	0.48
2.13	0.84	0.14	1.25	0.24	5.07	2.35	4.10	0.51	1.10	0.31	0.47	0.62	0.48
2.24	0.80	0.14	1.22	0.11	5.13	2.54	4.09	0.57	1.05	0.31	0.41	0.62	0.48
2.4	1.49	0.12	1.24	0.24	5.23	1.45	4.66	0.38	1.22	0.32	0.47	0.61	0.48
2.21	0.81	0.15	1.63	0.05	5.23	2.22	4.39	0.49	1.13	0.31	0.39	0.62	0.49
...													
...													
2.16	1.37	0.02	1.21	0.05	8.09	2.00	7.64	0.59	1.12	0.32	0.31	0.62	0.51
2.7	1.19	0.02	1.70	0.16	8.25	1.82	7.81	0.48	1.45	0.31	0.29	0.61	0.50
2.9	1.47	0.02	1.56	0.05	9.23	1.85	8.81	0.55	1.48	0.32	0.30	0.62	0.52
Normalising factors:						0.07	3e-3	44.8	2.42	26.88	1.50	0.04	0.07

The radial basis function metamodel, built to construct a surrogate model of the input and output relation in the calibration Batch 2, suggested a best parameter set with $KpH = 1.50$, $KdH = 0.15$, $KpC = 1.67$ and $KdC = 0.24$. This point was suggested by finding the minimum of the metamodel that was constructed to match the combined goal function. The fit accuracy of this metamodel achieved an R^2 -value of 0.987, which can be compared to the same metamodel built based on the results from the first calibration batch, that achieved an R^2 -value of 0.54. A high R^2 -value (close to 1.00) indicates that there is a clear trend in variation of a parameter on the variation of a response. An example of an independent variation of the tested parameters is the NRMS values of the steering wheel force and seat belt force in Batch 2, where most of the values computed are similar ($SBF=0.62$ and $SWF = 0.48$). The explanation is that the parameters used in Batch 2 have low impact (sensitivity) on these responses. In Batch 2, the best metamodel fit on an individual response was found on the head rotation output (HR) with $R^2 = 0.99$, and the worst metamodel fit was found on the seat belt force (SWF) with $R^2 = 0.58$.

In Figure 4.10 the response curves of the best parameter set from Batch 1 and Batch 2 (simulation 2.3) is displayed together with reference simulations conducted on both a passive THUMS model and a model with the parameters used prior to the calibration. The results of the simulation with passive muscles gave a combined RMS score of 24.23, with all of the responses except the steering wheel force being outside of one standard deviation. A sequential comparison of the SAFER AHBM and a passive THUMS model can be seen in Figure 4.11. The passive model falls into the seat belt and drops its head forward until the chin hits the manubrium and bounces up and down. Furthermore, the response of the model with the initial parameters achieved a combined NRMS value of 5.03, with the response of the head (rotation and displacement) containing an unwanted unstable frequency at 5 Hz, see Figure 4.10. Additional passive damping and an increase of the muscular co-contraction in the muscles of the head and cervical spine improved the 2.3 parameter settings, primarily by decreasing the response amplitude and model eigenfrequency of the head kinematics. This resulted in a combined NRMS value of 3.10 compared to the originally damped 2.3 model, with 4.95. The major improvement in individual responses was, as expected, seen in the frequency content of the head rotation (NRMS of 2.51 instead of 4.40) and head *X*-displacement (NRMS of 0.16 instead of 0.31). Also, the more damped head settings had a calming effect on the frequency content of the steering wheel force (NRMS of 0.73 instead of 1.14) and on the sternum *X*-displacement (NRMS of 0.51 instead of 1.22). Finally, the damped 2.3-parameter set was tested with a settling phase included prior to the brake pulse. The results show that the rotation of the head did not overshoot as much as it did without the settling, and that most matches were better to the average volunteer. The combined NRMS for the settled run was 2.78 and the NRMS for the rotation of the head was 0.69.

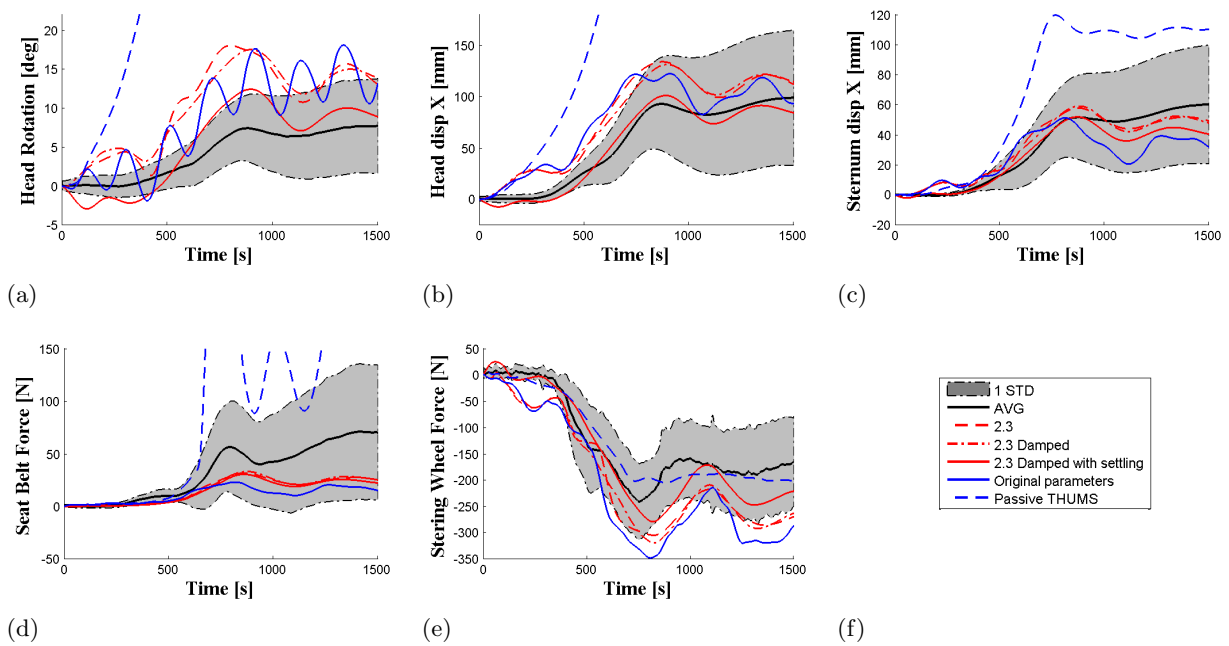


Figure 4.10: Response curves for the best found parameter combinations with and without damping and/or settling, the original parameter settings, and a completely passive THUMS. (a) Head rotation about the Y-axis [deg], (b) Head displacement in the X-direction [mm], (c) Sternum displacement in the X-direction [mm], (d) Change in seat belt force [N], (e) Change in axial steering column force [N], (f) Legend explaining the colours of the curves.

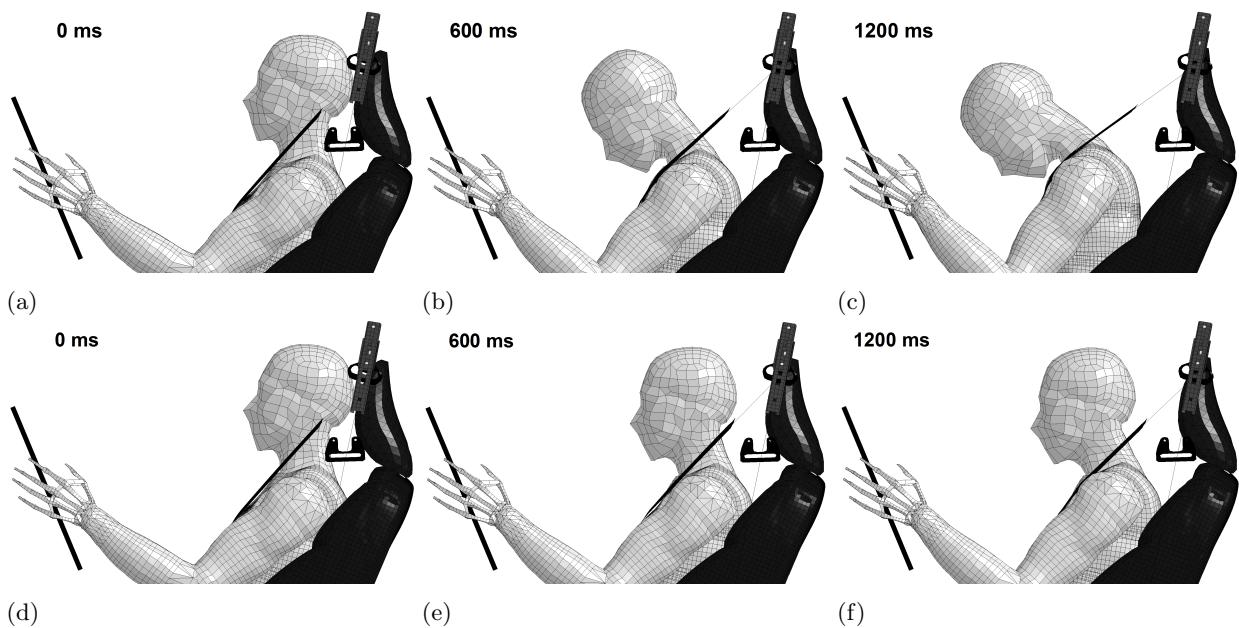


Figure 4.11: Series plot of a pre-crash scenario with a passive vs. an SAFER AHBM model. ((a) passive 0 ms, (b) passive 600 ms, (c) passive 1200 ms, (d) active 0 ms, (e) active 600 ms, (d) active 1200 ms)

Validation results

The validation simulations were conducted with the regulator parameters of the 2.3-calibration setup, both with the original muscle settings and with the increased damping and co-contraction for the head and cervical spine. In Figure 4.12, the kinematic response of the HBM and the influence of the active seat belt can be seen on both the head X-displacement and shoulder X-displacement. After the autonomous braking is initiated the shoulders

and head X -displacement has a peak of 42 mm and 94 mm respectively, around 850 ms into the simulation, for both the tested model settings. At this initial peak, the response of the SAFER AHBM overshoot the responses by the average volunteer with more than one standard deviation. However, after the initial phase 1200 ms and further, with the active seat belt pulling with its full capacity, both the X -displacement of the head and shoulders are found within the corridor of 1 standard deviation even though the SAFER AHBM is pulled further back than the average volunteer. In the first phase, before the seat belt reaches full activation, a behaviour similar to the calibration simulations is seen in the model response. The active seat belt starts pulling 600 ms after the brake pulse is initiated, and does not reach its full capacity (380 N) until 900 ms into the brake event. During the brake event, the SAFER AHBM model is pulled back further into the seat than its initial position, which is seen by the negative values of the shoulder X -displacement in the end of the simulations, see Figure 4.12. A behaviour which is seen in the volunteers and not captured by the SAFER AHBM, is that in the second phase (past 1200 ms), the volunteers tends to continue falling forward while the SAFER AHBM holds a constant level of X -displacement. This can be seen in Figure 4.12 and in the sequential pictures of an example volunteer in Figure 4.13. The same example volunteer is also seen as the dashed lines in Figure 4.12.

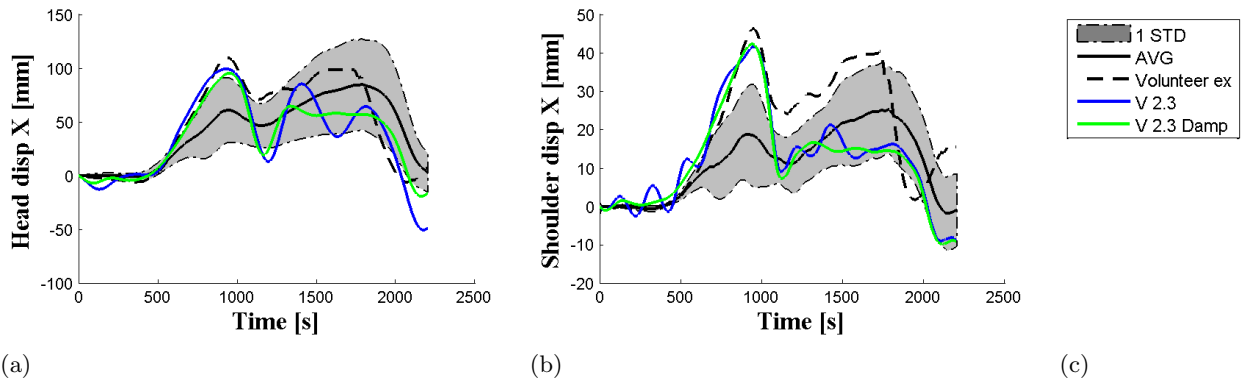


Figure 4.12: Response curves for the head and shoulder X -displacement from the validation simulations. The regulator parameters are from calibration 2.3 using one model with the original muscle settings and one model with increased passive damping and co-contraction. One volunteer curve is also plotted for reference.

Using the same analysis as in the calibration, with NRMS values for each measured response, it was found that the damped version of the 2.3 settings resulted in a better match with the validation data. The combined value of the damped 2.3 setting gave a score of 1.76, while the less damped had 2.04. In Figure 4.12, it can be seen that the 2.3 simulation, with original muscle settings, have a higher frequency content in both the head and shoulder X -displacement, compared to the damped version. However, in Table 4.4, this effect is only seen in the response of the shoulders. This is because the frequency content of the head X -displacement was measured between 1 - 7 Hz, and therefore not captured by the NRMS value.

Table 4.4: Results of the validation; showing the best parameter set seen in the calibration with increased and original damping. The following abbreviations are used for the comparative NRMS values: HX - Head X -displacement, $ShlX$ - Shoulder X -displacement, SBF - Seat Belt Force, SWF - Steering Wheel Force, Fr - frequency amplitude

Validation	Parameters				Normalised RMS				
SimID	KpH	KdH	KpC	KdC	Comb	HX	HXFr	ShlX	ShlFr
V 2.3 Damp	1.50	0.15	1.62	0.25	1.76	0.72	0.86	1.11	0.77
V 2.3	1.50	0.15	1.62	0.25	2.04	1.03	0.65	1.13	1.19
Normalising factors:						27.5	1.47	7.09	0.42

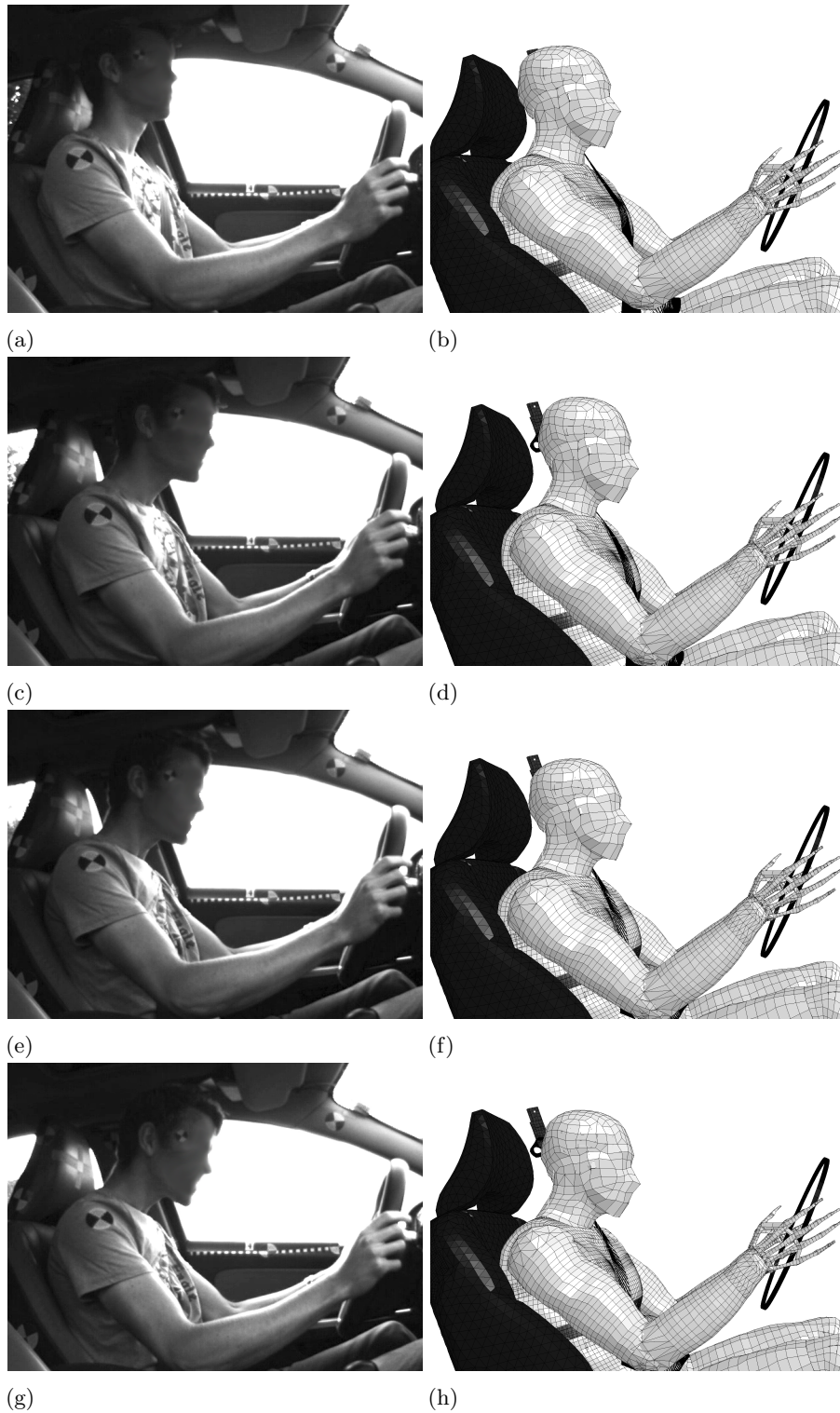


Figure 4.13: Series plot of a pre-crash scenario with a passive vs. an SAFER AHBM model. ((a) passive 0 ms, (b) passive 600 ms, (c) passive 1200 ms, (d) active 0 ms, (e) active 600 ms, (d) active 1200 ms)

5 Discussion

In this thesis a method for positioning an HBM model has been developed and utilised for positioning according to PMHS postures and volunteers in pre-crash scenarios. Additionally, the SAFER AHBM was made to complete a full pre-crash crash simulation without numerical instabilities after some changes was made. Finally, calibration and validation simulations of the neuromuscular control system, that regulates the active muscles, was performed to achieve a response comparable with volunteers subjected to autonomous braking events.

Positioning

The method developed in this thesis for positioning an HBM in a car interior model enables both positioning and seat squashing to be conducted in a single simulation setup. The belt fitting then needs to be done manually once the final position of the model is achieved. The method has been tested for different postures, both in a seat and in space, and gives the user precise control of the model to set up various scenarios. Since the displacements are prescribed, the results show that it is possible to obtain the desired posture with higher precision, compared to using a force based method. Unfortunately the article by Poulard et al. (2015) [26], which was used for comparison with the method developed in this thesis, does not clearly specify in which coordinate system the reported errors were measured. Hence, the developed Prescribed Displacement method cannot be strictly compared to any of the reported positions achieved by the Marionette method. For the measured error in position (estimated from Poulard et al.'s data, explained in Section 3.1), the method achieves a close fit with the goal position, average error in position 0.3 mm while the head angle error is 0.05° and the error in lean angle is 0.1° . For the same PMHS, Poulard et al. reported an average error in position of 9.5 mm, an average angle error of 4.3° and an error in lean angle of 0.1° . Even though a direct comparison should not be made between these results, because of the estimated measurements mentioned above, one can still argue for the indicated potential of the Prescribed Displacement method. The cost for the improved control over the HBM position is an increased risk of building in high stresses or even distorting the FE-mesh. This can lead to failed simulations due to negative volumes in the FE-elements if excessive bending of e.g. the spine is introduced. To minimise the risk of such errors the user should try to constrain as few DOFs as possible during the positioning, to allow the model to move freely, and always take extra care when prescribing rotational displacements on individual vertebrae. Success of the positioning simulation will be governed by the chosen nodes and DOFs.

Positioning, within one standard deviation in X -direction, of an average volunteer posture [37] was achieved for all target nodes by using the Prescribed Displacement method. The simulation was completed within the requirements of an over-night simulation (9 h, using the computer resources listed in Section 1.4) if the interior was scaled down to only include the SAFER AHBM and the seat model, but did not complete in time (21 h) if the full interior model was used. However, the computer cluster used is from 2008 so with a state of the art computer cluster the simulation times would be reduced. Extracting the seat model from the rest of the interior can be done quickly with good knowledge of the models interfaces but can otherwise take some time. What is most time efficient will be up to the user to decide but if multiple positionings are simulated, within the same interior, it is probably worth the time needed to extract the seat model for separate simulations.

When extracting the new position from the simulation results this thesis presents a MATLAB script for the update of all nodes. There are, however, an alternative way to performing this update by saving the model directly from a pre-processor, such as Ls-PrePost. This is possible for all kinds of models that are not encrypted. However, for more advanced models that are commercially distributed amongst companies, there is an industrial demand not to re-structure the model keyfiles, which is the case when saving from Ls-PrePost or OASYS Primer. Re-structuring in this context means adding or removing existing comments and changing the current order of keywords in the keyword files. Since the new nodal definitions are written as one collection of nodes from the output files, a manual replacement of the nodes is not feasible because the nodal definitions are found in multiple locations in different input files. The script, even though it makes the method slightly more complicated to use, is a way to keep the structure of the keyfiles and letting the computer do the update of all nodes. If all nodes were collected in a single definition for the HBM and seat model respectively, the update would be much easier.

When the HBM model is positioned in a seat the file including the element stresses should always be included for subsequent simulations since it defines the state of equilibrium between the HBM and the seat. On the other hand, when the HBM is positioned in space, it is recommended to exclude the stresses for subsequent simulation, especially for lateral changes in position. This is because changing the position of e.g. the spine

introduces high stresses in the ligaments which could be considered unphysical. The new position extracted from the simulation could instead be thought of as the "stress free" state of the model and hence, not include any initial stresses. In general, if a big change in position (e.g. leaning out of the sagittal plane) is desired, as well as a positioning in a seat model, it is recommended to do two simulations. The first simulation creates the positioning in space, where stresses are excluded, while the second simulation positions the HBM created in the first simulation into a seat. The nodal coordinates are then read from the second simulation and the stress state is included in subsequent setups. This is because the stress state produced when doing large alterations in position could make the model spring back towards its original posture in subsequent simulations. An example of this effect can be seen in the results of the calibration, see Figure 4.10. In the first 200 ms of simulation there is a small perturbation in head rotation, head X -displacement and steering wheel force. This is because the model produced in the positioning for this setup has internal stresses which creates a small jerk when the simulation starts. Looking at the results from the validation, see Figure 4.12, one can note that these perturbations are no longer present. This is because a 300 ms initialisation phase was included before the braking event started so that the model could stabilise.

The mesh quality assessment done on the original THUMS model and the model which was positioned with the Prescribed Displacement method, showed that the positioning had little effect on the general mesh quality. In small local areas a negative affect on the mesh quality could be found since an alteration of e.g. the spine always will cause compression/extension of the intervertebral discs. None of these elements were however deemed to be bad enough to affect the general response of the model and was hence accepted. When doing large alterations of the original model the user should always be careful not to have too much of a negative effect on the elements in critical regions, since this will effect the outcome of the simulations. The most striking result of the mesh quality assessment is the quality of the original mesh for which both solid and shell elements have far more elements than the specified 5% by Burkhart et al. (2013) [4] which fails in almost all measurements, the worst being aspect ratio of solid elements (32% failed). However, since the mesh of the THUMS model is not the main focus of this thesis it is simply noted together with the fact that the positioning method does not have a further negative effect on these measurements.

Calibration

A calibration was conducted to improve the kinematics of the SAFER AHBM, by comparing the model response against experimental data from a volunteer study by Östh et al. (2013) [37]. Autoliv and other partners that are interested in the model want to use the SAFER AHBM in design and to verify their safety systems. Therefore, it is important to ensure the model response and numerical stability in various setups with different boundary conditions. Doing so will improve the validity of the model and help understand its limitations.

When conducting the calibration study the single iteration method was chosen over a sequential iteration method, since the simulation times are long while the initial parameter set and the range of the design space had considerable uncertainties. A sequential iteration could get stuck in a local minimum and leave a larger part of the design space unexplored when the calibration deadline was met. For parameter sampling the maxi-mini method with simulated annealing was chosen over a full factorial design or an LHS. The motivation for this is that a full factorial design could not be implemented because of the restrictions on time and that an LHS method is more suited for sampling around a good initial guess of parameters, something which was highly uncertain for the starting model. This means that the sampling is done with an even spread in the parameter space, for the number of simulations specified, but that all parameter combinations are not tested separately.

In order to capture the effect of the parameter space in calibration Batch 1 (48 simulations) and 2 (24 simulations), the optimisation algorithm suggested six/four parameters to be included in each of the calibrations. This meant reducing the total set of 21 parameters, governing the PID-controllers, to a much smaller subset while keeping as much of the significant parameter space as possible. A restriction on the parameter space will always limit the possibility of finding the best match. Therefore, the calibration was not defined as an optimisation but rather as a tuning of the model. In reality problems are often both large and complex but with restrictions on time and resources, making constrictions on parameter space the only feasible option. The challenge is to come up with the set of parameters which has the most significant effect on the measured response, while still fitting within the restrictions on resources. When doing such a large reduction of parameters, as was done in this thesis, there is also a big risk of missing interactions that might occur between different parameters in different regions of the parameter space. The strategy used to minimise these risks was to first determine which parameters had the least influence on the response functions, and then to identify which type of control strategy that would be best for following the volunteer's response curves. By looking at results from a previous

calibration, done by Jonas Östh (see Appendix C), the following controller ranking was determined; elbow, cervical spine, head, shoulder, lumbar. From this ranking, the lumbar regulator was seen to have the least effect on model response and was therefore excluded from the calibration. The head and shoulder regulators were determined to have a medium influence on the response and was hence included with their proportional gain but with the derivative gain set to a fix scale factor of the proportional. Both elbow and cervical spine regulators were seen to have large influence on the results and was hence included with both their proportional and derivative gain. The integral gain of all regulators were set to a relatively low value, fix scale factor of 50% of the proportional gain, since analysis of the volunteer's response indicated a low tendency to force their body back through the deceleration field while subjected to the autonomous braking event. This was interpreted as; if the unaware volunteers found a satisfactory equilibrium point in front of the normal seated position, while being subject to the brake event, the volunteer would stay at this position rather than using a higher muscular activation to move back to his original position. Since the regulator system is defined around angles, and the initial angles are defined as zero, a large integral gain would make the SAFER AHBM push back towards the starting position earlier than what is seen in the volunteers. At the same time, a large integral gain is known to lead to stability problems in regulator design [17] and should therefore be used with caution. The choice of using a scale factor, instead of a constant value, was done to avoid having the integral or derivative gain suddenly become much larger/smaller than the proportional.

The results from Batch 1, see Table 4.2, shows that most of the tested parameter space results in a frequency content with NRMS values above 1.00, indicating that the deviation from the average volunteer was higher than one standard deviation. These results are most significant for the head rotation, where most of the simulations lead to an unstable control system. This unstable response was found to be a result of high derivative gains in the head and cervical spine regulators. Contrary to simple control problems, where a derivative gain normally increase the stability margins for the system [17], the opposite effect seems to be true for the SAFER AHBM, where a decrease in derivative gain increases the stability margin. One possible explanation for this is the significant signal delays in the system (neural delay, muscle activation dynamics, neural excitation and low-pass filtering), which is estimated to total approximately 60 ms. Considering that most of the simulations which showed an unstable response had a peak in frequency content around 5-6 Hz, resulting in a period of approximately 180 ms, indicate that the signal resulting from the derivative gain is almost completely out of phase with the dynamics of the system. This phase lag could explain why a large derivative gain leads to an unstable response. However, if the high frequency content could be reduced in the model, the derivative gain would again help with the control of the system. Since all response curves, excluding head response, was within one standard deviation from the average volunteer, Batch 2 was solely focused on the controller gains of the head and cervical spine. In order to have more results within the stable region, the ranges of derivative gains were reduced significantly to [0.015 0.15] and [0.05 0.25] for head and cervical spine respectively, compared to Batch 1 where the ranges were set to [0.26 1.67] and [0.2 1.0].

The results from Batch 2, see Table 4.3, shows a decent response in all measurements except head frequency, which is still clearly worse than one standard deviation from the volunteer response. Head rotation is on average slightly better than what was seen in Batch 1 but with the drawback of a higher rotational frequency content. The conclusion made from these results is that in order to have a good match of the amplitude in head rotation and head x-displacement, a slightly higher proportional and/or derivative gain is needed than what is presented for the best cases in Batch 1 and Batch 2. The cost of this is an increase in frequency which means lower stability margins for the model. This is a difficult balance since, on one hand, the model needs to have good correlation in distance between the head and the steering wheel when evaluating a safety system design but, on the other hand, an unstable model will not be able to perform a parameter study with varying boundary conditions, since any small change can lead to widely varying results in the response. Again, the conclusion made was that if the high frequency content could be reduced in the model it would help to improve both the stability margins and the possible range of regulator gains to allow for a stronger control.

In order to solve this problem, an attempt at looking outside of the PID-regulator was made. It is noted that an increased damping of a system leads to stabilising forces and dissipation of energy which results in lower frequencies and higher stability margins. In addition to this, an increased neck stiffness could help with reducing the head rotational amplitude and forward X-displacement without increasing the strength of the regulator signal. All muscle elements includes a passive part, explained further in Section 2.3, which results in a passive force as a result of the muscle being subjected to strain or strain rate. This passive element is modelled as a spring and damper in parallel (Kelvin-Voigt model), meaning that it has viscous properties. The viscous properties of the model works as damping to the system since they dissipate energy when subjected to a change in strain (strain rate). It was found that the damping constant governing this viscous property was

set equal for all muscle elements in the model, and that this value was achieved by tuning the elbow joint in comparison with experimental studies, see Östh et. al. (2011) [36]. However, this value has not been confirmed against experimental studies on the cervical spine. Considering that the elbow joint has a single rotational axis while the neck bends around every vertebrae, and that each vertebrae is separated by intervertebral discs, one could argue that there should be more viscous damping in the neck than in the elbow. This could motivate a higher damping value for the neck muscles, compared to the upper extremities muscles, if this damping isn't fully captured by the geometry of the model itself. Viviani and Berthoz (1975) [31] studied the dynamics of the head-neck system in response to small perturbations by both volunteer experiments and by mathematical modelling. In their mathematical model they simplified the head-neck system as a double inverted pendulum, with one rotational joint at approximately the level of C6-C7 and one rotational joint close to the atlanto-occipital articulation [31], using torsional springs with variable stiffness and viscosity in each joint. In their calibration of the model they found that the viscoelastic parameters were both non-linear with increasing frequency and that the two joints differed by a factor of $\approx 50 - 100$ times. Since their model is very different from the SAFER AHBM, and the viscous term is implemented in a different way, it is difficult to make a direct translation of their reported damping value to something that could be used in the SAFER AHBM. However, it does confirm that different joints can have highly varying damping coefficients. This could make the implemented damping value, which is tuned from the elbow joint, questionable as a good choice for the head and cervical spine damping.

All muscles also include a co-contraction value which is the activation level of the muscle when it is fully relaxed. The co-contraction adds a constant tension of the muscles in both extension and flexion, resulting in an increased bending stiffness of the controlled joint, see Lee (2006) [16]. For the head and cervical spine muscles this value is set to 3% which has been estimated from EMG data on volunteer drivers in a normal driving event [37]. This value would then correspond to a driver which is completely unaware of the impending accidents [37]. Benderius (2014) [2] discusses the involvement of a stretch reflex which tends to counteract the motion when a muscle is pulled externally. This reflex would then increase the co-contraction of the muscles when the driver is suddenly subjected to the autonomous braking event, possibly motivating a higher co-contraction value for the model. Arguing that the driver might not be completely unaware just before the brake event, but rather tense up in anticipation of the accident because of some visual cue, could further motivate an increased co-contraction.

The above argumentation for co-contraction and viscous damping was used when trying to improve the model response. Since no numerical values which could be directly translated to the SAFER AHBM was found in the literature (except the one already implemented in the model), it was decided to test a significantly higher value to clearly see the effect. Hence, a fifty times higher damping constant ($4 * 50 = 200$ [kNs m⁻²]) and a co-contraction level of 10% was implemented with the control parameters from calibration 2.3. The results from this change can be seen in Figure 4.10 where it is shown that the model response has improved compared to the volunteer average. NRMS values tells us that both frequency content as well as rotational amplitudes and sagittal displacements have improved; combined NRMS of 3.1 instead of 4.95, frequency content NRMS of 2.51 instead of 4.4 and head X-displacement NRMS of 0.16 instead of 0.31. These changes results in a more stable model towards small perturbations in boundary conditions, which is crucial for its usability in industry. The downside is that since no experimental references has been found to back up these values, the bio-fidelity of these solutions could be questionable. These results should therefore primarily be considered as guidance for future work. Before these values are fully trusted, it is advisable to more in detail investigate the level of damping that would be appropriate for the passive muscle properties in the SAFER AHBM.

Validation

The validation of the SAFER AHBM was set up using an active seat belt, instead of the standard passive seat belt used for calibration. The validation data was obtained from an experimental study testing autonomous braking events, conducted at Autoliv 2013. Using a different test case is standard procedure when performing a validation to ensure that the model is not only calibrated for one specific case. If the calibrated model gives a satisfactory response, compared to the validation test data, the parameters found are considered to work in a general setting for frontal pre-crash simulations. The validation simulations were done with the parameter setting found from calibration 2.3, with the original muscle model, and for the same parameter setting with increased co-contraction and passive damping.

The results from the validation can be seen in Table 4.4 and Figure 4.12, where the model with increased co-contraction and passive damping has a better response than the original muscle model, combined NRMS

value of 1.76 instead of 2.04. For the damped model, all NRMS values except shoulder X -displacement indicate a match which is within one standard deviation of the volunteers. The results also show that when the boundary condition from the seat belt is significantly altered, compared to the calibration study, the model with increased damping still behaves as a stable control system while the original muscle model gets an increased frequency content in the response curves. This indicates that the model with increased co-contraction and passive damping should be able to handle parameter studies with varying interior design, without resulting in an unstable response.

When comparing the response curves for head and shoulder X -displacement of the SAFER AHBM with the volunteers, one can see a considerable difference in the time interval of 600 ms to 1200 ms and a small difference after 1200 ms. In the first phase the SAFER AHBM keeps moving forward, with the brake pulse, while the volunteers do not display the same amplitude in motion. In the second phase, after 1200 ms, the SAFER AHBM instead moves back towards the seat while the volunteers keep moving a little bit forward. The response shown by the SAFER AHBM is however what is expected considering the boundary conditions of the system and the control implementation. Since the active belt isn't activated until 600 ms into the pre-crash event, there is no reason for the model to behave differently than what was found in the calibration study. After approximately 900 ms the model is pulled back once the force in the active belt gets high enough. The intended design of the system is to let the driver first fall forward during the initial phase of the pre-crash and then pull him back into the seat with the active seat belt, before the crash occurs. This is done to have as much time as possible to slow down the motion of the driver, and to position him correctly for the upcoming crash. This motion is just what the SAFER AHBM shows so one must then ask: *Why doesn't the volunteers behave as we expect them to do?*

All attempts to answering this question is purely based on speculations from a limited set of data and should be thought of with this in mind. One reason for the limited X -displacement during the initial phase of the pre-crash event, compared to what was registered in the experiments done by Östth et al.(2013) [37], could be that the volunteers experienced discomfort from the belt pull-in. The force applied to the chest is relatively high but gets reduced the further back into the seat the driver is positioned (because of the belts loading path). If the driver anticipates the force, the driver might tense up to minimise the forward motion and hence lower the discomfort level. This would explain the lower X -displacement in the initial phase. Once the driver feels that the seat belt carries his weight, the driver might instead relax his neck and shoulders because of the supporting constraint. This relaxation would explain the small increase in X -displacement after 1200 ms, even though the seat belt pulls back with full force since the head and shoulders can "fold" over and around the seat belt. Another factor which could affect the response of the volunteers is that all of them work with testing of vehicle safety systems and that they therefore might be biased for the study. If the volunteers expected the upcoming force from the active seat belt during the pre-crash event, because of their own experience in working with vehicle safety systems, they might have tensed up in anticipation of this force in a way that an unknowing driver would not. It is also known from previous experiments that aware drivers have a substantially lower head forward displacement [28]. Finally the boundary conditions for this seat belt has not been completely confirmed from the test setup which means that the validation simulation might not be a good enough estimation of the actual event. Still, this does not fully explain the differences in the initial phase of the pre-crash, where the active belt is still passive, when comparing the two sets of volunteer data. To capture these behaviours the SAFER AHBM would need a more advanced regulator design which could include effects such as dealing with muscle tension due to anticipation of the pre-crash, muscle relaxation when the model feels supported by e.g. the seat belt, habituation to the brake event etc.

One volunteer has been singled out and highlighted in the validation results to show that the SAFER AHBM response is close to the volunteers in some cases, see Figure 4.12. In this volunteer the peak in forward displacement during the initial phase matches that of the SAFER AHBM which would indicate that the control system is tuned properly. However, in the second phase, when the seat belt is fully activated, the SAFER AHBM is pulled further back than the volunteer. This could be explained, but has not been confirmed, if the volunteer has his shoulders placed closer to the seat back than the positioned SAFER AHBM, since this would allow the shoulder and head to travel a further distance when being pulled back into the seat. If this is the case it would indicate that this is not produced by a control system which is badly tuned, but rather be a result of a miss match in initial position.

6 Conclusions

In this thesis, the SAFER AHBM has been made easier to use in the industrial development process, by development of a positioning tool using prescribed displacements. Furthermore, the kinematic response of the model was improved through systematic calibration and was validated with respect to a new data set. The model was found to give a satisfying match with the experimental data in both calibration and validation. Solutions to numerical issues have been found and incorporated into the SAFER AHBM. These issues were hourglassing of finite elements, bad scaling properties in muscle contact definitions and error terminations due to muscle nodes running through slip rings. The industrialised version of the model completed a combined pre-crash crash event with a valid response and without any of these errors. Hence, the industrialisation considered in this thesis is deemed successful, even though future improvements are always possible.

Seat-squash, positioning and/or adjustments in posture of the SAFER AHBM (and other HBMs) can be conducted in a single stage simulation with the developed Prescribed Displacement method. If the user wants to include internal stresses in the model, an initialisation phase via dynamic relaxation needs to be included prior to any subsequent simulation. There is a risk of over-constraining the model during positioning, and thereby induce distorted finite elements or cause error terminations, if the user is not cautious with the choice of prescribed DOFs. A correct usage of the Prescribed Displacement method uses a minimal number of DOFs to achieve a desired posture/position, ensuring that the quality of the mesh can be sustained without distortion.

In an autonomous braking event, all of the measured responses on the calibrated SAFER AHBM were able to match the average volunteer within 1 standard deviation, except the rotation of the head in the sagittal plane which rotated slightly more than the volunteers. The measured responses that matched within one standard deviation was head X -displacement, sternum X -displacement, seat belt force, and axial steering column force. It was found that the muscular control system of the SAFER AHBM is sensitive to high derivative gains, which could cause instability and oscillations in its response. Additional viscous damping and muscular co-contraction was added to the material model of the muscles connected to the head and cervical spine, which increased the stability margins for various boundary conditions. A validation simulation was conducted to test the calibrated SAFER AHBM with an active seat belt pulling with 380 N at 600 ms after an autonomous braking event was initiated. This indicated that the increased viscous damping and added co-contraction was necessary in order to obtain a stable response for varying boundary conditions, such as the active seat belt.

7 Future Work

The set of parameters found in the calibration should not be considered an optimum for the model but rather a good starting point for future tuning. The calibration performed in this thesis faced stability issues, resulting in a large number of calibrations with response curves far from one standard deviation of the average volunteer. These results, and the knowledge gained about stable parameter regions, should be used as a starting point for future calibrations in order to find an even better fit with the volunteer data.

Since the calibration done in this thesis had stability issues, some different ways to solve this was tested. The addition of increased passive damping and muscle co-contraction proved to be effective for reducing the frequency content of the response. However, no reference to substantiate these changes was found in the literature. Since the changes were effective it is recommended that a study which evaluates these factors and confirms the biofidelity of the model, both by simulations and further literature research, is conducted.

In order to simplify future work with the SAFER AHBM model, it is recommended to solve the issue with having to update the reference angles when a new positioning is tested. This requires manual work and good understanding of the regulator implementation to be done correctly. If the angles instead could be updated automatically at the start of the simulation there would be no need for the user to worry about this issue. From what has been found in the LS-DYNA manual, there is today no way of defining a function which measures an output at a specified time and then stores this value as a constant. If this was possible the function would be able to measure the initial angles when the simulation starts and then give them as input to the regulator.

To avoid numerical instabilities in the model, for different pre-crash crash scenarios, it is recommended that a node to node contact is included in all slip rings connected to muscles. If a muscle gets shortened/lengthened in such a way that it gets pulled through a slip ring the simulation will fail, even though this would probably have had an insignificant effect on the model response. If a node to node contact is included this risk will be eliminated, possibly saving many hours of simulation data. A second risk of numerical instability was found at the end of a crash event, where the rib case sometimes included a lot of hourglass energy. For future crash simulations this might become a problem that needs to be addressed.

Future development work should also be focused on adding muscle control in the lateral direction to facilitate studies of pre-crash events in curves. This means adding muscles to the SAFER AHBM model that controls this motion and will make the regulator design more complex. A model of only the head and neck system could be extracted from the SAFER AHBM and further developed for testing a lateral implementation.

References

- [1] M. Barnes. Form Finding and Analysis of Tension Structures by Dynamic Relaxation. *International Journal of Space Structures* 14 (1999), 89–104.
- [2] O. Benderius. Modelling driver steering and neuromuscular behaviour. PhD thesis. Chalmers University of Technology, 2014.
- [3] A. van den Bogert, K. Gerritsen, and G. Cole. Human Muscle Modelling from a User’s Perspective. *Journal of Electromyography and Kinesiology* 8 (1998), 119–124.
- [4] T. Burkhart, D. Andrews, and C. Dunning. Finite Element Modeling Mesh Quality, Energy Balance and Validation Methods: A Review with Recommendations Associated with the Modeling of Bone Tissue. *Journal of Biomechanics* 46 (2013), 1477–1488.
- [5] R. Courant, K. Friedrichs, and H. Lewy. On the Partial Difference Equations of Mathematical Physics. *IBM Journal* (1967), 215–234.
- [6] C. Desai et al. A generic Positioning Tool for Human Body FE Models. *IRCOBI Conference Proceedings*. Vol. IRC-12-69. International Research Council on the Biomechanics of Injury. 2012, pp. 610–621.
- [7] Dummy positioning tutorial. Livermore Software Technology Corporation. 2012. URL: <http://www.lstc.com/lssp/content/tutorials/6/t6p1.shtml> (visited on 05/08/2015).
- [8] R. Fletcher. Practical Methods of Optimization, Second Edition. John Wiley & Sons, Ltd, 2013.
- [9] S. Gayzik et al. Development of the Global Human Body Models Consortium Mid-Sized Male Full Body Model. *Proceedings of the 39th International Workshop*. Injury Biomechanics Research.
- [10] Global status report on road safety. World Health Organisation, WHO, 2013.
- [11] P. Hovenga et al. Improved Prediction of Hybrid-III Injury Values Using Advanced Multibody Techniques and Objective Rating. Tech. rep. SAE International, 2005.
- [12] M. Iwamoto et al. Development of a Finite Element Model of the Total HUMAN Model for Safety (THUMS) and Application to Injury Reconstruction. Toyota Central R&D Labs., Inc., 2002.
- [13] G. Jacobs, A. Aeron-Thomas, and A. Astrop. Estimating global road fatalities. Official Report. Berkshire, England: Transport Research Laboratory, 2000.
- [14] D. Jani et al. Repositioning the Knee Joint in Human Body FE Models Using a Graphics-Based Technique. *Traffic Injury Prevention* 13 (2012), 640–649.
- [15] P. Knupp. Remarks on Mesh Quality. *Proceedings of the 45th AIAA Aerospace Sciences Meeting and Exhibition, Reno, NV*. 2007.
- [16] P. Lee, E. Rogers, and K. Granata. Active trunk stiffness increases with co-contraction. *Journal of Electromyography and Kinesiology* 16 (2006), 51–57.
- [17] B. Lennartsson. Reglerteknikens grunder. Studentlitteratur, 2002.
- [18] LS-Dyna Keyword User’s Manual Volume 1. Livermore Software Technology Corporation. 2014.
- [19] LS-Dyna Keyword User’s Manual Volume 2, Material Models. Livermore Software Technology Corporation. 2012.
- [20] LS-Dyna Theory Manual. Livermore Software Technology Corporation. 2006.
- [21] LS-OPT User’s Manual. A Design Optimization and Probabilistic Analysis Tool for the Engineering Analyst. Livermore Software Technology Corporation. 2012.
- [22] Oasys PRIMER manual v. 12: Occupant Set-Up. Livermore Software Technology Corporation. 2012. URL: <http://www.oasys-software.com/dyna/en/software/primer.shtml> (visited on 05/08/2015).
- [23] M. Orr. Introduction to Radial Basis Function Networks. Centre for Cognitive Science, Edinburgh, Scotland, 1996.
- [24] PIPER project; Position and Personalise Advanced Human Body Models for Injury Prediction. European Union Seventh Framework Programme. 2015. URL: <http://www.piper-project.eu> (visited on 05/15/2015).
- [25] B. Pipkorn and K. Mroz. Validation of a Human Body Model for Frontal Crash and its Use for Chest Injury Prediction. *SAE International* (2008).
- [26] D. Poulard et al. Development of a computational framework to adjust the pre-impact spine posture of a whole-body model based on cadaver tests data. *Journal of Biomechanics* 48 (2015), 636–643.
- [27] S. Robin. HUMOS: Human Model for Safety - A Joint Effort Towards the Development of Refined Human-Like Car Occupant Models. France: LAB PSA Peugeot-Citroën RENAULT, 297:2001.
- [28] L. van Rooij et al. Driver head displacement during (automatic) vehicle braking tests with varying levels of distraction. *Proceedings of the 23rd Enhanced Safety of Vehicles Conference*. 2013.

- [29] L. Råde and B. Westergren. *Mathematics Handbook for Science and Engineering*. Studentlitteratur, 1998.
- [30] L. Threfethen. *Finite Difference and Spectral Methods for Ordinary and Partial Differential Equations*. Department of Computer Science and Center for Applied Mathematics, Cornell University, 1996.
- [31] P. Viviani and A. Berthoz. Dynamics of the Head-Neck System in Response to Small Perturbations: Analysis and Modeling in the Frequency Domain. *Biological Cybernetics* 19 (1975), 19–37.
- [32] J. Winters and L. Stark. Analysis of fundamental human movement patterns through the use of in-depth antagonistic muscle models. *IEEE Trans BioMed Eng.* 32(10) (1985), 826–839.
- [33] F. Zajac. Muscle and Tendon: Properties, Models, Scaling, and Application to Biomechanics and Motor Control. *Critical Reviews in Biomedical Engineering* 17(4) (1989).
- [34] K. Åström and R. Murray. *Feedback Systems. An Introduction for Scientists and Engineers*. Princeton University Press, 2008.
- [35] J. Östh. *Muscle Responses of Car Occupants - Numerical Modeling and Volunteer Experiments under Pre-Crash Braking Conditions*. PhD thesis. Chalmers University of Technology, 2014.
- [36] J. Östh, K. Brodin, and R. Happee. Active muscle response using feedback control of a finite element human arm model. *Computer Methods in Biomechanics and Biomedical Engineering* 15(4) (2012), 347–361.
- [37] J. Östh et al. Driver Kinematic and Muscle Responses in Braking Events with Standard and Reversible Pre-tensioned Restraints: Validation Data for Human Models. *Stapp Car Crash Journal* 57 (2013), 1–41.
- [38] J. Östh et al. The Occupant Response to Autonomous Braking: A Modeling Approach That Accounts for Active Musculature. *Traffic Injury Prevention* 13(3) (2012), 265–277.

Appendices

A Positioning Manual

This is a step-by-step instruction of how to set up a positioning of an HBM using the Prescribed Displacement method in LS-Dyna. The instructions include both positioning with a seat model (seat squashing) and positioning in space, with comments for steps that are not needed if the seat is excluded.

1. (*Not needed if only positioning in space*) Start by translating and rotating the HBM to be as close to the seat as possible without introducing initial penetrations. The closer you can get the model to the desired position the better since this will result in a shorter displacement, and thereby a more stable simulation. This can be done manually by specifying `*INCLUDE_TRANSFORM` for all input files that corresponds to the HBM (**except** the muscle control file if you use the SAFER AHBM). The reason for not including the muscle control file is that it needs to be aligned with the global X -axis in order to work properly. An example of initial position and translated position of the HBM relative to the seat can be seen in Figure A.1.

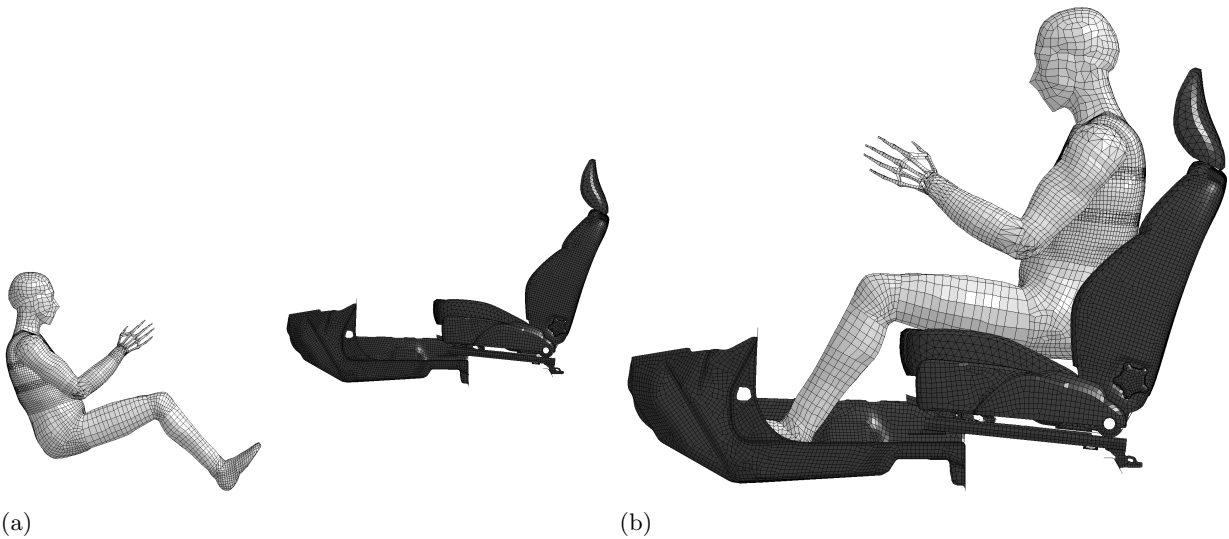


Figure A.1: (a) Initial position of the HBM and (b) translated position of the HBM, used to minimise displacement during simulation.

2. Determine the parts to position and the displacement measures needed to obtain the desired posture, see Figure A.2. This can for example be X - and Y -displacement of the head and spine to achieve the correct back angle or spine curvature, X - and Z -displacement of the hip to push the HBM into the correct seat position or X -, Y - and Z -displacement of the hands and feet to position them in space close to the steering wheel and foot pedals respectively. The segments are chosen by specifying a node on the part that should be positioned. Since the positioning will pull the node to a new position it is advisable to use hard structures such as bone or rigid bodies.

NOTE: Be careful not to over constrain the model since this will lead to *Error Termination* in the simulation. Consider, for example, constraining Z -displacement for multiple points along the spine while trying to get the correct back angle and spine curvature in X - and Y -direction. If the Z -values specified are not exactly compatible with the HBM for the goal position, and for every point in between the initial position and the goal position, you will cause an *Error Termination* due to excessive compression or shearing of an intervertebral disc. Instead, only prescribe X - and Y -displacements for the spine while leaving Z free for all points but a base, advisably put in the pelvis. This is not as big of a problem for hands and feet since the connection to the rest of the body includes two joints. A general recommendation is to prescribe as few DOFs as possible so that the model is allowed to move and adapt to the new position.

3. Enter the nodal IDs for the parts that should be positioned and the DOFs and displacements that you want to prescribe using `*BOUNDARY_PRESCRIBED_MOTION_NODE` in a .key-file that will include all information related to the positioning, see Appendix A.1 for an example file of positioning.

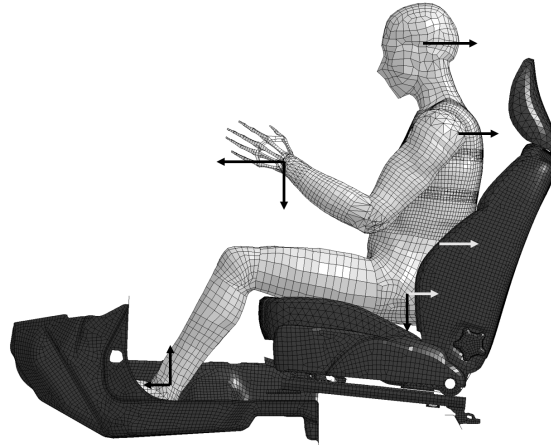


Figure A.2: Example of parts to consider for positioning with prescribed displacement direction indicated by arrows.

4. Other than *BOUNDARY_PRESCRIBED_MOTION_NODE the .key-file should include a ramp curve, see Figure A.3, and a *DAMPING_GLOBAL to avoid vibrations from the positioning (recommended damping value of 0.15). For moderate positioning distances a positioning time of 150 ms and a settling time of 150 ms has been successfully implemented but the times needed are dependent on the positioning distance to ensure a stable simulation. Try getting the model as close to the desired position as possible, using translations and rotations, and consider increasing the positioning time if the desired position is still far from the initial position.

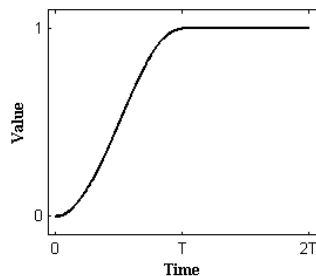


Figure A.3: Continuous ramp curve defining the prescribed motion in the positioning method (T is the total positioning time)

5. (Not needed if only positioning in space) If the positioning is conducted with the full interior model, exclude the belt system before running the simulation since this might interfere with the HBM. Also, if there is a risk that the HBM hits the steering wheel during the positioning or if there is an initial penetration between e.g the hands and the steering wheel, make sure to exclude this contact definition from the simulation since it will hinder the positioning of the model.
6. (Not needed if stress state is not saved) If your model includes *DATABASE_EXTENT_BINARY make sure that SIGFLG=1 so that the stress tensor is included in the shell LS-Dyna database.
7. If you use the SAFER AHBM, include a passive muscle control file for the simulations instead of the active. This is because the muscles will try to move the model back to its original position if left active.
8. If you use the SAFER AHBM model with redefined joints for knee, shoulder, hip and elbow, consider setting the rotational stiffness to zero in the *DEFINE_CURVES associated with each *CONSTRAINED_JOINT_STIFFNESS_GENERALIZED, before running the simulation. This is especially important for the lateral stiffness of the hip joint which is very high. If lateral positioning of the legs is desired this stiffness will build up high joint stresses which will make the legs spring back in subsequent simulations if stresses are included.

9. Include the positioning .key-file with the rest of your model and run the simulation.
10. Once the simulation has completed it is time to extract the new position and element stresses. Open the d3plot file in LS-PrePost and go to Post - Output. Then chose Format: Dynain ASCII, Entire Model and type in the number of the final simulation state, see Figure A.4. Press *Write* and save the dynain file with a name of your choosing, recommended to use a name which describes the current positioning and model file so that the position can be saved for future use.

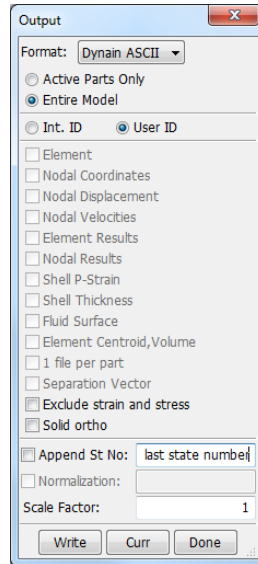


Figure A.4: *Output dialog from LS-PrePost used to write dynain file.*

11. Place all files that you want to update in a folder with the dynain file and the MATLAB script *post_positioning_script.m* with its function files. The script will go through all .key-files in the folder and check for nodal IDs that match the dynain file. The matching nodes will get updated coordinate values corresponding to the final state of the simulation. The script will also go through all joint definitions to make sure that the nodes used for the joint definitions has the exact same coordinates. This is because the constraints are penalty based so when the final state is read from the model it is not guaranteed that the nodes are exactly on top of each other. This will cause an error termination in subsequent simulations if it isn't fixed.

NOTE: If the positioning only includes the HBM then place all files in the folder for the update. If the positioning is done with the full interior it is recommended to only include all files corresponding to the HBM and the seat model. This is because the interior moves slightly when it gets subjected to gravity and including these small stresses and displacements will only slow down the subsequent simulations.

12. Open the MATLAB script *post_positioning_script.m*, change the variable *dynainFileName* to your saved file name and run the script.
13. The updated files and a dynain file that only includes element stresses is found in the new folder *NewKeyFiles*. Copy the files into your simulation setup and your new model will now be positioned according to the simulation results.

NOTE: If you started with defining an **INCLUDE_TRANSFORM* for all HBM files, you need to remove this since the model now starts at the correct position. To be extra certain that no initial penetrations are present between the HBM and the seat, the **INCLUDE_TRANSFORM* could also be changed to e.g. only a translation in *Z*-direction of 1 mm.

14. If you use the SAFER AHBM, the reference angles now has to be updated for the new position, see Figure A.5. This is either done manually, by running a very short simulation and extracting the initial angles for all controllers so that the signal will start at zero, or by using the MATLAB script *update_controller_referenceAngles.m* which does this automatically, see Appendix B. The script can either update the angles directly from the .key files or from the corresponding dynain file, created in step 10. Simply follow the short instruction given in the MATLAB script.

```

$ y0
*DEFINE_CURVE
$# lcld      sidr      sfa      sfo      offa      offo      dattwp
43810000    0      1.000000  1.000000  0.000    0.000    0
$#
          al          ol
          0.00000e+000      -0.148836 ← Reference
          4.00000e+003      -0.148836
$ y(t)
*DEFINE_CURVE_FUNCTION
$# lcld      sidr      sfa      sfo      offa      offo      dattwp
43810001    0      1.000000  1.000000  0.000    0.000    0
$# function
ATAN((CX(43700101)-CX(43700121))/(CZ(43700101)-CZ(43700121)))-LC43810000 ← Subtracted to start from zero

```

Figure A.5: Reference angle specified for the head controller in the SAFER AHBM model.

15. If you deactivated the joint stiffness for all/some of the joints before running the positioning simulation, you should now reset them to their original values.
16. If you don't want to include stresses to the model you are now done, simply discard the dynain file created with your new model since this only includes stresses by now. Your model is positioned and if you use the SAFER AHBM it has updated reference angles that match this position.
17. To start the now positioned model from a state of pre-load, the new dynain file needs to be included in your simulation setup and a *CONTROL_DYNAMIC_RELAXATION with IDRFLG=1 needs to be defined. Doing so will ensure that each simulation begins with a dynamic relaxation where the element stresses and nodal coordinates finds an equilibrium to start from, see Figure A.6 for an implementation example. Recommended tolerance value is $2.5E - 2$.

```

*CONTROL_DYNAMIC_RELAXATION
$# nrcyck      drtol      drfctr      drterm      tssfdr      irelal      edttl      idrflg
      250      2.5E-2      0.995      0.0      0.0      0      4.0E-2      1

```

Figure A.6: Key card example for dynamic relaxation started from a dynain file.

18. (Optional) If the dynamic relaxation phase is slow you don't need to include this for every simulation, it is sufficient to run it only once. After a simulation that includes dynamic relaxation has completed (it is enough to run a 1 ms simulation) a file named *drdisp.sif* will be written. This file includes the coordinate values for each node which corresponds to a state of equilibrium with the applied pre-load. By saving this file with the rest of your simulation setup, setting IDRFLG=2 in *CONTROL_DYNAMIC_RELAXATION and including an extra flag (m=drdisp.sif) in all future simulations, it is possible to start from this state directly. Since dynamic relaxation moves the model slightly, the reference angles might not start exactly at zero. If this becomes a problem, running a dynamic relaxation and saving its drdisp.sif file can be a solution. It is then possible to update the angles from the exact position which is the result of the dynamic relaxation.
19. Your model is now positioned and, if you want to, you can start it from a state of pre-load corresponding to the current position by including the created dynain file in your simulation setup.

Since it is not recommended to include the element stresses if the positioning of the model is far from the original position, or if it includes a lot of compression of the intervertebral discs, a recommendation for these positions, if they also need to include a seat squash, is to divide the positioning in two phases. First, go through the steps as if only doing a positioning in space where the big change in posture is achieved. Then, only update the nodal coordinate values while discarding the element stresses. This will make the desired position the "stress free" state which is probably closer to reality than the high stresses which can be found otherwise. Second, do a new positioning with the model created in the first iteration but now include the seat and only do a seat squash. Update the nodal coordinates a second time and save the element stresses which will now only be created from the seat squash and not from large compressive forces due to bending of the spine.

B MATLAB code

Post Positioning Script

```
clc, clear all, close all
%%%%%%%%%%%%%%%%%%%%%%%%%%%%%%%%%%%%%%%%%%%%%%%%%%%%%%%%%%%%%%%%%%%%%%%%
% The script does the following:
%
% - All files that are copied, fixed or created are added to a folder:
%   "\NewKeyFiles\"
%   in the current directory.
% - Updates nodal coordinates from dynain in all the keyfiles that are
%   inside the current folder.
% - Copies encrypted files (.enc)
% - Adds all *INITIALSTRESS information in a new dynain file.
% - Merges nodal coordinates in spherical and revolute joints to avoid
%   problems with noodes not beeing coincident.
%
% Created by: Jacob Wass & Erik Eliasson
%%%%%%%%%%%%%%%%%%%%%%%%%%%%%%%%%%%%%%%%%%%%%%%%%%%%%%%%%%%%%%%%%%%%%%%%

%% INPUT FOR SCRIPT
% Give the dynain filename
dynainFileName = 'dynain.full.interior.20150601';

% Give the filenames of the files you want to include stresses in the new
% dynain file
filesToIncludeStress = {'01a.thums.am50.occ152-040526_main.06.ren.act3b.legla.key';...
                        'y352.dwg.front.seat.manual.220mm.lhs.euroncap.h350-0742.ml.k'};

%%%%%%%%%%%%%%%%%%%%%%%%%%%%%%%%%%%%%%%%%%%%%%%%%%%%%%%%%%%%%%%%%%%%%%%%
%% Start of script

% Read dynain file
disp('');
disp('-----Starting post positioning script-----');
disp('           Written by: Erik Eliasson & Jacob Wass');
disp(' ');
disp(' ');
disp(' -Can take up to 20 minutes, please wait');
disp([' -Reading: ', dynainFileName]);
fileID = fopen(dynainFileName);
dynainKey = (textscan(fileID, '%s', 'Delimiter', '\n', 'Whitespace', '', ...
                    'CommentStyle', '$'));
dynainKey=dynainKey{1,1};
fclose(fileID);

%% Interpret dynain and divide information

initStrainSolidErr = find(~cellfun(@isempty, ((regexp(dynainKey, ...
                    '*INITIALSTRAIN.SOLID')))));
initStrainSolidErr =initStrainSolidErr(2:end);
dynainKey = dynainKey(setdiff(1:length(dynainKey), initStrainSolidErr));
% % Find NODE and INITIAL lines
starLine = find(~cellfun(@isempty, ((regexp(dynainKey, '^<.*')))));
nodeLine = find(~cellfun(@isempty, ((regexp(dynainKey, '*NODE')))));
initLine = find(~cellfun(@isempty, ...
                    ((regexp(dynainKey, '*INITIAL.'))));
nodeLines = (nodeLine+1:starLine(find(starLine==nodeLine)+1)-1)';
updateNodeStr = dynainKey(nodeLines);
allUpdateID = cell2mat(cellfun(@(cell) sscanf(cell, '%u', 1), ...
                    updateNodeStr, 'UniformOutput', false));

% % Include initial stress for found *INITIAL... lines

% library for elements to include initial stress,
% element name, rows dynain, cols IDdynain, rows key, cols IDkey, dynain
```

```

% inds
elemToInclInit = {'*INITIAL_STRESS_SHELL',4,10,1,8,[],[];...
 '*INITIAL_STRESS_SOLID',2,10,1,8,[],[];...
 '*INITIAL_STRESS_BEAM',2,10,1,8,[],[];
 '*INITIAL_STRAIN_SHELL',3,10,1,8,[],[];...
 '*INITIAL_STRAIN_SOLID',2,10,1,8,[],[];
dynainStress = {};
initElements = {};
tmp = elemToInclInit(1,:);
elemIDs={};
disp(' -Including the following keyword types for initialisation:')
for i = 1:size(dynainKey(initLine),1)
    initElements(i,1) = {dynainKey{initLine(i)}};
    ind = find(~cellfun(@isempty, strfind(elemToInclInit...
        (1:end,1),initElements{i,1})));
    if isempty(ind)
        continue;
    end
    initLines(i) = {(initLine(i)+1:starLine(...
        find(starLine==initLine(i))+1)-1)'};
    rows = elemToInclInit{ind,2};
    elemIDs(i) = {cellfun(@(cell) sscanf(cell,'%u',1),...
        dynainKey(initLines{i}(1:rows:end)))};
    tmp(i,:) = [elemToInclInit(ind,1:5) ,initLines(i),elemIDs(i)];
    disp(initElements{i,1})
end
elemToInclInit = tmp;

disp([' -Reading of ',dynainFileName ' finished: - found ',...
    num2str(length(nodeLines))...
    , ' node lines and ',num2str(length(initLines)), ' *INITIAL... definitions']);
disp('-----');
disp('');
clear starLine initLines initStressLine nodeLine initStressElements elemIDs ...
    tmp ind

%% Update nodal coordinates, Fix joints, add initial stress
% in all keyword files that have *NODE with corresponding nodal IDs as the
% dynain file
names = cellstr(ls);

for file_index=1:size(names,1)
    % Check if file is k or key file, or if it is not the dynainFile
    if (~isempty(strfind(names{file_index,:},'.k'))) &&...
        ~strcmp(names{file_index,:},dynainFileName)

        disp(['Checking: ',names{file_index,:}]);

        % Read current key file
        fileID = fopen(names{file_index,:});
        currentKey = textscan(fileID,'%s','Delimiter','\n','Whitespace','');
        currentKey=currentKey{1,1};
        fclose(fileID);

        % Identify the node lines
        nodeLineStart = find(strcmp(currentKey,'*NODE'));

        % Check if keycard contain any *NODE def,
        if ~isempty(nodeLineStart)
            nodeLineEnd = zeros(size(nodeLineStart));
            for k=1:length(nodeLineStart)
                nodeLineEnd(k,1)=nodeLineStart(k)+find(~cellfun(@isempty,...
                    ((regexp(currentKey((nodeLineStart(k)+1) ...
                    :end,1),'<*', 'start')))),1);
            end

            if isempty(nodeLineEnd)
                disp(['The file: "',names{file_index,:},...
                    "' have no nodal information']);
            end
        end
    end
end

```

```

        continue;
    end

    % Loops over each *NODE part in the currnet keyword file
    for currentNodeInd = 1:length(nodeLineStart)
        % Lines to search
        startLine = nodeLineStart(currentNodeInd)+1;
        endLine = nodeLineEnd(currentNodeInd)-1;
        lineVec = startLine:endLine;
        tmp=lineVec';

        % Check if current *Node was empty
        if startLine==endLine
            continue;
        end

        % find all commented lines
        commentLineID=startLine-1+find(~cellfun(@isempty,...
            ((regexp(currentKey(lineVec,1),'\$\w*')))));

        % Lines to update
        if ~isempty(commentLineID)
            tmp(commentLineID+1-startLine)=[];
            updKeyLines = tmp';
        else
            updKeyLines=lineVec;
        end

        oldnodeID = cellfun(@(cell) sscanf(cell,'%u',1),...
            currentKey(updKeyLines,1));

        for j = 1:length(oldnodeID);
            % Find where to get the updated nodal info
            updInd = find(allUpdateID==oldnodeID(j));
            % Check existence
            if isempty(updInd)
                continue;
            end
            updIndAll = find(allUpdateID==oldnodeID(j));
            currentKey{updKeyLines(j),1}(9:56)= ...
                updateNodeStr{updIndAll,1}(9:56);
        end
        end
        disp(' -Updated nodes from dyain file');
    end

    nodeLines = find(strcmp(currentKey,'*NODE'));
    nodeLineEnd = zeros(size(nodeLines));

    for i = 1:length(nodeLines)
        nodeLineEnd(i) = nodeLines(i)-1+find(~cellfun(@isempty,...
            ((regexp(currentKey(nodeLines(i)+1:end),'\<.*')))),1);
    end

    jointRevoluteLine = find(strcmp(currentKey,...
        '*CONSTRAINED_JOINT_REVOLUTE_ID'));
    jointSphericalLine = find(strcmp(currentKey,...
        '*CONSTRAINED_JOINT_SPHERICAL_ID'));

    if ~isempty(jointRevoluteLine)
        for i = 1:length(jointRevoluteLine)
            jointRevoluteLineEnd = jointRevoluteLine(i)-1+ ...
                find(~cellfun(@isempty,((regexp(currentKey( ...
                    jointRevoluteLine(i)+1:end),'\<.*')))),1);
            currentLines = jointRevoluteLine(i)+1:jointRevoluteLineEnd;
            currentCont = textscan(strjoin(currentKey(currentLines)',...
                '\n'),'%s','Delimiter','\b','CommentStyle','$');
            currentCont=currentCont{1,1};
            njoints = size(currentCont,1)/2;
        end
    end

```

```

for j = 1:njoints
    jointID = sscanf(strjoin(currentCont(j*2-1)', '\n'), ...
        '%8f'); jointID=jointID(1);
    nodes = sscanf(strjoin(currentCont(j*2)', '\n'), ...
        '%8f %8f %8f %8f');
    n1A = nodes(1);
    n2A = nodes(3);
    n1B = nodes(2);
    n2B = nodes(4);
    n1ALine=0; n2ALine =0; n1BLine =0; n2BLine =0;

    for k=1:length(nodeLines)
        currentNodeLines = nodeLines(k)+1:nodeLineEnd(k);
        n1ALinetmp = nodeLines(k)+find(~cellfun(@isempty, ...
            ((regexp(currentKey(currentNodeLines), ...
                num2str(n1A))))),1);
        if n1ALinetmp>0
            n1ALine=n1ALinetmp;
            break;
        end
    end
    for k=1:length(nodeLines)
        currentNodeLines = nodeLines(k)+1:nodeLineEnd(k);
        n2ALinetmp = nodeLines(k)+find(~cellfun(@isempty, ...
            ((regexp(currentKey(currentNodeLines), ...
                num2str(n2A))))),1);
        if n2ALinetmp>0
            n2ALine=n2ALinetmp;
            break;
        end
    end
    for k=1:length(nodeLines)
        currentNodeLines = nodeLines(k)+1:nodeLineEnd(k);
        n1BLinetmp = nodeLines(k)+...
            find(~cellfun(@isempty, ((regexp(currentKey(...
                currentNodeLines), num2str(n1B))))),1);
        if n1BLinetmp>0
            n1BLine=n1BLinetmp;
            break;
        end
    end
    for k=1:length(nodeLines)
        currentNodeLines = nodeLines(k)+1:nodeLineEnd(k);
        n2BLinetmp = nodeLines(k)+find(~cellfun(@isempty, ...
            ((regexp(currentKey(currentNodeLines), ...
                num2str(n2B))))),1);
        if n2BLinetmp>0
            n2BLine=n2BLinetmp;
            break;
        end
    end
    currentKey{n1BLine}(9:56) = currentKey{n1ALine}(9:56);
    currentKey{n2BLine}(9:56) = currentKey{n2ALine}(9:56);
end
disp(' -Revolute joints updated')
end

if ~isempty(jointSphericalLine)
    for i = 1:length(jointSphericalLine)
        jointSphericalLineEnd = jointSphericalLine(i)-1+...
            find(~cellfun(@isempty, ((regexp(currentKey(...
                jointSphericalLine(i)+1:end), '^<[*]'))),1);
        currentLines = jointSphericalLine(i)+1:...
            jointSphericalLineEnd;
        currentCont = textscan(strjoin(currentKey(currentLines)', ...
            '\n'), '%s', 'Delimiter', '\b', 'CommentStyle', '$');
        currentCont=currentCont{1,1};
        njoints = size(currentCont,1)/2;

        for j = 1:njoints

```

```

jointID = sscanf(strjoin(currentCont(j*2-1), '\n'), ...
    '%8f');
jointID=jointID(1);
nodes = sscanf(strjoin(currentCont(j*2), '\n'), ...
    '%8f %8f');
n1A = nodes(1);
n1B = nodes(2);

n1ALine=0; n1BLine =0;
for k=1:length(nodeLines)
    currentNodeLines = nodeLines(k)+1:nodeLineEnd(k);
    n1ALinetmp = nodeLines(k)+find(~cellfun(@isempty, ...
        ((regexp(currentKey(currentNodeLines), ...
            num2str(n1A))))),1);
    if n1ALinetmp>0
        n1ALine=n1ALinetmp;
        break;
    end
end
for k=1:length(nodeLines)
    currentNodeLines = nodeLines(k)+1:nodeLineEnd(k);
    n1BLinetmp = nodeLines(k)+find(~cellfun(@isempty, ...
        ((regexp(currentKey(currentNodeLines), ...
            num2str(n1B))))),1);
    if n1BLinetmp>0
        n1BLine=n1BLinetmp;
        break;
    end
end
currentKey{n1BLine}(9:56) = currentKey{n1ALine}(9:56);
end
end
disp(' -Spherical joints updated')
end

printKeyFile(names{file_index, :}, currentKey);
disp(' -Copied keyword file');

% Find all element IDs and save the initial stress from the
% dynainFile
% allStressKey
% element name, rows dynain, cols IDdynain, rows key, cols IDkey
% elements.to_include_stress = {'*ELEMENT_SHELL',4,10,1,8;
%                               '*ELEMENT_SOLID',2,10,1,8;
%                               '*ELEMENT_BEAM',2,10,1,8};
% dynainStress

if ~isempty(find(strcmp(filesToIncludeStress, names{file_index, :}),1))
    for elemType = 1:size(elemToInclInit,1)
        % Identify the *element lines lines
        elemLineStart = find(strcmp(currentKey, ['*ELEMENT.', ...
            elemToInclInit{elemType,1}(17:end)]));

        % Check if keycard contain any *ELEMENT def,
        if ~isempty(elemLineStart)

            % Create *INITIAL_STRESS_DEF
            if isempty(dynainStress{1})
                dynainStress = {elemToInclInit{elemType,1}};
            else
                dynainStress = [dynainStress; ...
                    elemToInclInit{elemType,1}];
            end

            elemLineEnd = zeros(size(elemLineStart));
            for k=1:length(elemLineStart)
                elemLineEnd(k,1)=elemLineStart(k)+find(~cellfun(@isempty, ...
                    ((regexp(currentKey((elemLineStart(k)+1) ...
                        :end,1), '\<*', 'start'))),1);
            end
        end
    end
end

```

```

end

if isempty(elemLineEnd)
    disp(['The file: ', names{file_index, :}, ...
        ' have no element information']);
    continue;
end

% Loops over each *ELEMENT_ part in the currnet keyword file
for currentElemInd = 1:length(elemLineStart)
    % Lines to search
    startLine = elemLineStart(currentElemInd)+1;
    endLine = elemLineEnd(currentElemInd)-1;
    lineVec = startLine:endLine;
    tmp=lineVec';

    % Check if current *ELEMENT_ was empty
    if startLine==endLine
        continue;
    end

    % find all commented lines
    commentLineID=startLine-1+find(~cellfun(@isempty, ...
        ((regexp(currentKey(lineVec,1), '^$\$w*')))));

    % Lines to update
    if ~isempty(commentLineID)
        tmp(commentLineID+1-startLine)=[];
        updKeyLines = tmp';
    else
        updKeyLines=lineVec;
    end

    keyEleID = cellfun(@(cell) sscanf(cell, ['%'], ...
        num2str(elemToInclInit{elemType, 5}), 'u', 1), ...
        currentKey(updKeyLines, 1));
    allEleIdDynainlines = zeros(length(keyEleID)*...
        elemToInclInit{elemType, 2}, 1);
    rows = elemToInclInit{elemType, 2};
    for j = 1:length(keyEleID);
        tmp = find(keyEleID(j)==elemToInclInit...
            {elemType, 7}, 1)*rows-(elemToInclInit{elemType, 2}-1);
        if isempty(tmp)
            continue;
        end
        EleIdDynainlines = elemToInclInit...
            {elemType, 6}(tmp:(tmp+elemToInclInit...
            {elemType, 2}-1));
        allEleIdDynainlines((j*elemToInclInit...
            {elemType, 2}-(elemToInclInit...
            {elemType, 2}-1)):(j*elemToInclInit...
            {elemType, 2}))=EleIdDynainlines;
    end
    if ~isempty(find(allEleIdDynainlines>0))
        dynainStress = [dynainStress;...
            dynainKey(allEleIdDynainlines)];
    end
end
else
    continue
end
disp([' -Included ', ...
    elemToInclInit{elemType, 1}(2:end), ...
    ' in new dyain file']);
end
else
    disp([' -No stresses included'])
end
elseif (~isempty(strfind(names{file_index, :}, '.enc')))
    % Encrypted files are copied

```

```

        disp(['Checking: ',names{file_index,:}]);
        copyfile(names{file_index,:},['NewKeyFiles1\',names{file_index,:}])
        disp(' -Copied');
    else
        continue;
    end
end
dynainStress = [dynainStress; '*END'];
printKeyFile(dynainFileName,dynainStress);

disp('-----');
disp('');

disp('Done!')

```

Update Controller Reference Angles Script

```

%% Update reference angles in active THUMS controller keyword
clc, clear all, close all
%%%%%%%%%%%%%%%%%%%%%%%%%%%%%%%%%%%%%%%%%%%%%%%%%%%%%%%%%%%%%%%%%%%%%%%%
% The script does the following:
% - Updates controller angles in a specified muscle_control_active keyword
% - The new angles are calculated from nodal coordinate values that are
%   found, either in a dynain file or in the model key
%   files, dependent on the source of the new coordinates that you would
%   like the controller system to work with.
% - The controller keyword file is given as an input file to the script and
%   becomes updated in the end.
%
% Comments
% - The script can be modified if new controllers are added to the AHBM
%   by adding information in the cell-structure "CN" (line 40-50) and in
%   "refAngle" (line 141-147). Nothing else should need changes.
% - The script searches for a comment in the controller keyword "$ y0" which
%   comes before each define curve that sets the reference angle. It is
%   important not to remove or change this comment for the script to work.
%
% Created by: Jacob Wass & Erik Eliasson
%%%%%%%%%%%%%%%%%%%%%%%%%%%%%%%%%%%%%%%%%%%%%%%%%%%%%%%%%%%%%%%%%%%%%%%%

%% Inputs to set by the user!
% set the type of update reference. The following numbers mean:
% dynainUpdate = 1;
% keywordUpdate = 2;
typeOfUpdate = 2;

% Specify the filename of the dynain or drdisp.sif file
updateFileNameDynain = 'dynain.full';

% Specify the name of the current active controller keyword file
controllerKeyFileName = 'muscle_control_active_v3.key';

%% Script start
disp('');
disp('-----Update controller reference angles script-----');
disp('          Written by: Erik Eliasson & Jacob Wass');
disp(' ');
% Control nodes to be found and updated
CN(1,:)={'head',43700101,[]};
CN(2,:)={'sacrum',43300071,[]};
CN(3,:)={'T1',43900131,[]};
CN(4,:)={'T10',43900141,[]};

```

```

CN(5,:)={'Occ',43700121,[]};
CN(6,:)={'RElbow',43500101,[]};
CN(7,:)={'RShoulder',43500041,[]};
CN(8,:)={'Rhand',43500102,[]};
CN(9,:)={'LElbow',43600101,[]};
CN(10,:)={'LShoulder',43600041,[]};
CN(11,:)={'Lhand',43600102,[]};

%% Gets coordinates
switch typeOfUpdate
    % dynainUpdate
    case 1
        disp('    -Type of update: dynainUpdate');
        disp('    -Reading file');
        fileID = fopen(updateFileNameDynain);
        dynainKey = (textscan(fileID,'%s','Delimiter','\n','Whitespace',''));
        dynainKey=dynainKey{1,1};
        fclose(fileID);
        nodeLine = find(strcmp(dynainKey,'*NODE'));
        nodeLineEnd = nodeLine-1+find(~cellfun(@isempty,...
            ((regexp(dynainKey(nodeLine+1:end),'^\<.*')))),1);
        nodeLines = nodeLine+1:nodeLineEnd;
        updateMatrix = cell2mat(cellfun(@(cell) sscanf(cell,'%f',...
            [1,4]),dynainKey(nodeLines),'UniformOutput',false));
        % Get coordinate data from dynain file
        for i=1:length(CN) %for each node keyword
            currentLine = find(CN{i,2}==updateMatrix(:,1));
            CN{i,3}=updateMatrix(currentLine,2:4);
        end

        % From keyword files
    case 2
        disp('    -Type of update: keywordUpdate');
        disp('    -Reading files');
        names = cellstr(ls);
        filenum =1;
        for file_index=1:size(names,1)
            if (~isempty(strfind(names{file_index,:},'k')))
                fileID = fopen(names{file_index,:});
                currentKey = textscan(fileID,'%s','Delimiter',...
                    '\n','Whitespace','');
                currentKey=currentKey{1,1};
                fclose(fileID);
                % Identify the node lines
                nodeLines = find(strcmp(currentKey,'*NODE'));
                % Check if keycard contain any *NODE def,
                if ~isempty(nodeLines)
                    nodeLineEnd = zeros(size(nodeLines));
                    for k=1:length(nodeLines)
                        nodeLineEnd(k,1)=nodeLines(k)+find(~cellfun(...
                            @isempty,((regexp(currentKey((nodeLines(k)...
                                +1):end,1,'^\<.*','start')))),1);
                    end
                    % look for node IDs within the *Node lines
                    for k=1:length(nodeLines)
                        currentNodeLines = nodeLines(k)+1:nodeLineEnd(k)-1;
                        for i=1:size(CN,1)
                            if isempty(CN{i,3})
                                CNdLine = nodeLines(k)+find(~cellfun(@isempty,...
                                    ((regexp(currentKey(currentNodeLines),...
                                        num2str(CN{i,2}))))),1);
                                if ~isempty(CNdLine)
                                    updateCoords = cell2mat(cellfun(@(cell)...
                                        sscanf(cell,'%f',[1,4]),...
                                        currentKey(CNdLine),'UniformOutput',...
                                        false));
                                    CN{i,3}=updateCoords(2:4);
                                end
                            end
                            CNdLine=[];
                        end
                    end
                end
            end
        end
    end
end

```

```

                end
            end
        end
    end
    otherwise
        disp('Incorrect choice of "typeOfUpdate"! Stopping script')
        return;
    end
    if sum(~cellfun(@isempty,CN(:,3)))/size(CN,1)<1
        disp('      -Error! All coordinates was not found! Stopping script')
        return;
    else
        disp('      -Coordinates found!')
    end

    %% update angles
    disp(' ');
    disp('-----');

    disp('      -Calculating new angles and updates the controller keyword file')
    % Calculate new reference angles
    refAngle(1,:) = {'Head',43810000,atan((CN{1,3}(1,1)-CN{5,3}(1,1))/...
        ((CN{1,3}(1,3)-CN{5,3}(1,3)))));
    refAngle(2,:) = {'Cervical.spine',43710000,atan((CN{5,3}(1,1)-CN{3,3}(1,1))/...
        ((CN{5,3}(1,3)-CN{3,3}(1,3)))));
    refAngle(3,:) = {'Lumbar.spine',43310000,atan((CN{4,3}(1,1)-CN{2,3}(1,1))/...
        ((CN{4,3}(1,3)-CN{2,3}(1,3)))));
    refAngle(4,:) = {'Right.elbow',43541000,acos(dot(CN{6,3}-CN{7,3},...
        CN{8,3}-CN{6,3})/(norm(CN{6,3}-CN{7,3})*norm(CN{8,3}-CN{6,3})));
    refAngle(5,:) = {'Shoulder.right.arm',43551000,atan(...
        (CN{6,3}(1,1)-CN{7,3}(1,1))/((CN{6,3}(1,3)-CN{7,3}(1,3)))));
    refAngle(6,:) = {'Left.elbow',43641000,acos(...
        dot(CN{9,3}-CN{10,3},CN{11,3}-CN{9,3})/...
        (norm(CN{9,3}-CN{10,3})*norm(CN{11,3}-CN{9,3})));
    refAngle(7,:) = {'Shoulder.left.arm',43651000,atan(...
        (CN{9,3}(1,1)-CN{10,3}(1,1))/((CN{9,3}(1,3)-CN{10,3}(1,3)))));
    disp('      -New reference angles for control system: ');
    disp(' ');
    disp(refAngle);

    % Get control keyword file
    fileID = fopen(controllerKeyFileName);
    muscleControlKey = textscan(fileID,'%s','Delimiter','\n','Whitespace','');
    muscleControlKey=muscleControlKey{1,1};
    fclose(fileID);

    % Updates control keyword file with new reference angles
    UCnodeline = find(strcmp(muscleControlKey(:,1),'$ y0'));
    for i=1:length(UCnodeline) %for each node keyword
        k=UCnodeline(i)+3; % line index
        if refAngle{i,2}==sscanf(muscleControlKey{k,1},'%u',1)
            space=' ';
            if refAngle{i,3}>0, space = ' '; end
            muscleControlKey{k+2,1}(21:40)=[space, num2str(refAngle{i,3},'%16f')];
            muscleControlKey{k+3,1}(21:40)=[space, num2str(refAngle{i,3},'%16f')];
        end
    end
end

% print updated keyword file
fileID=fopen(controllerKeyFileName,'w');
fprintf(fileID,'%s',strjoin(muscleControlKey,'\n'));
fclose(fileID);

disp(['      -Updated controller keyword saved as: ', controllerKeyFileName]);
disp('-----');
disp('Done!');

```

C Calibration Results

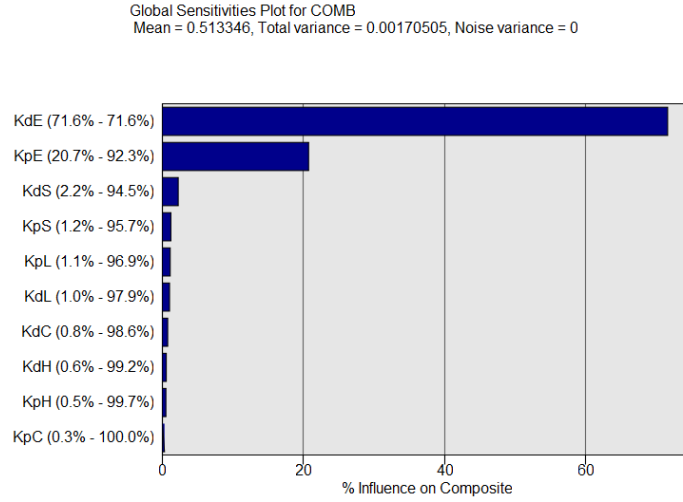


Figure C.1: Parameter statistical sensitivities for the combined goal function in the calibration conducted by Osth et. al. (2013) [37]

Table C.1: Complete results of calibration Batch 2; showing the tested parameter sets sorted after NRMS values for the seven best and three worst scoring combined values. The following abbreviations are used for the comparative NRMS values: *HR* - Head Rotation, *HX* - Head X-displacement, *StX* - Sternum X-displacement, *SBF* - Seat Belt Force, *SWF* - Steering Wheel Force, *Fr* - frequency amplitude

Batch 2		Parameters				RMS normalised							
SimID	KpH	KdH	KpC	KdC	Comb	HR	HRFr	HX	HXFr	StX	StFr	SBF	SWF
2.3	1.50	0.15	1.62	0.25	4.95	1.25	4.40	0.31	1.24	0.32	0.49	0.62	0.48
2.11	0.81	0.14	1.65	0.25	4.98	2.12	4.13	0.42	1.13	0.31	0.47	0.62	0.48
2.6	1.14	0.15	1.47	0.19	5.06	1.74	4.39	0.40	1.18	0.31	0.46	0.61	0.48
2.13	0.84	0.14	1.25	0.24	5.07	2.35	4.10	0.51	1.10	0.31	0.47	0.62	0.48
2.24	0.80	0.14	1.22	0.11	5.13	2.54	4.09	0.57	1.05	0.31	0.41	0.62	0.48
2.4	1.49	0.12	1.24	0.24	5.23	1.45	4.66	0.38	1.22	0.32	0.47	0.61	0.48
2.21	0.81	0.15	1.63	0.05	5.23	2.22	4.39	0.49	1.13	0.31	0.39	0.62	0.49
2.19	1.49	0.15	1.20	0.07	5.50	1.54	4.95	0.45	1.19	0.32	0.41	0.63	0.50
2.17	1.18	0.10	1.20	0.15	5.68	1.90	5.03	0.49	1.16	0.31	0.41	0.61	0.49
2.8	1.18	0.13	1.44	0.05	5.68	1.78	5.08	0.47	1.18	0.32	0.37	0.63	0.49
2.14	1.00	0.10	1.70	0.14	5.81	1.85	5.19	0.44	1.23	0.31	0.40	0.61	0.49
2.2	1.22	0.08	1.70	0.25	5.86	1.52	5.33	0.37	1.32	0.31	0.44	0.62	0.48
2.10	0.82	0.05	1.20	0.06	5.92	2.71	5.01	0.66	0.80	0.31	0.33	0.62	0.49
2.23	1.45	0.10	1.58	0.13	6.14	1.41	5.66	0.39	1.36	0.32	0.41	0.61	0.49
2.18	0.82	0.04	1.69	0.24	6.40	2.18	5.75	0.48	1.19	0.30	0.36	0.61	0.49
2.20	0.82	0.02	1.35	0.18	6.69	2.52	5.96	0.59	1.01	0.31	0.34	0.61	0.49
2.1	1.10	0.05	1.45	0.10	6.78	1.99	6.23	0.52	1.16	0.31	0.33	0.62	0.50
2.5	1.19	0.02	1.22	0.25	7.00	1.90	6.47	0.49	1.30	0.31	0.37	0.61	0.49
2.12	1.50	0.04	1.33	0.17	7.20	1.55	6.75	0.45	1.41	0.31	0.36	0.62	0.50
2.15	0.85	0.02	1.70	0.06	7.47	2.37	6.88	0.59	1.00	0.31	0.32	0.62	0.50
2.22	1.50	0.02	1.58	0.25	7.87	1.46	7.44	0.40	1.63	0.31	0.40	0.62	0.50
2.16	1.37	0.02	1.21	0.05	8.09	2.00	7.64	0.59	1.12	0.32	0.31	0.62	0.51
2.7	1.19	0.02	1.70	0.16	8.25	1.82	7.81	0.48	1.45	0.31	0.29	0.61	0.50
2.9	1.47	0.02	1.56	0.05	9.23	1.85	8.81	0.55	1.48	0.32	0.30	0.62	0.52
Normalising factors:						0.07	3e-3	44.8	2.42	26.88	1.50	0.04	0.07

Table C.2: Complete results of calibration Batch 1; showing the tested parameter sets sorted after NRMS values for the seven best and three worst scoring combined values. The following abbreviations are used for the comparative NRMS values: *HR* - Head Rotation, *HX* - Head *X*-displacement, *StX* - Sternum *X*-displacement, *SBF* - Seat Belt Force, *SWF* - Steering Wheel Force, *Fr* - frequency amplitude

Batch 1		Parameters						Normalised RMS								
SimID	KH	KpC	KdC	KS	KpE	KdE	Comb	HR	HRFr	HX	HXFr	StX	StFr	SBF	SWF	
1.17	0.71	1.35	0.23	0.28	1.01	0.49	3.27	1.92	2.15	0.19	0.85	0.44	0.22	0.66	0.39	
1.35	0.44	2.91	0.54	0.03	2.45	0.49	3.70	1.65	2.53	0.58	0.65	1.03	0.69	0.78	0.63	
1.20	0.60	2.96	0.26	1.82	1.58	0.44	4.25	1.77	3.27	0.26	0.54	0.65	0.61	0.77	0.82	
1.8	0.40	2.89	0.31	1.05	1.11	0.03	4.27	2.35	2.44	0.68	1.62	0.63	1.15	0.67	0.88	
1.14	0.87	2.92	0.95	0.43	1.01	0.01	4.43	1.65	3.03	0.61	1.43	0.71	1.75	0.65	0.73	
1.30	2.44	0.53	0.34	0.23	1.01	0.48	4.84	0.90	4.05	0.36	0.30	0.64	0.76	0.67	0.90	
1.36	1.17	0.52	0.92	1.22	1.01	0.01	4.90	2.47	3.29	1.07	1.29	0.63	1.27	0.64	0.91	
1.45	2.41	0.80	0.40	1.93	1.15	0.41	5.04	0.99	4.05	0.39	0.76	0.55	0.99	0.72	1.10	
1.32	0.54	0.53	0.21	0.13	1.03	0.09	5.16	3.93	2.58	1.00	1.02	0.50	0.83	0.63	0.55	
1.23	1.65	2.42	0.20	0.08	1.93	0.48	5.17	0.90	4.34	0.40	0.51	1.04	0.94	0.74	0.88	
1.5	1.86	2.04	0.20	1.85	1.26	0.02	5.24	0.71	4.58	0.55	1.13	0.66	1.15	0.71	0.93	
1.26	0.55	2.92	0.30	1.17	2.46	0.13	5.39	1.63	4.46	0.52	1.53	0.87	0.72	0.83	0.59	
1.40	0.43	1.15	0.75	0.50	1.01	0.28	5.45	3.06	3.90	0.56	1.32	0.31	0.73	0.64	0.58	
1.39	1.95	0.68	0.32	0.69	2.06	0.34	5.49	1.02	4.74	0.32	0.90	0.92	1.08	0.76	0.78	
1.9	0.43	2.99	0.76	0.04	2.08	0.01	5.51	2.02	3.70	0.53	2.30	0.87	1.95	0.69	0.68	
1.11	2.46	2.97	0.34	1.88	2.26	0.03	5.57	2.21	4.21	0.81	1.53	0.94	1.01	0.80	0.82	
1.21	0.41	2.04	1.00	0.61	1.83	0.47	5.64	2.50	4.37	0.17	0.98	0.82	0.79	0.74	0.87	
1.33	1.37	0.50	1.00	1.06	1.72	0.32	5.64	1.70	4.54	0.47	0.92	0.81	1.22	0.73	0.88	
1.41	2.41	1.03	0.40	0.03	2.48	0.01	5.68	0.96	4.88	0.63	1.40	1.15	1.01	0.77	0.58	
1.16	1.13	2.87	0.52	0.02	1.07	0.30	5.72	1.02	5.14	0.20	1.02	0.62	0.93	0.64	0.62	
1.27	0.99	2.30	0.96	1.99	1.12	0.09	5.77	1.80	4.74	0.58	1.54	0.48	1.03	0.72	0.88	
1.24	1.31	1.06	0.81	0.03	2.48	0.44	5.83	1.41	4.37	0.25	1.36	1.11	1.59	0.72	1.06	
1.19	1.21	1.86	0.55	1.99	2.12	0.25	5.88	1.44	5.20	0.31	0.93	0.88	0.67	0.80	0.77	
1.47	0.90	0.51	0.99	0.05	2.40	0.01	5.93	2.45	4.15	0.42	2.48	1.05	1.31	0.76	0.57	
1.44	0.72	0.60	0.27	1.90	1.71	0.04	5.99	3.23	4.26	0.73	1.53	0.66	1.09	0.77	0.87	
1.15	2.39	2.16	0.24	1.69	2.17	0.44	6.05	2.01	4.76	0.50	0.57	0.94	0.97	0.76	1.11	
1.12	0.71	0.59	0.51	1.64	1.26	0.47	6.08	3.36	3.51	0.86	1.07	0.54	1.12	0.71	1.09	
1.1	0.86	1.30	0.47	0.44	2.00	0.06	6.11	3.02	4.03	1.56	1.27	0.97	0.89	2.22	0.42	
1.25	1.35	2.92	0.99	0.03	2.48	0.29	6.18	0.81	5.58	0.48	0.73	1.15	1.15	0.76	0.77	
1.37	2.24	0.88	0.36	0.41	1.22	0.04	6.19	0.72	5.63	0.47	1.29	0.61	1.39	0.66	0.65	
1.18	2.36	0.92	0.78	1.97	1.63	0.05	6.26	1.47	5.48	0.32	1.51	0.71	0.98	0.79	0.78	
1.28	2.31	2.06	0.97	0.17	1.54	0.02	6.29	1.74	5.15	0.54	2.03	0.80	1.76	0.66	0.60	
1.29	2.34	2.86	0.69	1.43	1.21	0.16	6.31	2.45	5.35	0.48	1.02	0.56	0.78	0.74	0.64	
1.46	2.39	1.13	1.00	0.74	2.47	0.16	6.40	2.00	5.64	0.58	0.83	1.04	0.52	0.79	0.55	
1.10	2.44	2.82	0.25	0.19	1.08	0.08	6.49	1.90	5.80	0.54	0.98	0.58	1.18	0.64	0.56	
1.38	2.35	0.89	0.23	1.81	2.37	0.02	6.53	0.86	5.65	0.45	2.03	0.92	1.12	0.80	0.88	
1.22	1.92	2.98	0.90	1.37	2.07	0.42	6.58	2.04	5.19	0.57	0.93	0.96	1.20	0.73	1.13	
1.7	2.00	0.59	0.89	0.00	1.02	0.21	6.60	0.99	6.01	0.19	1.04	0.54	1.25	0.64	0.60	
1.3	1.75	2.91	0.93	1.27	2.28	0.00	6.70	1.83	5.75	0.74	1.52	0.97	1.22	0.80	0.72	
1.2	1.96	1.77	0.98	1.99	1.19	0.45	6.70	1.68	5.33	0.19	0.49	0.64	1.20	0.70	1.31	
1.13	2.21	2.95	0.21	0.06	2.48	0.02	6.75	1.62	6.03	0.97	0.89	1.15	0.79	0.78	0.51	
1.6	0.41	1.61	1.00	1.18	1.97	0.00	6.76	3.04	5.05	0.44	2.15	0.81	1.54	0.76	0.81	
1.48	0.40	0.50	0.72	1.29	2.50	0.23	7.19	4.09	5.32	0.52	1.22	0.90	0.94	0.80	0.75	
1.31	0.46	1.54	0.20	1.09	2.44	0.50	7.55	3.34	5.75	0.25	1.02	0.90	0.97	0.76	1.19	
1.4	0.45	1.09	0.99	1.98	2.13	0.50	7.81	3.49	4.90	0.51	1.14	0.76	1.50	0.68	1.54	
1.42	2.46	2.94	0.70	0.02	1.76	0.33	7.89	3.08	6.72	0.96	1.16	1.00	1.01	0.75	0.82	
1.34	2.50	1.53	0.98	0.59	1.65	0.50	10.27	3.48	8.43	0.66	1.09	0.84	1.70	0.68	1.42	
1.43	2.31	1.05	0.91	1.95	2.49	0.43	11.42	3.05	9.88	0.58	0.36	0.96	1.52	0.70	1.49	
Normalising factors:								0.07	3e-3	44.8	2.42	26.88	1.50	0.04	0.07	

D SAFER AHBM Industrial Version Bug Fixes

Table D.1: Solutions and fixes that have been added to the SAFER AHBM within this thesis work, to solve numerical issues, improve scaling properties, and other errors found in the work process.

Nr.	Short description	Changed files	Change info	Date
1.1	Controller keyword	All muscle	All keywords associated with the active muscle control is cut from the muscle files and pasted into a separate controller keyword file, called "muscle control active v1.key"	15-02-06
1.2	Update SSP	Trunk	All SSP values were set to 0, to active the passive properties	15-02-06
1.2	Update SSP	Lowex	all M.gluteus maximus inferior changed to SSP=1, all M.adductor changed to SSP=1, to deactivate passive properties and fix problem with initial movement of the sacrum.	15-02-06
1.3	Pnode knee	lowex	Pnode in knee and ankle fixed to not end up in COG, and cause numerical instabilities	15-02-06
1.4	Tied contacts MPP	lowex, upex, trunk	Changed all *CONTACTTIED NODES TO SURFACE to *CONTACT TIED NODES TO SURFACE MPP with GRPABLE=1	15-02-19
1.5	Rigid node knee MPP	lowex	Got warning from rigid node in knee joint definition that was also part of contact segment. Changed node 41121576 and 41221576 to 41121598 and 41221598	15-02-22
2.5	Positioning	Entire AHBM	Positioning AHBM into seat, to match the volunteers for calibration	15-02-25
2.6	Wrong constraints	trunk	Nodes 43751062, 43751072, 43752052, 43755012, 43727022, 43728012 was constrained to 41910100 (T2) but should be constrained to 41910000 (T1)	15-03-03
2.7	Length of arm muscles	upex	Element 43610010, Node 43610013, halved length. Same muscle properties	15-03-05
2.7	Length of arm muscles	upex	Element 43610020, Node 43610023, halved length. Same muscle properties	15-03-05
2.7	Length of arm muscles	upex	Element 43610030, Node 43610033, halved length. Same muscle properties	15-03-05
2.7	Length of arm muscles	upex	Element 43510010, Node 43510013, halved length. Same muscle properties	15-03-05
2.7	Length of arm muscles	upex	Element 43510020, Node 43510023, halved length. Same muscle properties	15-03-05
2.7	Length of arm muscles	upex	Element 43510030, Node 43510033, halved length. Same muscle properties	15-03-05
2.8	PIDCTL	muscle control active v2	Implemented PID function to reduce *DEFINE CURVE FUNCTION and combined two *DEFINE CURVE FUNCTION for scaling flexor/extensor to one. Goal to improve scaling in MPP. This setups needs to be simulated with the new Dyna binary.	15-03-19
2.9	Joint nodes	upex, lowex	New binary is more strict with nodal coordinates for joint definitions. Values updated for upex, lowex and seat model to work with new binary.	15-03-19
3.9	New Position	Entire AHBM	New calibration position to avoid seat "bounce" and head tipping forward.	15-03-20
3.10	Length of arm muscles	upex	Element 43611032 Node 43611039, doubled length. Same muscle properties	15-03-24
3.10	Length of arm muscles	upex	Element 43511032 Node 43511039, doubled length. Same muscle properties	15-03-24
3.10	Length of arm muscles	upex	Element 43511042 Node 43511049, doubled length. Same muscle properties	15-03-24
3.10	Length of arm muscles	upex	Element 43611042 Node 43611049, doubled length. Same muscle properties	15-03-24
3.11	Muscle constraints	upex	A number of muscles were connected to wrong rigid parts along the spine. Probably an error from converting the model to THUMS v1.5, see Table D.2	15-04-01
3.12	New DELAY and PIDCTL	upex	Added a new version of the DELAY function for testing LS-Dyna r8.0 rev 98312	15-05-06

Table D.2: The following node ID:s where found to connect to incorrect parts using \times CONSTRAINED_EXTRA_NODES_NODE in the Industial SAFER AHBM trunk file. The table is a list over what nodal constraints that were changed from its old to new part.

Node ID	Old Part ID	New Part ID	Node ID	Old Part ID	New Part ID
43701031	41710500	41710200	43709062	41910400	41910200
43751031	41710500	41710200	43759062	41910400	41910200
43701041	41710500	41710200	43761011	41710100	41710000
43751041	41710500	41710200	43761021	41710300	41710100
43701051	41710600	41710300	43711031	41710400	41710200
43701061	41710600	41710300	43761031	41710500	41710200
43701082	41910300	41910100	43711041	41710500	41710300
43751082	41910300	41910100	43761041	41710600	41710300
43701092	41910300	41910100	43764012	41710100	41710000
43751092	41910300	41910100	43765011	41710100	41710000
43701102	41910400	41910200	43765012	41710300	41710100
43751102	41910400	41910200	43771012	41710100	41710000
43701112	41910400	41910200	43772012	41710100	41710000
43751112	41910400	41910200	43774011	41710300	41710100
43701122	41910600	41910300	43724021	41710400	41710200
43751122	41910700	41910300	43774021	41710500	41710200
43702012	41710600	41710300	43724031	41710500	41710300
43702062	41910300	41910100	43774031	41710600	41710300
43752062	41910300	41910100	43725011	41710400	41710200
43702072	41910400	41910200	43775011	41710500	41710200
43752072	41910400	41910200	43725021	41710500	41710300
43702082	41910600	41910300	43775021	41710600	41710300
43752082	41910700	41910300	43726012	41710400	41710200
43703011	41710300	41710100	43776012	41710500	41710200
43703012	41910300	41910100	43726022	41710500	41710300
43753011	41710400	41710100	43776022	41710600	41710300
43753012	41910300	41910100	43727011	41710200	41710100
43703021	41710400	41710200	43777011	41710300	41710100
43703022	41910400	41910200	43727021	41710200	41710100
43753021	41710500	41710200	43777021	41710300	41710100
43753022	41910400	41910200	43727031	41710400	41710200
43703031	41710500	41710300	43777031	41710500	41710200
43703032	41910600	41910300	43727041	41710600	41710300
43753031	41710600	41710300	43728022	41910200	41910100
43753032	41910700	41910300	43778022	41910300	41910100
43703042	41910800	41910400	43729012	41710400	41710200
43753042	41910900	41910400	43779012	41710500	41710200
43703052	41911000	41910500	43729022	41710600	41710300
43753052	41911100	41910500	43779022	41710600	41710300
43704011	41710500	41710300	43901012	41910600	41910300
43754011	41710600	41710300	43951012	41910700	41910300
43705021	41710500	41710200	43901022	41910800	41910400
43705022	41910300	41910100	43951022	41910900	41910400
43755021	41710500	41710200	43901031	41910200	41910100
43755022	41910300	41910100	43901032	41910800	41910400
43705031	41710600	41710300	43951031	41910400	41910100
43705032	41910400	41910200	43951032	41910900	41910400
43755031	41710600	41710300	43901041	41910200	41910100
43755032	41910400	41910200	43901042	41911000	41910500
43705042	41910600	41910300	43951041	41910400	41910100
43755042	41910700	41910300	43951042	41911100	41910500
43706012	41910800	41910400	43901051	41910400	41910200
43756012	41910900	41910400	43901052	41911000	41910500
43706022	41911000	41910500	43951051	41910400	41910200
43756022	41911100	41910500	43951052	41911100	41910500
43707012	41710500	41710300	43901061	41910400	41910200
43757012	41710600	41710300	43901062	41911100	41910600
43707052	41910400	41910200	43951061	41910400	41910200
43757052	41910400	41910200	43901071	41910700	41910300
43708012	41910700	41910300	43901072	41911100	41910600
43758011	41710100	41710000	43951071	41910800	41910300
43758012	41910800	41910300	43901081	41910700	41910300
43708022	41910800	41910400	43951081	41910800	41910300
43758021	41710300	41710100	43901091	41910800	41910400
43758022	41910900	41910400	43951091	41910900	41910400
43708031	41710400	41710200	43901101	41910800	41910400
43708032	41911100	41910500	43951101	41910900	41910400
43758031	41710500	41710200	43901111	41911000	41910500
43758032	41911100	41910500	43951111	41911000	41910500
43709052	41910300	41910100	43901121	41911000	41910500
43759052	41910400	41910100	43951121	41911000	41910500